BOLTED JOINT STUDIES IN GRP

by

David M. Fox

B.S., Chemical Engineering
Rose-Hulman Institute of Technology, 1984

Submitted to the Department of Ocean Engineering and the
Department of Materials Science and Engineering
in Partial Fulfillment of the Requirements for the Degrees of

Naval Engineer
and
Master of Science in Materials Science and Engineering

at the
Massachusetts Institute of Technology
May 1994

Signature of Author_____

Certified by_____
Frederick J. McGarry, Professor of ~~Civil Engineering~~ and Polymer Engineering
Thesis Advisor

Certified by_____
Koichi Masubuchi, Kawasaki Professor of Engineering
Thesis Reader

Accepted by_____
Carl V. Thompson II, Professor of Electronic Materials
Chairman, Committee on Graduate Students,
Department of Materials Science and Engineering

Accepted by_____
A. Douglas Carmichael, Professor of Power Engineering
Chairman, Committee on Graduate Students, Department of Ocean Engineering

BOLTED JOINT STUDIES IN GRP

by

DAVID M. FOX

Submitted to the Department of Ocean Engineering and the Department of Materials Science and Engineering on 6 May 1994 in partial fulfillment of the requirements for the Degrees of Naval Engineer and
Master of Science in Materials Science and Engineering.

ABSTRACT

An experimental study was carried out to determine the bolt clampup force relaxation behavior in countersunk, single-lap bolted joints between glass/vinylester resin laminates and steel panels. Additionally, the effect of bolt clampup force relaxation on the bearing strength of such joints was studied.

Specially-instrumented bolts were used to measure clampup force relaxation in ten countersunk joint specimens. A 100,000 pound capacity MTS testing machine was used to evaluate the bearing strength in tension of sixteen countersunk bolted joint specimens torqued to four different levels of initial torque, as well as four similar protruding-head bolted joint specimens (at the same levels of torque).

The results of the relaxation experiments indicate that clampup force varies widely in nominally identical joints at identical torque levels, by as much as a factor of two. In countersunk bolt joints with sufficiently high initial clampup force, the clampup force relaxed in accordance with the inverse power equation proposed by Shivakumar and Crews for protruding-head bolt joints in graphite/epoxy laminates. Relaxation in the present experiments proceeded faster than in the protruding-head joints studied by Shivakumar and Crews; this is believed to have been due to the relative lack of constraint provided at the GRP surface by the countersunk bolt.

The results from the bearing strength experiments suggest that clampup force has only a small beneficial effect on bearing strength in both countersunk and protruding head single-lap joints, when compared to double-lap joints. The reduced effectiveness of clampup force in increasing the bearing strength is believed to be a result of the increased joint rotation and bolt bending inherent in single-lap joints. These phenomena lead to delamination and brooming failure in the GRP, which can be avoided in double lap joints with sufficient bolt clampup force. The countersunk joints failed at a load approximately 20% lower than the protruding head joints.

Thesis Advisor: Frederick J. McGarry
Title: Professor of Civil Engineering and Polymer Engineering

Table of Contents

List of Illustrations and Figures

List of Tables

Acknowledgements

Many persons aided me in my search for knowledge as I prepared this thesis. Although I cannot publicly acknowledge all of these people, the following deserve special recognition:

Professor Fred McGarry, whose advice, counsel, and good will kept me on the right path;

Professor Jeff Reed, who kept an active interest in my research, helped smooth out the programmatic details, and who was always available for advice or friendly discussions;

Scott Bartlett and Dr. Milt Critchfield of the Carderock Division, Naval Surface Warfare Center, who proposed that I study the behavior of bolted joints in composites, and provided financial support and materials for my research;

Noel Tessier of Grace Composites, Inc. of Canton, Massachusetts, who graciously allowed me to use their equipment to cut and drill composite samples, and who was willing to help me with any problems that developed along the way;

Noah Eckhouse, John Mass, and the boys in the Marine Instrumentation and Computation Laboratory at MIT, for lending me equipment and letting me use their facilities for building my relaxation experiment set-up;

My parents, Daniel and Patricia Fox, for their love, support, and encouragement throughout my life;

My colleague, LCDR Greg Thomas, whose advice and example helped motivate and challenge me;

My colleague, LCDR Melissa Smoot, who took care of things for me without needing to be asked when I was in the hospital with a fractured hip;

Professor Elias Gyftopoulos, who taught me to challenge accepted ideas;

The U.S. Navy, for providing me with the opportunity to further my education at MIT; and

Adolphe Sax, whose marvelous invention provided me with an outlet for the inevitable tensions generated during my studies.

Chapter One
Introduction

1.1 Overview

Glass-reinforced polymeric (GRP) materials offer certain advantages to the designer of Naval ships. A large strength-to-weight ratio, coupled with electromagnetic transparency and (possibly engineered) sound-dampening properties, render GRP materials as attractive materials for ship decks and deckhouse skins. Unfortunately, these materials, which use a thermosetting resin as a matrix material, cannot be welded as steel can. Thus, if a large structure is to be built of GRP, the inevitable joints must be either adhesively bonded or mechanically fastened. These joining techniques are frequently combined in joints which must support large loads. Because of this, an understanding of the mechanical behavior of joints in GRP is important.

In a properly designed bolted lap joint in GRP, the failure mode in tension is bearing failure, which occurs when the loaded edge of the bolt hole becomes crushed under the load imposed by the bolt. The stress at which this failure occurs is called the bolt-bearing strength. It is well-known that the bearing strength in a bolted joint in GRP can be increased by increasing the torque on the nut [1]. Shivakumar and Crews have shown, however, that the clampup force in the bolt (which is proportional to the torque applied to the nut) relaxes over time, as the viscoelastic matrix material in the GRP panel creeps under the influence of the load [2]. This effect is exacerbated by high temperature or high humidity. The overall result is a decrease in the bearing

strength of the material.

The Advanced Structures Group of the Carderock Division, Naval Surface Warfare Center (CD/NSWC) is interested in the possible use of a vacuum-assisted resin transfer molding (VARTM)-produced glass-reinforced vinylester resin for decks and bulkheads in future Naval combatants. For reasons related to producibility and radar cross section, they envision bolting panels of this material to the steel hull using flat-head, countersunk bolts. There is thus a need for an understanding of the mechanical behavior of such joints. The aims of the current thesis were as follows:

(1) To measure clampup force relaxation in countersunk bolt joints in glass/vinylester resin laminates, under different conditions of initial force;

(2) To compare the countersunk bolt, GRP results with Shivakumar and Crew's results for standard hex head bolts in carbon-fiber reinforced epoxy; and

(3) To determine the effect of this clampup force relaxation on the bearing strength of the VARTM-produced GRP panels.

1.2 Background

Like all polymeric materials, cured vinylester resin behaves viscoelastically at relatively low temperatures (when compared to the creep behavior of metals). This behavior manifests itself as either a stress relaxation effect under the influence of a constant strain, or a creep effect under the influence of a constant stress. These effects are detrimental over a long period of time when the material is used in structural applications.

In GRP materials, the viscoelastic behavior of the resin matrix is mitigated by the presence of the elastic glass fibers. In directions parallel to the fibers, the fibers carry the loads and restrain the matrix from creeping. If the structural application of the laminate is such that the loads remain in-plane and parallel to the fibers, the behavior of the composite will be elastic, even over long periods of time. If, however, the laminate is subjected to loads perpendicular to the laminar planes, the fibers can no longer carry loads. The laminate behavior is then dominated by the matrix material, and will be viscoelastic over long periods of time.

In order to achieve maximum bolted joint strength in GRP panels loaded in-plane, bolt holes in GRP materials must be perpendicular to the ply orientations. Thus, any clampup force applied to the laminate by a bolt acts in the matrix-dominated thickness direction, and will cause viscoelastic creep over time. This behavior is complicated by the small area over which the bolt clampup force acts; the material under the force application area is geometrically constrained by the unloaded material to which it is attached. Additionally, as the material creeps, there will be a corresponding relaxation of stress in the bolt.

Because of the anisotropic nature of GRP viscoelasticity, in which viscoelastic behavior is maximized in the thickness direction, any viscoelastic effects in bolt joints will be strongly affected by the geometry of the joint. In particular, the area of clampup force application, and its orientation with respect to the fibers, will affect the viscoelastic behavior of the laminate.

In order to predict the strength of bolted joints in GRP laminates, an

understanding of bolt clampup force relaxation and its effect on bolt bearing strength is required. The goal of this thesis is to quantify and describe the actual clampup force relaxation behavior of countersunk bolts in GRP, and to determine the effect of this relaxation on the bearing strength of the joint.

Theoretical Models of Bolted Joint Mechanical Behavior

The prediction of stress distributions near bolted joints in fiber-reinforced composite materials is made difficult by the many parameters involved. Because of geometric issues, and the anisotropic behavior of the non-homogeneous composite laminate, simplifying assumptions must necessarily be made.

The theory of elastic stresses in panels in the vicinity of holes is presented by Savin [3]. The two-dimensional development for isotropic materials begins with the combination of the static equilibrium and compatibility equations into the biharmonic equation,

$$\frac{\partial^4 U}{\partial x^4} + 2\frac{\partial^4 U}{\partial x^2 \partial y^2} + \frac{\partial^4 U}{\partial y^4} = 0 \qquad (1.1)$$

in which U is the stress function U(x,y), by which the stresses at any point are defined by:

$$\sigma_x = \frac{\partial^2 U}{\partial y^2} \qquad \sigma_y = \frac{\partial^2 U}{\partial x^2} \qquad \tau_{xy} = -\frac{\partial^2 U}{\partial x \partial y} \qquad (1.2)$$

The solution to equation (1.1) was shown by N. I. Muskhelishvili [3] to be of the form:

$$U(x, y) = Re[z\varphi_1(z) + \chi_1(z)] \tag{1.3}$$

where ϕ_1 (z) and χ_1 (z) are analytic functions of the complex variable z = x + iy, in which x and y are the in-plane Cartesian coordinates. Determination of the functions ϕ_1 and χ_1 thus establishes the two-dimensional state of stress at any point in the plane, subject to specific boundary condition equations that are dependent on the type of problem (i.e., whether stresses or displacements are specified on the boundary contour).

For anisotropic plates, S. G. Lekhnitskii [3] has shown that equation (1.1) can be generalized as:

$$S_{22}\frac{\partial^4 U}{\partial x^4} - 2S_{26}\frac{\partial^4 U}{\partial x^3 \partial y} + (2S_{12}+S_{66}) - \frac{\partial^4 U}{\partial x^2 \partial y^2} - 2S_{16}\frac{\partial^4 U}{\partial x \partial y^3} + S_{11}\frac{\partial^4 U}{\partial y^4} = 0 \tag{1.4}$$

where the S_{ij}'s are the compliance constants of the material as defined by, for example, Ward [4], with directions 1, 2 and 3 corresponding to linear displacement in the x ,y and z directions, respectively, and 4, 5 and 6 corresponding to rotation around the x, y and z axes, respectively. The solution to equation (1.4) can be expressed [3] as :

$$U(x,y) = F_1(x + s_1 y) + F_2(x + s_2 y) + F_3(x + s_3 y) + F_4(x + s_4 y) \tag{1.5}$$

where $s_1 = \alpha_1 + i\,\beta_1$, $s_2 = \alpha_2 + i\,\beta_2$, $s_3 = s_1^*$, $s_4 = s_2^*$, and the α_j's and β_j's are real constants. (The * signifies the complex conjugate of the starred expression.) The functions F_j are analytic functions of their respective arguments.

Now, since U(x, y) must be real, equation (1.5) can be expressed as:

$$U(x,y) = F_1(z_1) + F_2(z_2) + F_1^*(z_1) + F_2^*(z_2) \tag{1.6}$$

where $z_1 = x + s_1 y$ and $z_2 = x + s_2 y$.

If the following functions are introduced:

$$\varphi(z_1) = \frac{dF_1}{dz_1} \qquad \psi(z_2) = \frac{dF_2}{dz_2} \tag{1.7}$$

the stresses at any point are given [3] by:

$$\sigma_x = 2Re[s_1^2 \frac{d\varphi}{dz_1} + s_2^2 \frac{d\psi}{dz_2}] \tag{1.8a}$$

$$\sigma_y = 2Re[\frac{d\varphi}{dz_1} + \frac{d\psi}{dz_2}] \tag{1.8b}$$

and

$$\tau_{xy} = -2Re[s_1 \frac{d\varphi}{dz_1} + s_2 \frac{d\psi}{dz_2}] \tag{1.8c}$$

The corresponding displacements can be expressed [3] as follows:

$$u(x,y) = 2Re[p_1 \varphi(z_1) + p_2 \psi(z_2)] - \gamma_0 y + \alpha_0 \tag{1.9a}$$

$$v(x,y) = 2Re[q_1 \varphi(z_1) + q_2 \psi(z_2)] + \gamma_0 x + \beta_0 \qquad \textbf{(1.9b)}$$

where p_j and q_j are defined as follows:

$$p_1 = S_{11}s_1^2 + S_{12} - S_{16}s_1 \qquad p_2 = S_{11}s_2^2 + S_{12} - S_{16}s_2 \qquad \textbf{(1.10)}$$

$$q_1 = \frac{S_{12}s_1^2 + S_{22} - S_{26}s_1}{s_1} \qquad q_2 = \frac{S_{12}s_2^2 + S_{22} - S_{26}s_2}{s_2} \qquad \textbf{(1.11)}$$

and constants α_0 , β_0 , and γ_0 are constants of integration. (The additional terms associated with these constants in equations (1.9a) and (1.9b) represent total body displacement, and should be set to zero for equilibrium situations.)

The addition of a hole to the panel complicates the analysis. The development of expressions for the stress distribution in finite composite panels near frictionless pin-loaded holes was performed by T. de Jong [5], based on the analysis methods of Muskhelishvili as applied to anisotropic materials by Lekhnitskii.

The functions ϕ and ψ defined in equations (1.7) take the following forms for a frictionless, pin-loaded hole in a plate of infinite extent [5]:

$$\varphi(z_1) = A_1 \ln \zeta_1 + \varphi^o(z_1) \qquad \psi(z_2) = A_2 \ln \zeta_2 + \psi^o(z_2) \qquad \textbf{(1.12)}$$

In these expressions, ζ_j is defined as:

$$\zeta_j = \frac{z_j + \sqrt{z_j^2 - s_j^2 - 1}}{1 - is_j} \qquad \textbf{(1.13)}$$

and the functions ϕ° and ψ° are analytic everywhere outside the hole.

The physical geometry requires that the pin can only apply a load to approximately one-half the circumference of the hole. If we shift to polar coordinates r and θ, with θ measured from the positive y-axis (which is parallel to the loading direction), a load distribution function which satisfies the load boundary condition ($P = 0$ for $\pi/2 < \theta < 3\pi/2$) is the product of a sine series and a step function, resulting in the following expression [5]:

$$P_r = p_0[\frac{1}{2}\sum_{n=1,3}^{\infty} a_n \cos n\theta + \frac{1}{\pi}[\sum_{m=1,3}^{\infty}\frac{a_n}{n} + \sum_{m,\,n}^{*} a_n(\frac{1}{n-m}+\frac{1}{n+m})\sin m\theta]] \tag{1.14}$$

in which the special summation operator is defined as follows:

$$\sum_{m,\,n}^{*} = \sum_{n=1,3}^{\infty}\cdot\sum_{m=2,4}^{\infty}\cdot\sum_{n=2,4}^{\infty}\cdot\sum_{m=1,3}^{\infty} \tag{1.15}$$

The functions ϕ and ψ are then determined in terms of the series coefficients a_n after the application of the stress boundary conditions. The a_n coefficients, in turn, are determined by application of the displacement boundary condition at the hole edge. The stress distribution around the hole is then determined using Lekhnitskii's method as presented above.

There are several aspects of bolted joints in composite material that complicate theoretical analyses beyond the developments listed above. The first of these is the presence of friction between the bolt and the panel. This phenomenon complicates the analysis because of the existence of regions of slip and non-slip around the

contact area of the pin. Additionally, the coefficient of friction is variable around this arc. Several workers, including de Jong, Oplinger, and Oplinger and Gandhi, have developed mathematical models of the pin-loaded hole including friction. As an indicator of the difficulties associated with such analyses, all of these models (with the exception of de Jong's latest) exclude treatment of the non-slip regions [5].

The addition of frictional effects generally results in a decrease in the tangential and radial stresses near the hole; this beneficial effect is increased as the coefficient of friction is increased [5].

Other complicating factors besides friction include clamp-up force in the bolt; the size of the contact area (e.g. washer area) between the bolt and the laminate; and the amount of clearance between the bolt and the hole and between the bolt and the washer. Although these phenomenon have been investigated empirically (by, for example, Stockdale and Matthews [6] and Herrington and Sabbaghian [7]), the three-dimensional effects caused by variations in these parameters have so far apparently precluded the development of theoretically-based predictive models which account for their effects.

When considering the behavior of countersunk bolted joints in composite laminates, the three-dimensional nature of the clampup force must also be considered, as well as the non-prismatic nature of the bolt hole. In the same manner as for the parameters described above, no theoretical analyses of elastic (let alone viscoelastic) behavior seems to have been performed, because of the complicated geometry. Thus, at the present, analyses of the countersunk bolted joint in composite laminates must be

performed numerically.

Finite Element Modelling of Bolted Joint Mechanical Behavior

Depending on the nature of the phenomenon under study (e.g., bolt-bearing behavior, clampup force relaxation, etc.), the finite-element modelling technique can be applied to the mechanical analysis of bolted joints in composite materials. Typically, bolt-bearing behavior models have been two-dimensional in nature, because of the high cost of three-dimensional models [5].

Shivakumar and Crews [2] have performed a finite element analysis of viscoelastic clampup force relaxation in conventional protruding-head bolted joints in carbon fiber/epoxy composites, using the viscoelastic finite-element code VISCEL. They modelled a plane section through the joint, perpendicular to the bolt axis, using two-dimensional membrane elements. Because of the uni-directional, through the thickness nature of the clampup force load in a protruding-head bolt joint, they were able to treat the entire laminate as viscoelastic. This finite-element analysis correlated rather well with experimentally determined clampup force relaxation behavior.

Any finite-element model of a countersunk bolt joint would require the use of three-dimensional model elements which allow the inclusion of anisotropic viscoelastic properties. The development of such elements would be a formidable task; there are apparently no commercially-available finite-element codes which allow the use of such elements.

Empirically-Derived Relaxation Predictive Equation

Based on experimental data and the finite-element analysis described above, Shivakumar and Crews have developed a simple equation which predicts the clampup force relaxation in a carbon fiber/epoxy laminate bolted with standard protruding-head bolts [2]. This non-dimensional equation is expressed as follows:

$$\frac{F_t}{F_0} = \frac{1}{1 + F_1(\frac{t}{a_{TH}})^n} \tag{1.16}$$

where F_t is the clampup force at time t, F_0 is the clampup force at time 0, F_1 is a constant, n is the viscoelastic power law constant for the laminate, and a_{TH} is a hygrothermal shift factor defined by, for example, Schapery [2], which accounts for variations in temperature or humidity.

Related Work

My experimental approach to the relaxation problem was inspired by the work of Kunigal N. Shivakumar and John H. Crews, who performed empirical and finite-element studies as described above. The idea of using load-sensing bolts to measure clampup force was theirs; I adopted this technique and applied it to bevel-head bolt joints in glass-reinforced vinylester resin.

Other work upon which my research rests includes that of J. H. Stockdale and F. L. Matthews [6], who performed experimental studies that documented the effect of

bolt clampup force and washer fit on the protruding-head bolt-bearing strength of GRP.

Finally, I must give credit to F. L. Matthews for another endeavor. He served as the editor of a very informative collection of information on joints in composites, the book Joining Fibre-Reinforced Plastics. He also contributed an excellent chapter [5] on theoretically-based analyses of mechanically-fastened joints. In this same volume, L. J. Hart-Smith contributed a chapter [1], complementary to Matthews', on the empirical analysis and design of mechanically-fastened joints. Both of these chapters were very helpful during the development of my research program.

Chapter Two
Experimental Procedure

2.1 Experimental Materials

Overview

The materials used in each of the two types of experiment performed (clampup force relaxation and bearing strength) were selected based on several criteria. The first was the stipulation that the experimental set-ups must model, to the extent practicable, composite materials and composite-to-steel joint designs proposed for U.S. Navy shipboard use. These proposed materials and joint designs were suggested by my research sponsor, the Carderock Division of the Naval Surface Warfare Center (Code 66, Surface Ship Structures). Other materials selection criteria included easy availability and low cost for steel panels and fastener components. Finally, special instrumented bolts were selected for their demonstrated precision in the measurement of bolt stresses.

Description of Materials

The composite laminate panels used in the experiments consisted of E-glass reinforcement in a vinylester resin matrix, and were manufactured by the Seeman Composite Company of Gulfport, Mississippi. Each glass ply consisted of Owens-Corning 24-weight woven roving in a balanced weave, with the filling oriented perpendicularly to the warp. The lay-up sequence consisted of alternating 0° , +45°,

-45°, and 90° (warp orientation) layers, to a nominal thickness of 0.5 inches requiring 20 plies. The final sequence was thus $[(0/\pm45/90)_5]_T$, resulting in a "quasi-isotropic" laminate. The resin used was Dow Derakane 510A vinylester resin.

The laminate was formed by the Vacuum-Assisted Resin-Transfer Molding (VA/RTM) process. In this process, the glass plies are laid up dry in a mold. The resin is pumped into the mold until the plies are totally saturated and all air has been forced from the mold. The mold is then placed in a bag. A partial vacuum is applied to the inside of the bag, and the resin is allowed to cure at room temperature. The resulting laminate generally has a void content of less than 2%. Table 2-1 lists the mechanical properties of this material , as provided by the manufacturer.

Table 2-1. Mechanical Properties of Vinlyester/Glass Laminate (i = 1,2)

E_i , tension	4.07×10^6 psi
E_i , compression	4.01×10^6 psi
E_i , flexural	3.605×10^6 psi
Ultimate Tensile Strength	62.8×10^3 psi
Ultimate Compressive Strength	65.7×10^3 psi
Ultimate Flexural Strength	85×10^3 psi
Poisson's Ratio (υ_i)	0.27
In-Plane Shear Strength	18.41×10^3 psi
In-Plane Shear Modulus	6.20×10^6 psi
Short Beam Shear Strength	6.715×10^3 psi
Specific Gravity	1.968

The GRP material was supplied as two square panels, 24 inches by 24 inches each.

For the clampup-force relaxation experiments, ten 6-inch by 6-inch (nominal) specimens were cut from the GRP laminate panels supplied by the manufacturer. A nominal 0.625-inch hole was drilled in the exact center of each of these specimens. Each hole was then countersunk to a nominal depth of 0.292 inches, using a six-fluted, carbide, 5/8-inch pilot, 82° countersink drill. (The actual depth was set by drilling a pilot hole, and noting the depth at which a standard, countersunk 5/8 -inch bolt head was flush with the surface.) For the bearing strength experiments, twenty 3-inch by 12-inch (nominal) specimens were cut from the supplied panels. A nominal 0.625-inch hole, countersunk as described above, was drilled in each of these specimens. The center of each of these holes was nominally four inches from one of the short edges of the specimen, and centered with respect to the long edges of the specimen.

The steel panels used in the experiments were of AISI Type 1018 cold-rolled steel, 0.375 inches thick. The panels used in the relaxation experiments and in four of the bearing strength experiments were supplied (by Matt McDonald Special Steels of Boston, Massachusetts) in long strips of either 3-inch or 6-inch width, and were cut and drilled to the same dimensions as the corresponding composite specimens, except that none of the holes in the steel were countersunk. Additionally, a nominal 0.5-inch hole was drilled in each bearing test steel specimen, 1.75 inches from the end opposite the 0.625 inch hole. Ten steel panels were prepared for the relaxation experiments; four panels were prepared for the bearing-strength experiments.

After the conduct of the first four bearing strength experiments, it became

apparent that the bearing strength tests caused permanent distortion of the bolt hole in the steel panels. It was then necessary to obtain sixteen additional panels, identical to the initial four. These were prepared by the Grant Steel Company of Holbrook, Massachusetts, including the cutting and drilling. (Grant Steel was selected due to their overall lower price for the complete panel, including cutting to size and drilling.)

Two additional steel panels were prepared for the bearing strength experiments, as spacers to prevent bending. These were prepared from 0.375-inch Type 1018 cold rolled steel, and were each 3.5-inches by 3.0-inches, drilled with a 0.50-inch hole in the exact center. To pin these panels to the steel half of the joints, a 36-inch long section of 0.50-inch steel drill rod was obtained, and cut to 1-inch lengths for use in the experiments.

The ten bolts used in the relaxation experiments were specially instrumented load-sensing bolts, prepared by the Strainsert Company of West Conshohocken, Pennsylvania. These bolts were standard 5/8 - 11UNC x 2¾ hex-head cap screws, SAE Grade 8, modified by the insertion of a full-bridge resistance-type strain gage circuit (350 Ohms nominal resistance) into a small hole drilled through the head of the bolt along its axis. These bolts were calibrated at the factory, in both load directions, up to a load of 22,000 pounds.

In order to simulate countersunk bolt heads in the relaxation experiments, special washers in the shape of a cone frustrum were machined, using steel rod stock. Each washer was 0.285 inches thick; the large diameter was 1.125 inches, and the small diameter was 0.630 inches. A 0.630-inch hole was bored along the axis of the

frustrum. These dimensions were selected to match the head dimensions of a standard flathead, countersunk 5/8-inch bolt as closely as possible; additionally, these dimensions ensured that the washers would fit over any standard 5/8 inch bolt. Figure 2-1 is a drawing of one of these washers.

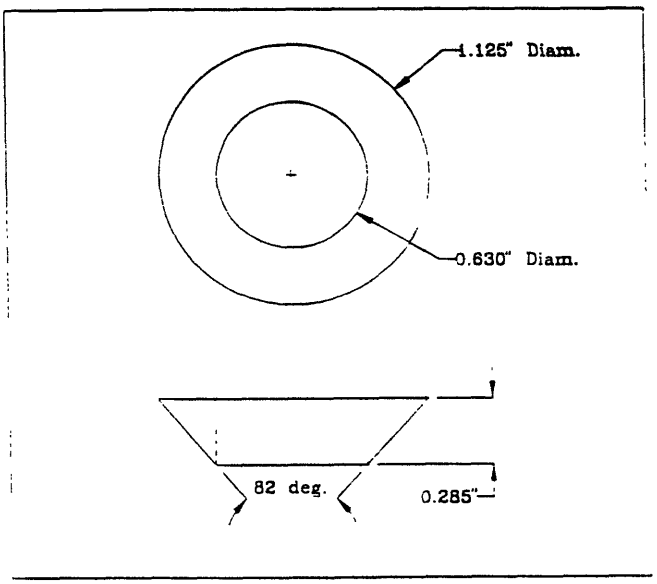

Figure 2-1. Conical Washer

Two types of bolts were used in the bearing strength experiments: standard 5/8 - 11UNC x 2 hexagon-socket flat countersunk head cap screws, alloy steel (minimum yield strength 120,000 psi, equivalent to SAE Grade 8); and standard hex-head cap screws, 5/8 - 11UNC x 2-3/4, SAE Grade 8. Flat washers used in both types of experiment were standard Type A Plain 5/8 W washers, SAE Grade 8. Nuts used in both types of experiment were standard 5/8 - 11UNC hex nuts, SAE Grade 8. All of these items except the hex-head cap screws were obtained from the McMaster-Carr Company of New Brunswick, New Jersey; the hex-head cap screws were obtained

from the Allied Bolt and Screw Company of Boston, Massachusetts.

2.2 Experimental Set-Ups

Relaxation Experimental Set-Up

The purpose of the relaxation experiments was to measure the clampup force relaxation in a countersunk bolted joint, in which a composite laminate was bolted to a steel panel. In order to measure the force in the bolts, specially instrumented bolts as described above were used. To facilitate testing with only one metering system, a pair of terminal boards was constructed, each capable of holding enough terminals for five bolts. Each board consisted of a nominally 7-inch by 7-inch, 1/4-inch thick Masonite panel, drilled to accept twenty binding-post type banana jacks. The jacks were arranged in five rows of four; each row of four contained two jacks for the gage excitation voltage and two for the gage signal voltage. Each terminal pair was spaced at 3/4 inches, to permit the use of a standard double banana plug. The four leads from each bolt were soldered in turn to the jacks in a single row. The finished boards allowed the quick change of electrical connections.

To provide a stable excitation voltage, and to amplify the relatively weak bridge signal, an Amot Controls Model 8351/B2111 pressure transducer amplifier was used. This device combines a power supply and signal amplifier in a very compact package. The power source was a pair of Yuasa 12-volt rechargeable batteries wired in series, producing a nominal voltage of 24 volts DC. The amplifier converted this

voltage to 10.00 volts DC, which was used to excite the bridge. The returning signal was amplified with a gain of 250, and measured with a Fluke model 77 multimeter. Figure 2-2 is a notional diagram of the testing circuit.

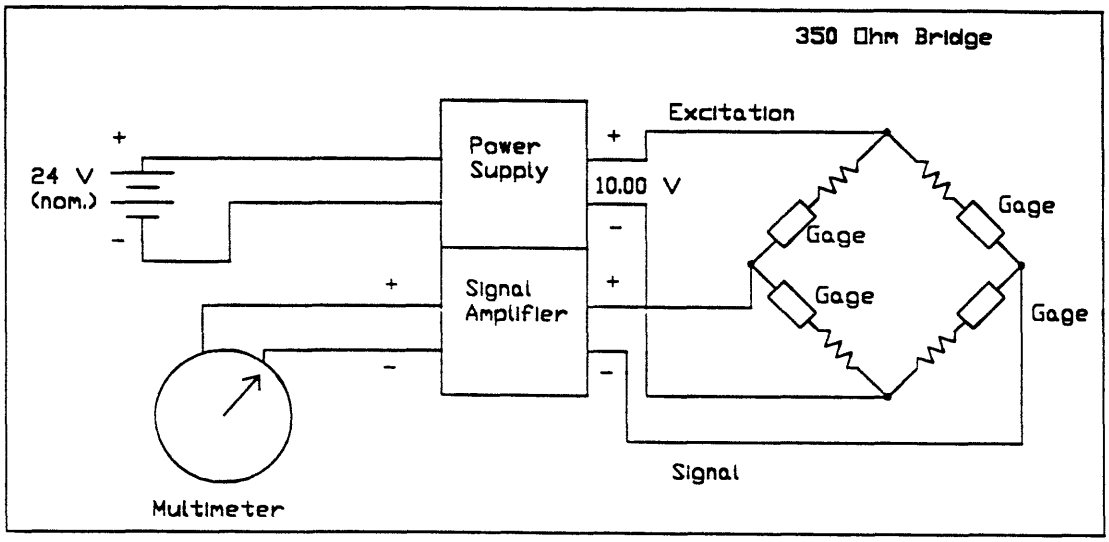

Figure 2-2. Relaxation Experiment Notional Strain Gage Circuit Diagram

In each experiment, a nominally 0.5-inch thick, 6-inch by 6-inch composite laminate specimen was bolted to a nominally 0.375-inch thick, 6-inch by 6-inch steel panel. The thicknesses were chosen based on proposed shipboard panel thickness; the length and width were made sufficiently long to avoid edge effects in the vicinity of the bolt-hole. Shivakumar and Crews have shown that stresses in composite laminates due to bolt clampup loads become negligible approximately three hole diameters away from the hole [2]. This would require an edge length of 3.75 inches for a 5/8 inch hole. Because Shivakumar and Crews studied carbon-fiber reinforced laminates bolted

with standard hex-head bolts, while the present study concerns glass-reinforced laminates bolted with countersunk bolts, the edge length was set at 6 inches for conservatism.

After alignment of the laminate and steel panels, the ten instrumented bolts were assembled with one conical washer each, such that the large diameter of the washer was flush with the underside of the head of the bolt. The bolts were inserted in the boltholes, starting at the countersunk side of the laminate, and continuing through the steel panel until the conical washers were snug in the countersunk holes. In order to prevent bottoming of the nuts at the end of the threads, five of the flat washers were placed over the protruding end of each bolt. The threads were lubricated using LPS® Force 842°™ dry moly lubricant, in an effort to improve the correlation between bolt force and torque as recommended by, for example, Shigley and Mitchell [8]. Finally, a hex nut was threaded onto the bolt, and made up finger-tight.

At this point, there were ten identical bolted joint samples, each as illustrated in Figure 2-3 . These were divided into two groups of five. The first group was torqued to 60 ft-lbs; the second was torqued to 35 ft-lbs.

The initial tensile force in each bolt was measured, as well as the time of the measurement. Because the bolts were calibrated at 70°F, the samples were left in the ambient air (i.e., no temperature control was used). The ambient temperature was recorded during each round of measurements. Clampup force measurements were taken once every eight hours after the initial assembly of the joints, for six days.

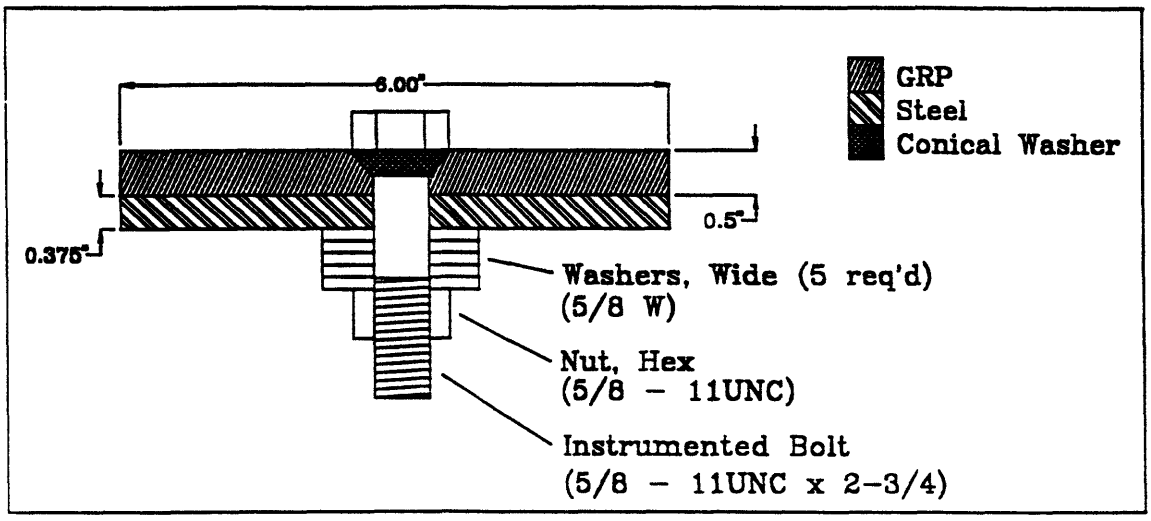

Figure 2-3. Relaxation Experiments Joint Specimen Configuration

Bearing Strength Experimental Set-Up

The purpose of the bearing strength experiments was to determine the effect of clampup-force relaxation on the bolt-bearing strength of the composite laminate, when bolted with countersunk bolts. Because of the head configuration of these bolts, a single-lap joint is the most likely joint design; thus, single-lap joints were tested. Since bearing strength tests generally destroy bolts, and clampup force is difficult to measure directly without expensive instrumented bolts, bolt torque was used as the measure of clampup force in these experiments. Thus, torque was varied as the independent variable, and bearing strength was measured as the dependent variable.

In order to measure the bearing strength, an MTS 100,000 pound capacity testing machine with hydraulic grips was used. The hydraulic grips, which were 3.5 inches wide, were set to grip the specimens at a pressure of 1000 psi . The load range

was limited to 50,000 lbs, and the extension rate was set at a constant 950 seconds per half-inch of displacement. A plot of load versus displacement was generated by a graphic plotter.

Single-lap joint specimens were prepared by overlapping one twelve-inch long steel panel with one twelve-inch long composite laminate panel, and bolting the composite to the steel using one of the countersunk, flathead bolts. A single flat washer was placed over the protruding end, and the threads were lubricated with the dry moly lubricant. A nut was then threaded on and made up finger-tight. Sixteen such specimens, all identical, were prepared; the configuration of each was as illustrated in Figure 2-4.

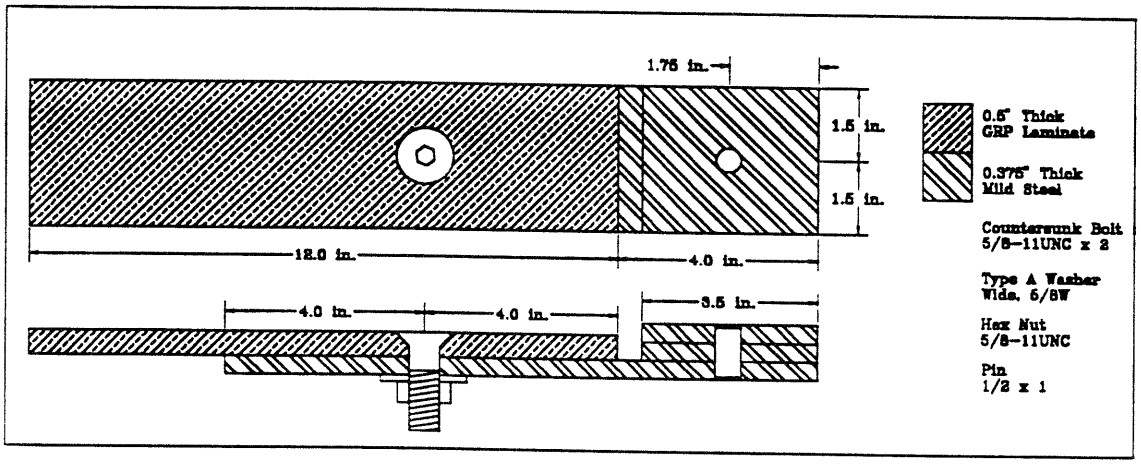

Figure 2-4. Bearing Strength Experiments Joint Specimen Configuration

The twelve specimens were divided randomly into four groups of four each. The first group was to be torqued to 50 ft-lb, the second to 33 ft-lb, the third to 17 ft-lb, and the last group to 0 ft-lb. (The last group was tightened finger tight, using a wrench to hold the bolt stationary.) The actual torquing of the bolts was performed just prior to each test, such that no stress relaxation would occur in the joint prior to the test.

In order to establish a baseline against which the performance of countersunk bolts could be measured, four single-lap joints with standard hex-head bolts were assembled. These were similar to the countersunk bolt joints, except that a washer was placed under the head of each hex-head bolt, and two washers were used under the nut to prevent bottoming out of the threads. One of these joints was torqued to 50 ft-lbs, one to 33 ft-lbs, one to 17 ft-lbs, and one to 0 ft-lbs (finger-tight). Table 2-2 shows the number of specimens receiving each type of treatment.

Table 2-2. Bearing Strength Tests Treatment Matrix

Number of Joint Specimens Receiving Each Type of Treatment		**Bolt Head Type**	
		Countersunk	**Hex-Head**
Torque	**0 ft-lbs**	4	1
	17 ft-lbs	4	1
	33 ft-lbs	4	1
	50 ft-lbs	4	1

To eliminate bending to the maximum extent practical, the end of each steel panel away from the joint was pinned to the two 3.0 x 3.5 inch steel panels, resulting in a thickness of 0.75 inches. The effect of this was to better align the centers of the ends of the joint specimens, so that when the specimens were placed in the testing machine, the closing of the grips on the specimen ends did not cause excessive specimen bending. Figure 2-5 illustrates this bending effect, and how the building up of the steel panel virtually eliminates it.

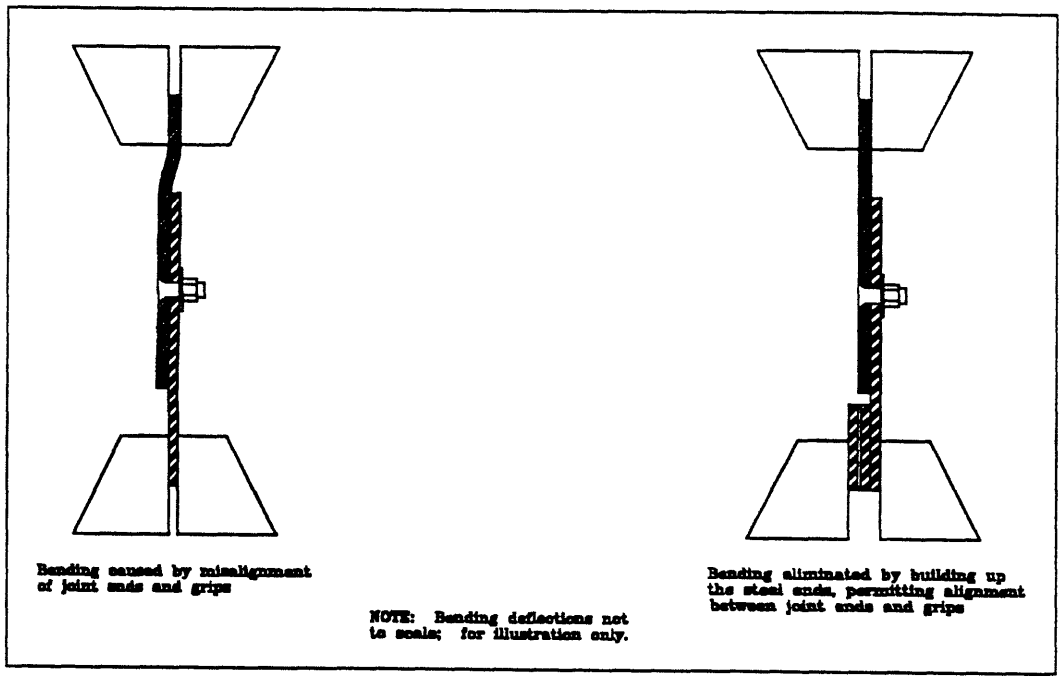

Figure 2-5. Testing Configuration to Minimize Initial Bending

At the start of each test, a joint specimen was placed between the grips on the testing machine. The sample axis was aligned as best as possible with the load axis of

the machine, and the grips were closed on the specimen. The joint specimen was then loaded in tension, and the load was increased until bearing failure of the composite. The load at which failure occurred was recorded, as well as a graph of load versus displacement. This was repeated until all twenty joint specimens had been tested.

Chapter Three
Experimental Results and Discussion

3.1 Results of the Relaxation Experiments

The data collected in the relaxation experiments consisted of output voltages from the instrumented bolt strain gage circuits, measured at nominal 8-hour intervals after the initial torquing of the ten specimen joints. These voltages were converted to bolt clampup force by the following equation:

$$F = \frac{V_O}{GV_E} C \tag{3.1}$$

where: F is bolt clampup force (pounds);

V_O is measured output voltage (volts) from the signal amplifier;

G is the signal amplifier gain (volts per millivolt);

V_E is the bridge excitation voltage (volts); and

C is the slope of the strain gage calibration curve (pounds per millivolt per volt).

Individual strain gage calibration data, for each bolt at an ambient temperature of 70°F, were provided by the manufacturer of the instrumented bolts. These data are provided in Appendix A.

The measured output voltages and corresponding clampup forces, as well as force relaxation graphs for each specimen, are provided in Appendix B. Figure 3-1 is a relaxation curve based on specimens R-1 through R-5, each of which was torqued to

an initial torque of 60 ft-lbs. Figure 3-2 is a relaxation curve for specimen R-6, which is representative of the behavior of specimens R-6 through R-9, each of which was torqued to an initial torque of 35 ft-lbs. Finally, Figure 3-3 is a plot of the relaxation behavior of specimen R-10, which was torqued to an initial torque of 35 ft-lbs. This curve is provided separately because of the significantly different behavior of specimen R-10 when compared to the other specimens.

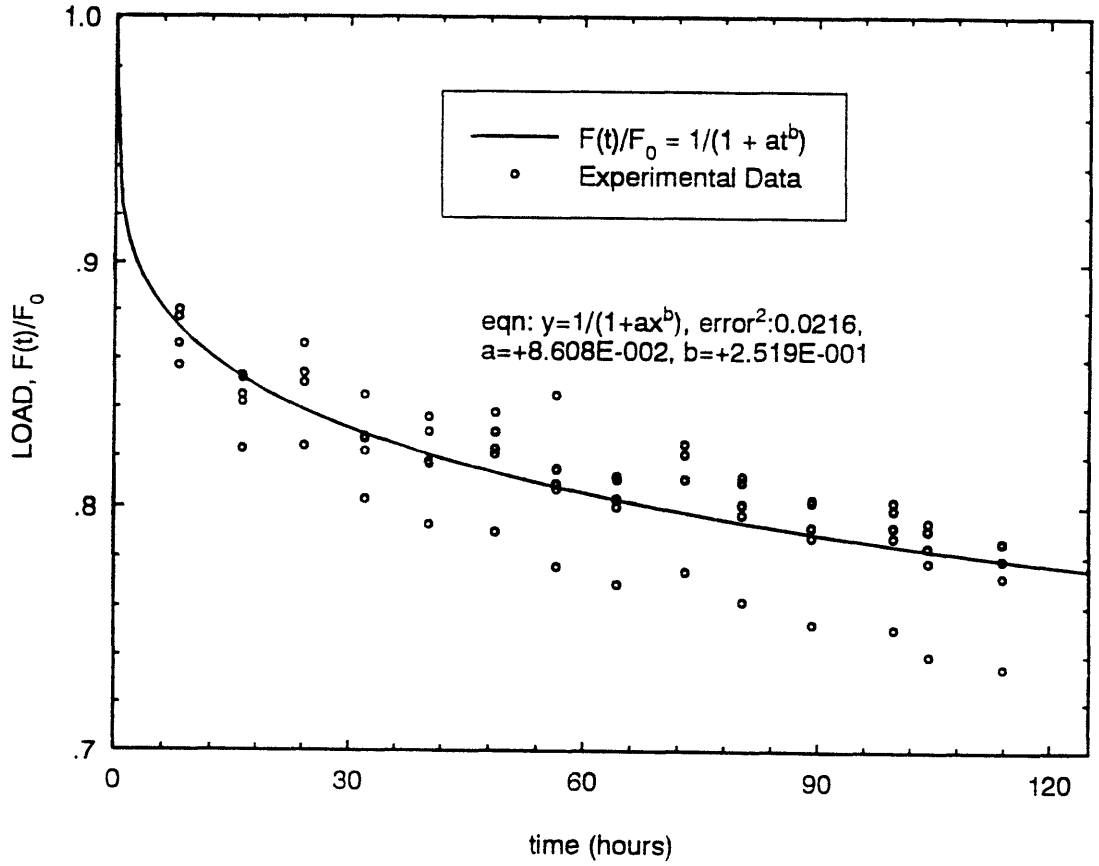

Figure 3-1. Relaxation Behavior, Specimens with 60 ft-lbs Initial Torque

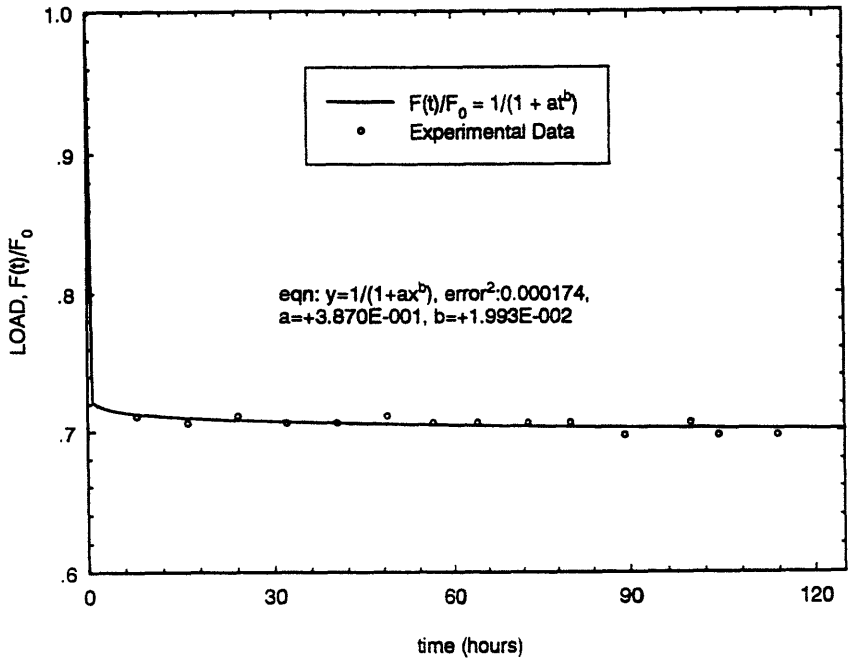

Figure 3-2. Sample R-6 Relaxation Behavior (35 ft-lbs Initial Torque Specimen)

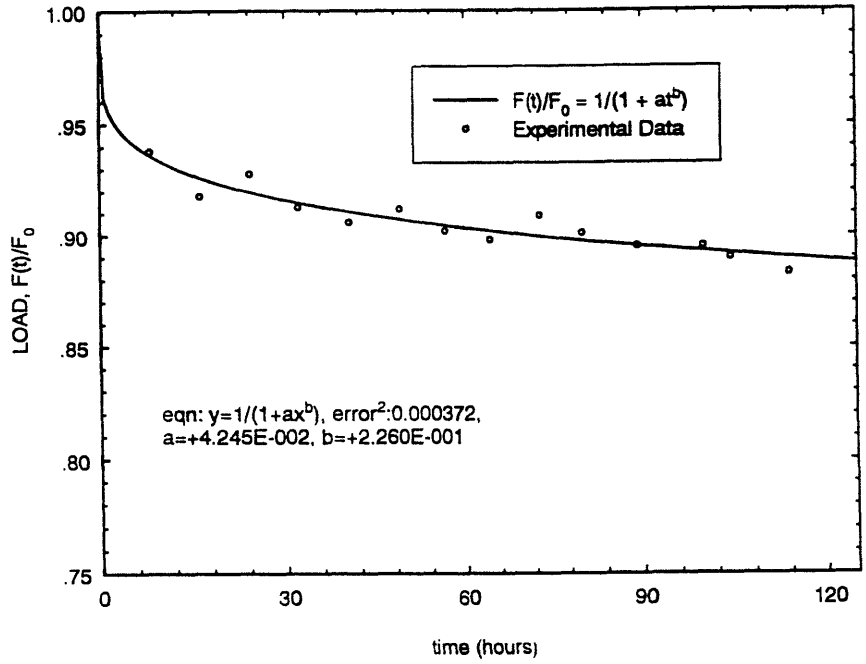

Figure 3-3. Relaxation Behavior of Specimen R-10

3.2 Results of the Bearing Strength Experiments

The data collected in the bearing strength experiments consisted of load-displacement curves generated by the testing machine (contained in Appendix C), videotapes of each test, and the failed physical specimens themselves. The load-displacement curves describe the behavior of the overall specimen/testing machine combination, and as such do not precisely describe the mechanical behavior of the GRP laminate. Nevertheless, these curves are useful indicators of the progression of events from initial load to failure, and were used to determine the onset of bearing failure in the samples. Table 3-1 summarizes the failure loads and maximum loads (where applicable) reached in each bearing strength experiment.

Table 3-1. Bearing Strength Experimental Results

Sample Number	Bolt Type	Torque (ft-lb)	Failure Load (lb)	Max. Load (lb) (Note 1)	Bearing Strength (psi)	Average Fail Load (lb)	Average Bearing Str. (psi)
BS-2	Flathead	50	19,400	N/A	68,613	19,594	69,199
BS-3	Flathead	50	18,550	N/A	64,900		
BS-4	Flathead	50	20,450	N/A	72,170		
BS-5	Flathead	50	19,975	N/A	71,112		

BS-7	Flathead	33	18,400	N/A	63,619	19,350	68,037
BS-8	Flathead	33	19,750	N/A	69,098		
BS-9	Flathead	33	19,875	19,875	69,006		
BS-10	Flathead	33	19,750	19,750	70,425		
BS-12	Flathead	17	19,075	19,075	67,317	18,694	65,632
BS-13	Flathead	17	18,350	19,800	64,759		
BS-14	Flathead	17	17,000	19,500	59,253		
BS-15	Flathead	17	20,350	20,350	71,198		
BS-17	Flathead	0	17,500	18,700	63,004	17,481	62,041
BS-18	Flathead	0	17,350	19,100	61,638		
BS-19	Flathead	0	15,825	19,250	55,730		
BS-20	Flathead	0	19,250	19,625	67,791		
BS-1	Hexhead	50	24,250	N/A	84,934	N/A (due to variable torque)	N/A (due to variable torque)
BS-6	Hexhead	33	23,125	N/A	81,795		
BS-11	Hexhead	17	22,100	N/A	78,988		
BS-16	Hexhead	0	22,075	N/A	77,191		

(1) Maximum loads are only provided for those samples which were allowed to fail catastrophically subsequent to bearing failure.

An Analysis of Variance (ANOVA) table listing the results of an analysis of the effect of torque on bearing strength is presented as Table 3-2.

Table 3-2. ANOVA Table for Torque Effect on Bearing Strength					
Variance Source	**Sum of Squares**	**Degrees of Freedom**	**Mean Square**	**F ratio**	**Probability**
Torque	119,945,639	3	39,981,880	2.31	0.1283
Error	207,851,506	12	17,320,959		
Total	327,797,145	15			

In order to conclude from Table 3-2 that bolt torque has any effect on bolt bearing strength in countersunk bolt joints of the type tested, the F-ratio from the data must exceed $F(\alpha; k-1; N-k) = F(\alpha; 3; 12)$. At a reasonable tail probability (α) of 0.5, however, $F(0.05; 3; 12) = 3.49$ [9]. Thus, the data do not support the conclusion that torque has any effect on bearing strength.

Examination of the data, however, suggests that there is probably a positive correlation between torque and bearing strength . (Verification of this hypothesis would require that the experiments be repeated withn a sample size of at least 45.) A graph of the bearing strength data is provided as Figure 3-4.

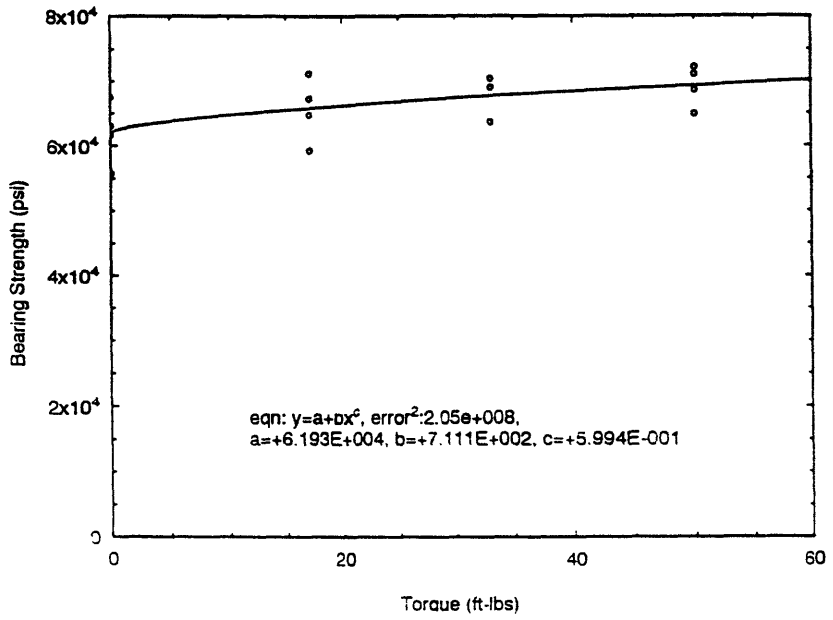

Figure 3-4. Bearing Strength of Countersunk Bolt Joints, GRP/Steel

3.3 Discussion of Relaxation Experiment Results

Correlation of Initial Torque with Initial Clampup Force

Specimen Variation

The first observation that can be made concerning the relaxation behavior data is that there is much variation in the observed initial clampup force produced by identical levels of initial torque in countersunk, bolted joints between vinylester/glass laminates and steel (henceforth termed "subject joints"). This is illustrated in Table 3-3.

Table 3-3. Initial Clampup Force in Relaxation Experiments		
Specimen	**Initial Torque (ft-lbs)**	**Initial Clampup Force (lbs)**
R-1	60	1474
R-2	60	925
R-3	60	1257
R-4	60	2028
R-5	60	1316
R-6	35	343
R-7	35	369
R-8	35	244
R-9	35	400
R-10	35	2016

Table 3-3 shows a general positive correlation between initial torque and initial clampup force, but the variation in clampup force at each torque level is very large. At 60 ft-lbs of torque, the clampup force ranges from 925 lbs to 2028 lbs, or by a factor of 2.19. At 35 ft-lbs of torque the variation is even more extreme, with clampup force ranging from 244 lbs to 2016 lbs, a factor of 8.26.

Shigley and Mitchell [8] suggest the following equation for correlation of torque and clampup force in protruding-head bolted joints in metal:

$$T = k_T F d \tag{3.2}$$

where: T is torque;

F is clampup force;

d is the bolt diameter; and

$$k_T = \frac{d_m}{2d} \cdot \frac{\tan\lambda + \mu\sec\alpha}{1 - \mu\tan\lambda\sec\alpha} + 0.625\mu_c \qquad (3.3)$$

where : μ is the coefficient of sliding friction between the nut and the bolt;

μ_c is the coefficient of sliding friction between the nut and the washer;

α, λ, d, and d_m are bolt thread geometrical parameters as defined in Figure 3-5.

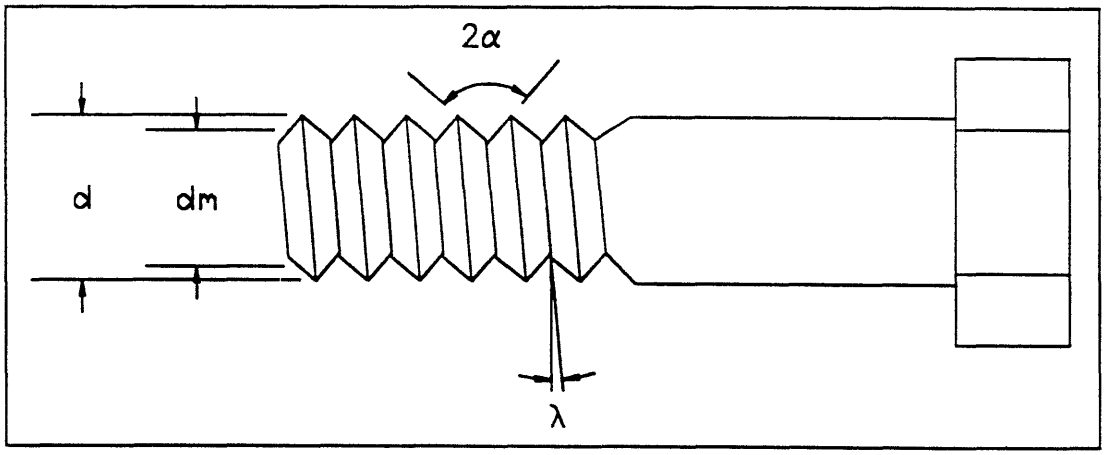

Figure 3-5. Bolt Thread Geometrical Parameters

There are many joint parameters that influence the correlation between torque and clampup force, as illustrated by the relative complexity of equation (3.3). A change in geometry from protruding-head bolt to countersunk bolt requires the consideration of additional parameters (e.g., the coefficient of friction between the

inclined portion of the bolt head and the panel, and the precision of the fit between the bolt head and the countersunk hole). If one or both of the panels being bolted are anisotropic, heterogeneous, and viscoelastic (e.g., GRP), there are yet more issues to consider. Finally, the normal dimensional variation in the bolt and the hole will have an effect on clampup force.

It is well-known that lubrication of the threads prior to joint assembly improves the torque-clampup force correlation by making the nut-bolt friction coefficients more uniform [8]. For this reason, all bolt threads in the relaxation and bearing strength experiments were lubricated. However, as illustrated in Table 3-3, there was still a wide variation in clampup force in countersunk bolt joints in GRP/steel, for a given amount of initial torque. The possible reasons for an individual observation of low clampup force for a given torque level include the following:

a. Relative poor mating of the nut threads to the bolt threads. In a joint with this phenomenon, a relatively large fraction of the total torque is used merely to rotate the nut ("running torque"); this torque is then unavailable for elastically lengthening the bolt and producing clampup force.

b. Relatively poor fit between the bolt head and the countersunk hole. Ideally, the clampup load is carried uniformly by the entire area of the countersunk hole. If the bolt head fit is poor, this load will be carried by local "high spots" on the hole surface, producing locally high stresses and local deformation. This deformation will allow the bolt to shorten under the clampup load, and thus

relax the load.

c. Location of the bolt hole at a locally "soft" area of the GRP panel. Because of the nature of GRP, there are always areas in the panel where imperfections (low fiber density, voids, inclusions, etc.) reduce the through-thickness stiffness of the panel. If the material near the bolt hole edges contain such imperfections, there will be more deflection of the GRP under the clampup load, which will permit bolt shortening and load relaxation.

d. A relatively large diameter of the non-countersunk portion of the bolt hole, relative to the bolt major diameter, d. Empty space between the bolt and bolt hole allows flow of the panel material towards the bolt, and thus more local panel deformation than in a joint in which the bolt fits snugly in the hole. This additional deformation allows bolt shortening and load relaxation.

Similarly, if the above conditions are favorable, the initial clampup force produced by a certain level of torque would be increased.

Variation Due to Measurement Technique

The final sources of clampup force variation were the inevitable measurement errors. Each relaxation experiment relied on a Wheatstone bridge circuit containing four strain gages and at least four resistors, a combination power supply/signal amplifier, and a digital multimeter. Due to the generally high reliability of electrical components, outright malfunctions would have been easy to detect.

The most likely sources of measurement error in the present study were non-

linearities in the signal amplifier, which would increase as the input signal approaches zero. Because the bridge circuits had very low impedances and the clampup force in the subject joints remained relatively low even with 60 foot-pounds of torque (compared with, say, steel), the output signals from the bridge circuits never exceeded four millivolts. This is at the low end of the linear range of the amplifier, which was designed for an input voltage range of 4 to 20 millivolts.

Another source of measurement errors was the relatively low signal-to-noise ratio associated with such a small signal.

Other error was associated with temperature fluctuations; it was noted that the voltages recorded in the afternoon frequently exceeded the readings from the same morning. This is believed to have been caused by resistance changes in the strain gages, as the ambient temperature rose over the course of the day.

These measurement errors would not, of course, result in an eightfold increase of measured voltage; additionally, the data were relatively well-behaved, with the readings decreasing in an orderly and predictable fashion. Thus, it is concluded that variation in the specimens themselves was the major source of clampup force variation at a certain torque level, and that the correlation between torque and clampup force in the subject joints is widely variable even for nominally identical specimens. In fact, an analysis of variance does not support the conclusion that clampup force is a function of torque ($F_{experimental} = 3.61 < F(0.05; 1; 8) = 5.32$ [9]).

Clampup Force Relaxation Behavior

Examination of the clampup force relaxation data for all ten specimens indicates that relaxation in countersunk bolted joints between vinylester/glass GRP laminates and steel can be described by an equation of the form proposed by Shivakumar and Crews [2] for describing relaxation in conventional bolt joints in carbon/epoxy laminates, namely:

$$\frac{F(t)}{F_0} = \frac{1}{1 + F_1(\frac{t}{a_{TH}})^n} \tag{3.4}$$

where the terms are defined as in Chapter One. If temperature and humidity are not varied, as in the present study, equation (2) can be simplified to:

$$\frac{F(t)}{F_0} = \frac{1}{1 + kt^n} \tag{3.5}$$

where the constant k is defined as:

$$k = \frac{F_1}{a_{TH}^n} \tag{3.6}$$

Equation (3.5) relaxation constants for each specimen, as well as overall relaxation constants based on specimens R-1 through R-5, are listed in Table 3-4.

Table 3-4. Experimentally-Determined Relaxation Equation Constants		
Specimen/Initial Torque	**n (dimensionless)**	**k (hours^{-n})**
R-1 / 60 ft-lbs	0.2450	0.08663
R-2 / 60 ft-lbs	0.2733	0.07059
R-3 / 60 ft-lbs	0.2580	0.08355
R-4 / 60 ft-lbs	0.2314	0.08718
R-5 / 60 ft-lbs	0.2816	0.09200
R-6 / 35 ft-lbs	0.01993	0.3870
R-7 / 35 ft-lbs	0.01409	0.4767
R-8 / 35 ft-lbs	0.1441	0.01261
R-9 / 35 ft-lbs	0.04683	0.5479
R-10 / 35 ft-lbs	0.2260	0.04245
Overall (R-1 thru R-5)	0.2519	0.08608

Differences in Relaxation Behavior Among the Specimens

Table 3-4 and the relaxation graphs in Appendix B reveal a marked difference in relaxation behavior between the joints with 60 ft-lbs of initial torque, and joints R-6 through R-9 with 35 ft-lbs of initial torque. The reason for this difference is the variation in initial clampup force among the ten specimens.

Specimens R-1 through R-5 were each torqued to 60 ft-lbs at the start of the experiment. As discussed earlier, the observed clampup forces varied widely, but the force in each of these five specimens was at least 925 lbs. Specimen R-10, while only torqued to 35 ft-lbs, nevertheless reached an initial clampup force of 2016 lbs. In all six of these specimens, the initial clampup force was high enough to preclude

relaxation to a level insufficient to cause further relaxation (designated as "effective zero") during the duration of the experiments (six days).

Specimens R-6 through R-9 were each torqued to 35 ft-lbs. Each of these specimens reached relatively low levels of initial clampup force; the highest was R-9 at 400 lbs. Shivakumar and Crews [2] describe an initial clampup force relaxation effect due to joint settlement, etc., that is observed even in metal-to-metal joints. It is the opinion of the author that the majority of the clampup force relaxation observed in specimens R-6 through R-9, almost all of which occurred in the first eight hours of the experiment, was due to this initial settling effect.

The limiting value of clampup force reached in these specimens, approximately 240 lbs, corresponds to a output voltage reading of approximately 0.100 volts. Disassembly of specimens R-6, R-7, and R-9 indicated that there is a residual output voltage of approximately 0.096 volts (0.0384 mV/V bridge output) remaining after complete unloading of the bolt. The output voltage associated with the limiting value of clampup force is only 4 millivolts above the residual voltage; this represents a bridge output signal of 0.0016 mv/V, which is comparable to the noise level in the system.

The differences in clampup relaxation between samples R-6 through R-9 and the remaining specimens are thus explainable by the low initial clampup force in the four indicated specimens, which quickly relaxed to an effective zero value, beyond which no relaxation occurred.

Subject Joint Relaxation Behavior Compared With Hex-Head, Carbon/Epoxy Results

Table 3-5 compares the relaxation behavior of the subject joints with the relaxation behavior of protruding head bolt double-lap joints in carbon fiber/epoxy laminates, as reported by Shivakumar and Crews [2].

Table 3-5. Relaxation Behavior in Bolted Joints

Time (hours)	Clampup Force, Countersunk Bolt, Glass/Vinylester ($F(t)/F_0$)	Clampup Force, Protruding-Head Bolt, Carbon/Epoxy ($F(t)/F_0$)
0	1.00	1.00
10	0.87	0.93
100	0.78	0.86

The data indicate that clampup force in the protruding-head bolt joints in carbon/epoxy relax more slowly than the subject joints. This difference is explainable by:

a. Material Properties; and

b. Joint Configuration.

Differences in the mechanical properties of the two types of laminates compared in Table 3-5 undoubtedly account for a portion of the relaxation behavior differences. However, without viscoelastic property data for the vinylester/glass panels

used in the present experiments, this effect cannot be quantified.

The difference in joint configuration is likely the major reason for the observed relaxation behavior difference. Figure 3-6 illustrates the two types of joint configuration.

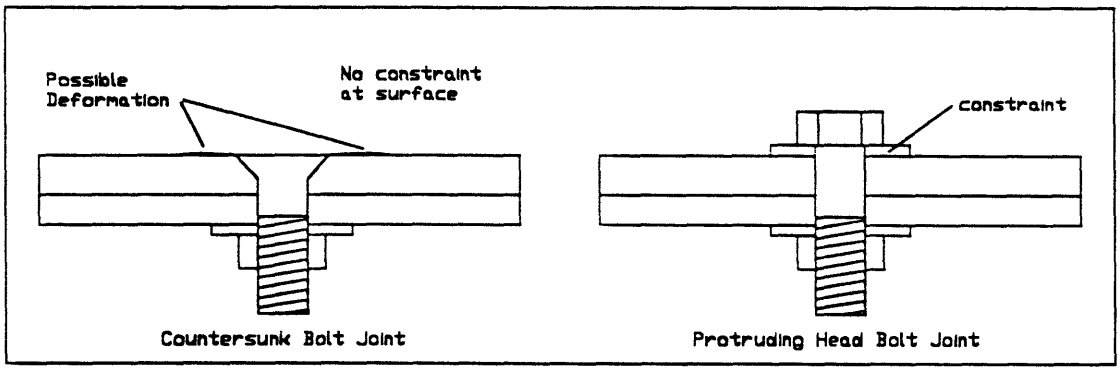

Figure 3-6. Bolted Joint Configurations

As illustrated in Figure 3-6, the protruding-head bolt joint allows the use of washers on both sides of the joint. The washers provide constraints on the creep behavior of the panels. Because of this, the only allowable deformations of the panel in the vicinity of the bolt hole are compression (volume reduction) through the joint

thickness, and creep (linear displacement) in the radial direction away from the bolt.

The countersunk bolt joint, on the other hand, precludes the use of a washer under the bolt head. Because of this lack of constraint due to washer absence, the material near the panel surface around the bolt head is free to creep upwards near the hole (illustrated in Figure 3-6). This additional freedom would permit upward lateral translation in addition to the deformation modes for the protruding head bolt, thus permitting more rapid relaxation.

The mode of contact and force load transfer between the bolt head and the panel is another probable cause of the more rapid relaxation behavior in countersunk joints. As illustrated in Figure 3-6, in the protruding-head joint configuration, the washer applies the load to the surface of the panel, which is distinct from the inside surface of the hole. There is thus no possibility of creep parallel to the interface between the contact area of the bolt/washer combination and the contact area on the surface of the panel.

In the countersunk joint, however, the contact area between the bolt head and the panel is not only a load-bearing surface; it also forms a portion of the inside surface of the bolt hole. As a result, since this contact area is at an angle, the applied clampup force resolves into a normal force and a tangential force, as illustrated in Figure 3-7. (In reality, the three-dimensional force resolution is more complicated, but the two-dimensional resolution in Figure 3-7 is adequate to explain the phenomenon.)

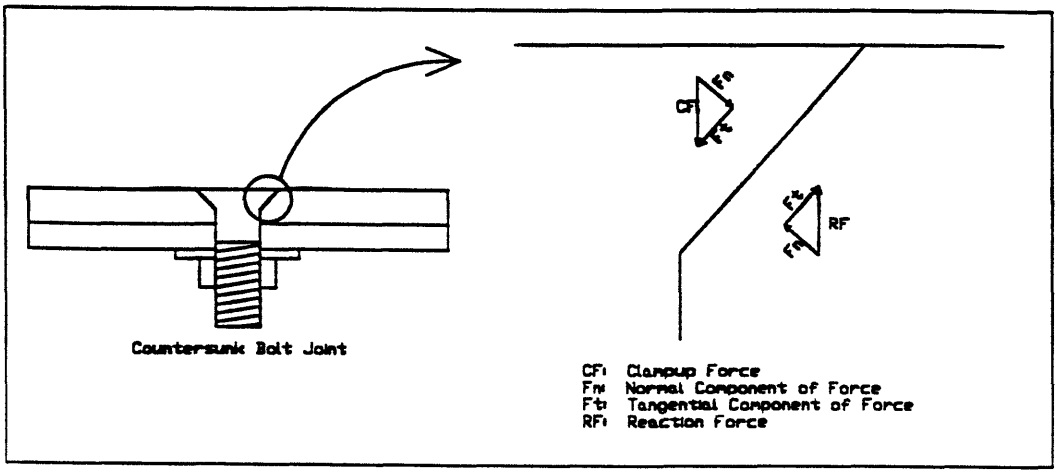

Figure 3-7. Resolution of Clampup Force in Countersunk Bolt Joint into Components

In equilibrium, the tangential force applied by the bolt to the panel must be balanced by a reaction force in the panel, equivalent to the frictional force (which is proportional to the normal force). This reaction force sets up shear stresses in the panel near the force application area; these will cause creep in the panel. This tangential creep effect will allow the bolt to shorten, because the creep will occur in the direction of bolt shortening. The result is more rapid bolt clampup force relaxation.

3.4 Discussion of Bearing Strength Experimental Results

Bearing Strength Definition

In the strictest sense, bearing failure in composite materials is a failure mode

requiring the fastener (pin, bolt, or rivet) to remain undeformed and perpendicular to the plane of the panels being joined. This restricts the effects to uniform crushing of the specimen under a uniformly-distributed normal load being applied to the hole surface.

It is recognized that the behavior of real joints is more complex than the simple model described above. Nevertheless, the bearing strength in composites is generally reported as an stress acting on the hole cross-section [10]; this is calculated by the following equation:

$$\sigma_{BS} = \frac{P}{ndt} \tag{3.7}$$

where: σ_{BS} is bearing strength;

P is the load to failure;

n is the number of bolts in the joint;

d is the bolt diameter; and

t is the panel thickness.

This definition of bearing strength is used for both single-lap and double-lap joints, although it is recognized that specimen bending and fastener rotation in single-lap joint tests significantly alter the failure mechanism (and reduce the failure load).

The matter is further complicated by the use of countersunk bolts. The extra width of the head increases the available bearing area of the bolt, so it may be logical to include this extra area in equation (3.7). This would have the effect of lowering the

bearing strength for a given failure load, which would penalize countersunk fasteners when compared to non-countersunk fasteners. Such comparisons, however, should be conducted on the merits of each fastener type; the goal should be to evaluate each joint type's ability to support the load. If a 5/8 inch protruding head bolt joint and a 5/8 inch countersunk bolt joint between identical materials both fail in bearing at the same load, they should be assigned the same bearing strength.

For the purposes of this study, bearing strength for countersunk bolts was calculated using equation 3.7, taking the load application area to be the bolt diameter (at the outside of the threads) multiplied times the panel thickness; in other words, the possible contribution of the extra head width to bearing strength was ignored.

Sequence of Events in Bearing Strength Tests

In order to determine the effect of the countersunk bolt geometry and torque/clampup force on bearing strength in the GRP panels, it is useful to describe the entire loading sequence, from initial loading to bearing failure, and on to ultimate (catastrophic) failure, in whatever mode is dictated by the joint geometry. For comparison, the sequence of events in countersunk and protruding head joints will both be described. It should be noted that these discussions describe specifically the joint configurations tested, as described in Chapter Two. The dimensions of these joints were selected in order to restrict the failure mode to bearing failure; other joint designs may fail in different modes (tension through the hole, shear, etc.) depending on the dimensions.

These descriptions are based on the direct observation of 16 countersunk bolt joint bearing strength tests, 4 protruding-head bolt joint bearing strength tests, and the review of videotapes recorded during each test. The videotapes were made from two different angles: focused on the area surrounding the bolt head, and focused on the edge of the specimen. The first camera angle was useful for observing the delamination behavior near the bolt hole; the second was useful for observing specimen bending, bolt tipping, bolt bending, and "brooming" near the surface of the GRP.

In each test, the grip displacement rate was kept constant throughout the test

Typical Countersunk Bolted Joint Test Behavior

0 to 5000 pounds load: During the first phase of the test, the joint "settles"; this effect is observable in the load-displacement curves as a concave-upward portion of the curve near the origin. (The curve is concave upward because the overall joint becomes more stiff after the initial "slop" in the fastener-panel fit is taken up. This effect is minimized in close-fitting joints.) In Appendix C, this is evident (for example) in the curves for specimens BS-4, BS-7, and BS-10.

Specimen bending begins in this phase. This bending is caused by the rotational moment resulting from the specimen mis-alignment inherent in single-lap joints. The portion of the joint containing the bolt rotates because of this moment, causing specimen bending; equilibrium is achieved when the panels are bent sufficiently to counteract the moment with a reaction force proportional to the bending

stiffness EI, in which E is Young's modulus, and I is the moment of inertia of the panel.

5000 to 10000 lbs load: Bolt tipping occurs in this phase. In tipping, the bolt shifts its position in the hole such that its axis is no longer aligned with the axis of the hole. This is permitted by elastic deformation of the hole, and by the difference in diameter between the hole (in the non-countersunk portion) and the bolt shank. Tipping occurs later in joints with a close fit between the bolt and the hole.

Additionally in this phase, specimen bending becomes more pronounced.

10000 to 15000 lbs load: During this phase, actual bending of the bolt occurs. By this time, the top of the bolt head makes an appreciable angle (up to 15°) with the surface of the GRP panel. Also in this phase, delamination of the laminate begins to occur near the edge of the hole; this is manifested as a thin ring of white. At the same time that delamination occurs (near the end of the phase), "cracking" sounds can be heard.

15000 lbs to Bearing Failure: Cracking sounds are emitted periodically; delamination continues to spread slowly outward from the hole edge. "Brooming" (in which the laminae near the surface of the GRP in the vicinity of the hole on the loaded side are pushed upward, producing a bulge) begins to occur . The load-displacement curve slope decreases.

At the Point of Bearing Failure (load range approximately 17000-19500 lbs):
Delamination on the loaded side of the hole, which has been occurring very slowly, suddenly happens all at once; the white area rapidly expands to become a crescent with an area roughly equivalent to the area of the bolt head, about 1 in^2. (Appendix D contains photographs of representative failed specimens.) The load, which has been continually increasing, stops rising or even decreases.

After Initial Bearing Failure, to Ultimate (Catastrophic) Failure: The load either remains virtually constant or increases very slowly. Brooming and delamination continue, and the "damage crescent" expands further. The load, if rising, levels out; it then begins to decrease rapidly, as the bolt finally fractures at one of the threads at a point between the two panels. This fracture can either be crack initiation only (samples BS-9 and BS-19), or complete brittle fracture separating the bolt head from the shank (samples BS-13, BS-14, BS-15, BS-17, BS-18, and BS-20); in either case the load drops off to near zero almost instantaneously. It is worth noting that in all cases where loading was continued to ultimate failure, the ultimate failure mode was fracture of the bolt. Additionally, the ultimate failure load was generally no more than 2000 lbs. greater than the initial failure load; in some cases it was less than 500 lbs greater (e.g. specimen BS-9), or was even equal to the initial failure load (e.g. specimen BS-20).

Typical Protruding-Head Bolt Joint Test Behavior

0 to 5000 lbs: Joint settlement occurs; panel bending begins.

5000 to 10000 lbs: The bolt begins to tip, but with less of an angle change than observed in a countersunk bolt joint. Panel bending deflection increases.

10000 to 15000 lbs: Bolt begins bending as the load approaches 15000 lbs; the head rotation relative to the bolt shank is significantly less than in a countersunk joint.

15000 to 20000 lbs: Cracking sounds are emitted at about 15000 lbs. The bolt continues to bend.

20000 lbs to Bearing Failure: The washer under the bolthead begins to "dish-in", causing the half of the washer on the loaded side of the hole to lift away from the panel. Delamination and brooming commence.

At the Point of Bearing Failure (load range approximately 22000 to 26500 lbs): Delamination suddenly occurs all at once, as in a countersunk joint. The washer has lifted to a point roughly ⅛ inch above the GRP surface. The load stops rising, and remains constant or decreases.

After Initial Failure: (None of the four protruding head bolt tests was carried out to ultimate failure.) The load begins to rise slowly OR it continues decreasing OR it remains constant (this behavior was not consistent among all four specimens). If the load increases, brooming continues.

Effect of Clampup Force on the Failure Modes in Each of the Two Joint Types

It is clear from the visual observations of the bearing strength experiments that the events at failure (in addition to classic hole edge crushing) for both joint types (countersunk and protruding head single-lap) are identical: sudden, rapid delamination and brooming. The difference is in the load at which failure occurs; the countersunk joints all failed at or below 78% of the load at which the protruding head joint torqued to 50 ft-lbs failed. If the failure events are identical, why do the failure loads differ?

The answer, once again, lies in the different head configurations. As discussed in section 3.3, the protruding head bolt transfers the clampup force load to the GRP panel through a washer. The effect of the clampup force is to compress the GRP laminae in the through-thickness direction; as long as the washer remains undeformed, this compression effect prevents delamination and brooming. (The other effect of clampup force in this joint type is to delay bolt tipping and reduce bolt bending by limiting the relative motion of the two panels being bolted together.) It is noteworthy that delamination and brooming do NOT occur until the washer dishes-in and deforms out-of-plane.

In the countersunk joint, however, the bolt cannot at all constrain the laminae near the surface of the GRP panel near the bolt hole. Because of the smaller diameter of the bolt head with respect to a washer, the greater ability of the countersunk bolt to rotate because of low head constraint, and the greater bearing load transfer area than on a protruding head bolt, the countersunk bolt is also less efficient than a protruding-head bolt at resisting tipping, bending, and relative motion between the panels. (The bearing load is applied to the bolt on the same bolt surface which transfers clampup force, as well as on the shank; because of the larger bearing force area, the total load tending to tip and bend the bolt is higher than for a protruding head bolt.) Therefore, in a countersunk bolt joint, bolt tipping and bending will occur at a lower load and to a greater degree than in a protruding head joint. Additionally, delamination and brooming will occur at a lower load and to a greater extent than in a protruding head joint, because there is no compressive load on the surface of the GRP panel constraining the laminae from delamination and brooming.

Effect of Clampup Force on Bearing Strength

As illustrated in Table 3-3, bearing force in countersunk bolt joints varies widely for a certain level of torque. This variation undoubtedly occurred in the bearing strength experiments; analysis of variance (Table 3-2) did not support the conclusion that varying the torque had any effect on bolt bearing strength in the subject joints. This situation illustrates the difficulty in trying to determine the effect

of one variable on another, by controlling a third variable that is assumed to be proportional to the first variable. It also illustrates the danger in trying to apply principles applicable to a certain system (e.g., protruding head bolt joints in steel) to a superficially similar system that behaves quite differently (e.g., countersunk bolt joints in GRP).

Nevertheless, Figure 3-4 indicates that there is probably a slight positive correlation between torque and bearing strength (and, we assume, clampup force and bearing strength) in the subject joints. Confirmation of this hypothesis would require repeating the bearing strength experiments with approximately 45 total samples, or performing an experiment in which clampup force could be measured directly in bearing strength test specimens, thus (presumably) reducing the variation.

If Figure 3-4 is taken at face value, bearing strength in countersunk bolt joints can be predicted by the following empirical equation:

$$\sigma_{BS} = \sigma_{BS,0} + aT^b \tag{3.8}$$

where: $\sigma_{BS,0}$ is the zero-torque bearing strength;

T is torque; and

a and b are constants dependent on material properties and joint configuration, with b approximately equal to 0.5.

For the subject joints , the constants in equation (3.8) have the following values:

$\sigma_{BS,0}$ = 61,930 psi;

a = 711.1 $lb^{0.4}$ $ft^{-0.6}$ in^{-2} ; and

$$b = 0.6$$

It appears from Figure 3-4 and Table 3-1 that increasing the level of torque (and presumably clampup force) applied to a single-lap countersunk bolt joint has only a moderate effect on bearing strength. There is only a 12% increase in bearing strength associated with increasing torque from 0 ft-lbs to 50 ft-lbs. There is an even smaller increase in bearing strength (10%) associated with the same torque increase in the single-lap protruding head joints (which admittedly have a very small sample size).

Stockdale and Matthews [6] reported an increase of 44% in bearing strength in protruding head, double-lap bolt joints in glass/epoxy with a $[0/90/0/90/0/90/0]_T$ lay-up, as clampup force was increased from 0 to 14715 N (3306 lbs).

This difference between double-lap and single-lap joint behavior indicates that, overall, clampup force is less effective in single-lap joints of either configuration (countersunk or protruding head) in GRP than in double lap joints. This is because of the inevitable specimen bending and bolt tipping/bending that occurs in single lap tests. As the applied load increases, these effects eventually defeat the beneficial effects of clampup force, namely joint alignment and bolt integrity (in countersunk and protruding head joints) and surface laminae restraint (in protruding head joints). Since these adverse effects begin long before the load reaches even the zero-clampup force bearing failure load, the beneficial effects merely act to delay failure in the same mode associated with zero clampup force; they do not prevent a relatively low-load failure mode in favor of a high-low mode.

In double-lap protruding head bolted joints, on the other hand, clampup force can essentially eliminate delamination and brooming, since there is no tendency for the washer to dish-in (if the bolt is sufficiently strong to prevent shear yielding of the bolt). The overall effect of clampup force in these joints is to eliminate the delamination and brooming modes of failure, in favor of the classic hole edge crushing that is the hallmark of straight bearing failure. As a result, the bearing strength increases appreciably with increased clampup force in double-lap, protruding-head bolted joints.

Chapter Four
Conclusions and Recommendations

4.1 Conclusions Concerning Relaxation Behavior

1. Based on observations of the initial clampup force in ten GRP/steel countersunk bolt joint (subject joint) specimens, it is concluded that the clampup force resulting from a certain level of torque in nominally identical countersunk bolted joints in GRP is widely variable, by a factor of two or more. It is therefore difficult to predict clampup force in such joints, even if the torque is known.

2. Based on the results of the experiments, it is concluded that clampup force relaxation in the subject joints relaxes according to the relaxation equation proposed by Shivakumar and Crews [2], which is:

$$\frac{F(t)}{F_0} = \frac{1}{1 + kt^n} \tag{4.1}$$

where: F (t) is the clampup force at time t;

F_0 is the clampup force at time zero; and

$$k = \frac{F_1}{a_{TH}^n} \tag{4.2}$$

where F_1 is a viscoelastic force constant, and a_{TH} is a hygrothermal shift factor.

For the subject joints under ambient conditions, a regression analysis of the experimental data yielded the following constants for equation (4.1):

$$k = 0.08608 \text{ hours}^{-0.2519}$$

$$n = 0.2519$$

Clampup force in the subject joints relaxed more rapidly than Shivakumar and Crews' results for protruding head bolt joints in carbon fiber/epoxy laminates [2]. This is believed to be a function of the countersunk joint geometry and its inherent lack of constraint at the surface of the GRP panel.

3. If the initial clampup force in the subject joints is at a sufficiently low level (as in four of the five samples torqued to 35 foot-pounds), it is concluded that the clampup force relaxes to an "effective zero" value within eight hours, after which relaxation behavior ceases. The relaxation which does occur in these specimens is believed to be almost entirely due to the initial "settling" which is reported by Shivakumar and Crews [2] to occur in all bolt joints, regardless of material.

It is further concluded that, in order to receive any benefit from clampup force in the bolt, countersunk joints must be torqued to a relatively high value (60 ft-lbs was shown to be reasonable in the joints tested).

4.2 Conclusions Concerning Bearing Strength Behavior

1. Because of the large variation in the bearing strength experimental data, there was no statistical basis for concluding that initial torque has any effect on bolt bearing strength in the subject joints. Nevertheless, examination of the data suggested that

there is probably a moderate positive correlation between torque and bearing strength in the subject joints. Confirmation of this hypothesis would require repeating the same experiments with a total sample size greater than 45.

A regression analysis of the bearing strength data suggests that bearing strength correlates to torque according to the following empirical equation:

$$\sigma_{BS} = \sigma_{BS,0} + aT^{b} \tag{4.3}$$

in which : σ_{BS} is the joint-specific bolt bearing strength;

$\sigma_{BS,0}$ is the zero-torque bolt bearing strength;

T is torque; and

a and b are constants dependent on joint geometry and material properties, with b approximately equal to 0.5.

For the subject joints, the various constants in equation (4.3) have the following values:

$$\sigma_{BS,0} = 61{,}930 \text{ psi}$$

$$a = 711.1 \text{ lb}^{0.4} \text{ ft}^{-0.6} \text{ in}^{-2}$$

$$b = 0.6$$

2. Based on the bearing strength experimental data, it is concluded that clampup force probably has only a modest effect on bearing strength in single lap joints (when compared to double lap joints), regardless of whether the joint is of a countersunk or protruding head configuration. This is because, in a single lap joint, the clampup force apparently serves only to delay failure in a delamination/brooming mode,

whereas in a double lap joint, the clampup force effectively precludes delamination and brooming failure in favor of classic bearing failure, which occurs at a much higher load.

3. Based on the bearing strength experimental data, it is concluded that bearing failure in the (countersunk) subject joints is followed soon after by catastrophic bolt fracture, without necessarily any increase in load. This indicates that in the subject joints, the stresses in the bolt become dangerously high as the bearing failure load is approached. These high bolt stresses are believed to be caused by the relative freedom of the bolt to bend (when compared to a protruding head bolt).

Because of the catastrophic failure of the subject joints soon after bearing failure, design of joints employing countersunk bolts must be performed carefully, to ensure that loads on individual bolts remain significantly below the bearing failure load.

4. The bearing strength of the single-lap subject joints was shown to be approximately 80% of the bearing strength of single-lap protruding head joints. This loss of bearing strength may be acceptable to a designer, if he has specific reasons for selecting countersunk fasteners. If he has no reason to prefer countersunk fasteners, he should always select protruding-head fasteners for use in single-lap joints in GRP.

4.3 Recommendations

1. Further research should be performed in the following areas in order to fully quantify the behavior of countersunk joints of the type studied:

   a. The bearing strength tests should be repeated with a sample size greater than 45, in an attempt to confirm the hypothesis that torque affects bearing strength in the subject joints;

   b. The relaxation experiments should be repeated, with variation of temperature and humidity to account for the full range of shipboard conditions; and

   c. The variation of clampup force resulting from constant torque levels in the subject joints should be investigated further, with an eye toward finding ways to improve the correlation.

2. Countersunk fasteners should only be used in applications where their advantages outweigh their significant mechanical behavior weaknesses.

3. Any composite-to-steel joint which is expected to carry significant transverse loads (and which therefore would tend to rotate out-of-plane) should be double-lapped, with a steel panel on either side of the GRP laminate. Countersunk fasteners should NOT be used for this application.

Appendix A. Instrumented Bolt Calibration Data

The next ten pages are the calibration data for the instrumented bolts as supplied by the manufacturer, the Strainsert Company of West Conshohocken, Pennsylvania. The calibrations were performed at 70°F, in both the loading and unloading directions, over the full range of safe loads from 0 to 23,000 lbs.

The final digit of the manufacturer's serial number corresponds to the sample numbers in the relaxation experiments.

STRAINSERT CALIBRATION DATA

Massachusetts Institute of Technology Cambridge, MA	Q-12172 Strainsert Job No.
	Date: APR 19 1994
Customer P.O. No. GG-R-470462	Sign: MAC

Transducer: Standard Hex Head Cap Screw
(SXS-FB) 5/8-11UNC x 2-3/4"-lg.
(350Ω/150°F) W To K(LU) So

Gages: EA-06-S1393-350 Type: W
Service Temp.: 150°F Max. Ins. Res.: Over 10,000 megohms

CAL TEMP 70°F S/N 012172-1

LOAD LBS	STRAIGHT LINE SIGNAL mv/V	DEVIATIONS μv/V RUN-1	RUN-2	RUN-3	REP μv/V
0	0.000	0.0	0.0	0.0	0.0
4,600	0.773	-3.5	-3.5	-3.0	0.5
9,200	1.545	-4.5	-5.0	-5.0	0.5
13,800	2.318	-5.5	-5.0	-5.0	0.5
18,400	3.090	-2.5	-2.5	-2.5	0.0
23,000	3.863	5.0	5.0	4.5	0.5
18,400	3.090	-3.0	-2.5	-2.5	0.5
13,800	2.318	-5.5	-5.5	-5.5	0.0
9,200	1.545	-4.5	-4.5	-4.5	0.0
4,600	0.773	-3.0	-3.0	-3.0	0.0
0	0.000	0.0	0.0	0.0	0.0
	HYSTERESIS	0.5	0.5	0.5	

CALIBRATION ANALYSIS:

NON-LINEARITY: 5.5 PARTS IN 3.863 = 0.14%

REPETITION
LOADING : 0.5 PARTS IN 3.863 = 0.01%
UNLOADING: 0.5 PARTS IN 3.863 = 0.01%
ZERO LOAD: 0.0 PARTS IN 3.863 = 0.00%
MAX. LOAD: 0.5 PARTS IN 3.863 = 0.01%

END POINT : 5.0 PARTS IN 3.863 = 0.13%

HYSTERESIS : 0.5 PARTS IN 3.863 = 0.01%

Calibration per GL-STD-4300I, traceable to NIST.

S-1150

STRAINSERT CALIBRATION DATA

Massachusetts Institute of Technology Cambridge, MA	Q-12172 Strainsert Job No.
	Date: APR 19 1994
Customer P.O. No. GG-R-470462	Sign: MAC

Transducer: Standard Hex Head Cap Screw
(SXS-FB) 5/8-11UNC x 2-3/4"-lg.
(350Ω/150°F) W To K(LU) So

Gages: EA-06-S1393-350 Type: W
Service Temp.: 150°F Max. Ins. Res.: Over 10,000 megohms

CAL TEMP 73°F S/N Q12172-2

LOAD LBS	STRAIGHT LINE SIGNAL mv/V	DEVIATIONS µv/V RUN-1	RUN-2	RUN-3	REP µv/V
0	0.000	0.0	0.0	0.0	0.0
4,600	0.772	-3.5	-3.0	-3.0	0.5
9,200	1.543	-4.5	-4.5	-4.5	0.0
13,800	2.315	-5.5	-5.5	-5.5	0.0
18,400	3.086	-3.0	-2.5	-3.0	0.5
23,000	3.858	5.0	5.0	5.0	0.0
18,400	3.086	2.5	3.0	2.5	0.5
13,800	2.315	4.0	4.0	4.0	0.0
9,200	1.543	3.0	3.5	3.0	0.5
4,600	0.772	5.5	5.5	5.0	0.5
0	0.000	0.0	0.0	0.0	0.0
	HYSTERESIS	9.0	9.5	9.0	

CALIBRATION ANALYSIS:

NON-LINEARITY: 5.5 PARTS IN 3,858 = 0.17%

REPETITION
LOADING : 0.5 PARTS IN 3,858 = 0.01%
UNLOADING: 0.5 PARTS IN 3,858 = 0.01%
ZERO LOAD: 0.0 PARTS IN 3,858 = 0.00%
MAX. LOAD: 0.0 PARTS IN 3,858 = 0.00%

END POINT : 5.0 PARTS IN 3,858 = 0.13%

HYSTERESIS : 9.0 PARTS IN 3,858 = 0.23%

Calibration per Micro Precision, traceable to NIST.

S-1150

STRAINSERT CALIBRATION DATA

Massachusetts Institute of Technology Cambridge, MA	Q-12172 Strainsert Job No.
	Date: APR 19 1994
Customer P.O. No. GG-R-470462	Sign: MAC

Transducer: Standard Hex Head Cap Screw
(SXS-FB) 5/8-11UNC x 2-3/4"-lg.
(350Ω/150°F) W To K(LU) So

Gages: EA-06-S1393-350 **Type:** W
Service Temp.: 150°F Max. **Ins. Res.:** Over 10,000 megohms

CAL TEMP 70°F S/N Q12172-3

LOAD LBS	STRAIGHT LINE SIGNAL mv/V	DEVIATIONS µv/v RUN-1	RUN-2	RUN-3	REP µv/V
0	0.000	0.0	0.0	0.0	0.0
4,600	0.760	-0.5	-0.5	-0.5	0.0
9,200	1.520	-3.5	-3.0	-3.5	0.5
13,800	2.280	-5.0	-5.0	-5.0	0.0
18,400	3.040	-3.5	-3.5	-3.5	0.0
23,000	3.800	2.5	2.5	2.5	0.0
18,400	3.040	-3.0	-3.0	-3.0	0.0
13,800	2.280	-5.0	-5.0	-5.0	0.0
9,200	1.520	-3.5	-3.5	-3.5	0.0
4,600	0.760	-2.5	-2.5	-2.5	0.0
0	0.000	0.0	0.0	0.0	0.0
	HYSTERESIS	2.0	2.0	2.0	

CALIBRATION ANALYSIS:

NON-LINEARITY: 3.0 PARTS IN 3,800 = 0.13%

REPETITION
LOADING : 0.5 PARTS IN 3,800 = 0.01%
UNLOADING: 0.0 PARTS IN 3,800 = 0.00%
ZERO LOAD: 0.0 PARTS IN 3,800 = 0.00%
MAX. LOAD: 0.0 PARTS IN 3,800 = 0.00%

END POINT : 2.5 PARTS IN 3,800 = 0.07%

HYSTERESIS : 2.0 PARTS IN 3,800 = 0.05%

Calibration per MIL-STD-45662A, traceable to NIST.

S-1150

STRAINSERT CALIBRATION DATA

Massachusetts Institute of Technology Cambridge, MA	Q-12172 Strainsert Job No.
	Date: APR 19 1994
Customer P.O. No. GG-R-470462	Sign: MAC

Transducer: Standard Hex Head Cap Screw
(SXS-FB) 5/8-11UNC x 2-3/4"-lg.
(350Ω/150°F) W To K(LU) So

Gages: EA-06-S1393-350 Type: W
Service Temp.: 150°F Max. Ins. Res.: Over 10,000 megohms

CAL TEMP 70°F S/N 012172-4

LOAD LBS	STRAIGHT LINE SIGNAL mv/V	DEVIATIONS µv/V RUN-1	RUN-2	RUN-3	REP µv/V
0	0.000	0.0	0.0	0.0	0.0
4,600	0.764	-6.0	-6.0	-6.5	0.5
9,200	1.528	-7.5	-7.5	-7.5	0.0
13,800	2.292	-6.0	-5.5	-6.0	0.5
18,400	3.056	-3.0	-3.0	-3.0	0.0
23,000	3.820	5.0	5.0	5.0	0.0
18,400	3.056	0.5	0.5	0.5	0.0
13,800	2.292	-2.5	-2.5	-2.5	0.0
9,200	1.528	-4.0	-4.0	-4.0	0.0
4,600	0.764	-4.0	-4.0	-4.0	0.0
0	0.000	0.0	0.0	0.0	0.0
	HYSTERESIS	2.0	2.0	2.5	

CALIBRATION ANALYSIS:

NON-LINEARITY: 7.5 PARTS IN 3.820 = 0.20%

REPETITION
LOADING : 0.5 PARTS IN 3.820 = 0.01%
UNLOADING: 0.0 PARTS IN 3.820 = 0.00%
ZERO LOAD: 0.0 PARTS IN 3.820 = 0.00%
MAX. LOAD: 0.0 PARTS IN 3.820 = 0.00%

END POINT : 5.0 PARTS IN 3.820 = 0.13%

HYSTERESIS : 2.5 PARTS IN 3.820 = 0.07%

Calibration per MIL-STD-45662, traceable to NIST.

S-1150

STRAINSERT CALIBRATION DATA

Massachusetts Institute of Technology Cambridge, MA Customer P.O. No. GG-R-470462	Q-12172 Strainsert Job No. Date: APR 1 1994 Sign: MAC

Transducer: Standard Hex Head Cap Screw
(SXS-FB) 5/8-11UNC x 2-3/4"-lg.
(350Ω/150°F) W To K(LU) So

Gages: EA-06-S1393-350 **Type:** W
Service Temp.: 150°F Max. **Ins. Res.:** Over 10,000 megohms

CAL TEMP 70°F S/N Q12172-5

LOAD LBS	STRAIGHT LINE SIGNAL mV/V	DEVIATIONS µV/V RUN-1	RUN-2	RUN-3	REF µV/V
0	0.000	0.0	0.0	0.0	0.0
4.600	0.780	1.5	1.0	1.0	0.5
9.200	1.560	-2.0	-2.0	-2.0	0.0
13.800	2.340	-3.5	-3.5	-3.5	0.0
18.400	3.119	-3.5	-3.5	-3.5	0.0
23.000	3.899	2.5	2.5	2.5	0.0
18.400	3.119	-2.5	-3.0	-3.0	0.5
13.800	2.340	-3.5	-3.0	-3.5	0.5
9.200	1.560	-1.0	-1.0	-1.0	0.0
4.600	0.780	1.0	1.5	1.0	0.5
0	0.000	0.0	0.0	0.0	0.0
	HYSTERESIS	1.0	1.0	1.0	

CALIBRATION ANALYSIS:

NON-LINEARITY:	3.5	PARTS IN	3.899	=	0.09%
REPETITION					
LOADING :	0.5	PARTS IN	3.899	=	0.01%
UNLOADING:	0.5	PARTS IN	3.899	=	0.01%
ZERO LOAD:	0.0	PARTS IN	3.899	=	0.00%
MAX. LOAD:	0.0	PARTS IN	3.899	=	0.00%
END POINT :	2.5	PARTS IN	3.899	=	0.06%
HYSTERESIS :	1.0	PARTS IN	3.899	=	0.03%

Calibration per MIL-STD-45662. Traceable to NIST.

S-1150

STRAINSERT CALIBRATION DATA

Massachusetts Institute of Technology Cambridge, MA	Q-12172 Strainsert Job No.
	Date: APR 19 1994
Customer P.O. No. GG-R-470462	Sign: MAC

Transducer: Standard Hex Head Cap Screw
(SXS-FB) 5/8-11UNC x 2-3/4"-lg.
(350Ω/150°F) W To K(LU) So

Gages: EA-06-S1393-350 Type: W
Service Temp.: 150°F Max. Ins. Res.: Over 10,000 megohms

CAL TEMP 70°F S/N 012172-8

LOAD LBS	STRAIGHT LINE SIGNAL mv/V	DEVIATIONS µv/V RUN-1	RUN-2	RUN-3	REP µv/V
0	0.000	0.0	0.0	0.0	0.0
4,600	0.777	-3.5	-3.0	-3.0	0.5
9,200	1.554	-5.5	-5.0	-5.0	0.5
13,800	2.331	-5.5	-5.0	-5.0	0.5
18,400	3.108	-1.5	-1.5	-1.5	0.0
23,000	3.885	5.0	5.0	5.0	0.0
18,400	3.108	-2.0	-2.0	-2.0	0.0
13,800	2.331	-4.0	-4.0	-4.0	0.0
9,200	1.554	-3.0	-3.0	-3.0	0.0
4,600	0.777	-1.0	-1.0	-1.0	0.0
0	0.000	0.0	0.0	0.0	0.0
	HYSTERESIS	2.5	2.3	2.0	

CALIBRATION ANALYSIS:

NON-LINEARITY: 3.5 PARTS IN 3,885 = 0.14%

REPETITION
LOADING . 3.5 PARTS IN 3,885 = 0.01%
UNLOADING: 0.0 PARTS IN 3,885 = 0.00%
ZERO LOAD: 0.0 PARTS IN 3,885 = 0.00%
MAX. LOAD: 1.0 PARTS IN 3,885 = 0.00%

END POINT . 5.0 PARTS IN 3,885 = 0.13%

HYSTERESIS . 2.5 PARTS IN 3,885 = 0.06%

Calibration Load Cell ID-[illegible] traceable to NIST.

S-1150

STRAINSERT CALIBRATION DATA

Massachusetts Institute of Technology Cambridge, MA	Q-12172 **Strainsert Job No.**
	Date: APR 19 1994
Customer P.O. No. GG-R-470462	Sign: MAC

Transducer: Standard Hex Head Cap Screw
(SXS-FB) 5/8-11UNC x 2-3/4"-lg.
(350Ω/150°F) W To K(LU) So

Gages: EA-06-S1393-350 Type: W
Service Temp.: 150°F Max. Ins. Res.: Over 10,000 megohms

CAL TEMP 70°F S/N Q12172-7

LOAD LBS	STRAIGHT LINE SIGNAL mv/V	DEVIATIONS µv/V RUN-1	RUN-2	RUN-3	REP µv/V
0	0.000	0.0	0.0	0.0	0.0
4,600	0.759	-5.0	-5.0	-5.0	0.0
9,200	1.517	-6.5	-6.5	-6.5	0.0
13,800	2.276	-5.5	-6.0	-5.5	0.5
18,400	3.035	-1.0	-1.0	-0.5	0.5
23,000	3.793	7.5	7.5	7.5	0.0
18,400	3.035	3.5	3.5	3.5	0.0
13,800	2.276	-2.0	-2.0	-2.0	0.0
9,200	1.517	-2.5	-2.5	-2.5	0.0
4,600	0.759	-3.0	-3.0	-3.0	0.0
0	0.000	0.0	0.0	0.0	0.0
	HYSTERESIS	4.0	4.0	4.0	

CALIBRATION ANALYSIS:

NON-LINEARITY: 7.5 PARTS IN 3,793 = 0.20%

REPETITION
LOADING : 0.5 PARTS IN 3,793 = 0.01%
UNLOADING: 3.0 PARTS IN 3,793 = 0.00%
ZERO LOAD: 0.0 PARTS IN 3,793 = 0.00%
MAX. LOAD: 0.0 PARTS IN 3,793 = 0.00%

END POINT : 7.5 PARTS IN 3,793 = 0.20%

HYSTERESIS : 4.0 PARTS IN 3,793 = 0.11%

Calibration per MIL-STD-45662, traceable to NIST.

S-1150

STRAINSERT CALIBRATION DATA

Massachusetts Institute of Technology Cambridge, MA	Q-12172 **Strainsert Job No.**
	Date: APR 19 1994
Customer P.O. No. GG-R-470462	**Sign:** MAC

Transducer: Standard Hex Head Cap Screw
(SXS-FB) 5/8-11UNC x 2-3/4"-lg.
(350Ω/150°F) W To K(LU) So

Gages: EA-06-S1393-350 Type: W
Service Temp.: 150°F Max. Ins. Res.: Over 10,000 megohms

CAL TEMP 70°F S/N Q12172-8

LOAD LBS	STRAIGHT LINE SIGNAL mv/V	DEVIATIONS µv/V RUN-1	RUN-2	RUN-3	REP µv/V
0	0.000	0.0	0.0	0.0	0.0
4,600	0.769	-0.5	0.0	0.0	0.5
9,200	1.538	-3.0	-2.5	-2.5	0.5
13,800	2.307	-3.5	-3.5	-3.5	0.0
18,400	3.076	-1.5	-1.5	-2.0	0.5
23,000	3.845	5.0	5.0	5.0	0.0
18,400	3.076	-2.0	-2.0	-2.0	0.0
13,800	2.307	-2.5	-2.5	-2.5	0.0
9,200	1.538	-1.0	-1.0	-1.0	0.0
4,600	0.769	1.0	1.0	1.0	0.0
0	0.000	0.0	0.0	0.0	0.0
	HYSTERESIS	1.5	1.0	1.0	

CALIBRATION ANALYSIS:

NON-LINEARITY: 5.0 PARTS IN 3.845 = 0.13%

REPETITION
LOADING : 0.5 PARTS IN 3.845 = 0.01%
UNLOADING: 0.0 PARTS IN 3.845 = 0.00%
ZERO LOAD: 0.0 PARTS IN 3.845 = 0.00%
MAX. LOAD: 0.0 PARTS IN 3.845 = 0.00%

END POINT : 5.0 PARTS IN 3.845 = 0.13%

HYSTERESIS : 1.5 PARTS IN 3.845 = 0.04%

Calibration per MIL-STD-45662, traceable to NIST.

S-1150

STRAINSERT CALIBRATION DATA

Massachusetts Institute of Technology Cambridge, MA	Q-12172 **Strainsert Job No.**
	Date: APR 19 1994
Customer P.O. No. GG-R-470462	Sign: MAC

Transducer: Standard Hex Head Cap Screw
(SXS-F8) 5/8-11UNC x 2-3/4"-lg.
(350Ω/150°F) W To K(LU) So

Gages: EA-06-S1393-350 Type: W
Service Temp.: 150°F Max. Ins. Res.: Over 10,000 megohms

CAL TEMP 70°F S/N 012172-9

LOAD LBS	STRAIGHT LINE SIGNAL mv/V	DEVIATIONS µv/V RUN-1	RUN-2	RUN-3	REP µv/V
0	0.000	0.0	0.0	0.0	0.0
4,600	0.769	-4.0	-4.0	-4.5	0.5
9,200	1.538	-5.5	-5.5	-6.0	0.5
13,800	2.307	-5.0	-5.0	-5.0	0.0
18,400	3.075	-1.5	-1.5	-1.5	0.0
23,000	3.844	5.0	5.0	5.0	0.0
18,400	3.075	0.0	0.5	0.5	0.5
13,800	2.307	-3.5	-3.5	-3.0	0.5
9,200	1.538	-3.0	-3.0	-3.0	0.0
4,600	0.769	-3.0	-2.5	-2.5	0.5
0	0.000	0.0	0.0	0.0	0.0
	HYSTERESIS	2.5	1.5	2.0	

CALIBRATION ANALYSIS:

NON-LINEARITY: 5.0 PARTS IN 3.844 = 0.16%

REPETITION
LOADING : 0.5 PARTS IN 3.844 = 0.01%
UNLOADING: 0.5 PARTS IN 3.844 = 0.01%
ZERO LOAD: 0.0 PARTS IN 3.844 = 0.00%
MAX. LOAD: 0.0 PARTS IN 3.844 = 0.00%

END POINT : 5.0 PARTS IN 3.844 = 0.13%

HYSTERESIS : 2.5 PARTS IN 3.844 = 0.07%

Calibration per MIL-STD-45662, traceable to NIST.

S-1150

STRAINSERT CALIBRATION DATA

Massachusetts Institute of Technology Cambridge, MA	Q-12172 **Strainsert Job No.**
	Date: APR 19 1994
Customer P.O. No. GG-R-470462	**Sign:** MAC

Transducer: Standard Hex Head Cap Screw
(SXS-FB) 5/8-11UNC x 2-3/4"-lg.
(350Ω/150°F) W To K(LU) So

Gages: EA-06-S1393-350 **Type:** W
Service Temp.: 150°F Max. **Ins. Res.:** Over 10,000 megohms

CAL TEMP 73°F S/N Q12172-10

LOAD LBS	STRAIGHT LINE SIGNAL mv/V	DEVIATIONS μv/V RUN-1	RUN-2	RUN-3	REP μv/V
0	0.000	0.0	0.0	0.0	0.0
4,600	0.774	-3.5	-3.5	-3.5	0.0
9,200	1.548	-2.0	-2.0	-2.0	0.0
13,800	2.322	2.0	2.0	2.0	0.0
18,400	3.096	4.0	4.0	4.0	0.0
23,000	3.870	-2.5	-2.5	-2.5	0.0
18,400	3.096	1.0	1.0	1.0	0.0
13,800	2.322	1.5	1.5	1.5	0.0
9,200	1.548	-1.5	-1.5	-1.5	0.0
4,600	0.774	-2.0	-2.0	-2.0	0.0
0	0.000	0.0	0.0	0.0	0.0
	HYSTERESIS	3.0	3.0	3.0	

CALIBRATION ANALYSIS:

NON-LINEARITY: 4.0 PARTS IN 3.870 = 0.10%

REPETITION
LOADING : 0.0 PARTS IN 3.870 = 0.00%
UNLOADING: 0.0 PARTS IN 3.870 = 0.00%
ZERO LOAD: 0.0 PARTS IN 3.870 = 0.00%
MAX. LOAD: 0.0 PARTS IN 3.870 = 0.00%

END POINT : 2.5 PARTS IN 3.870 = 0.06%

HYSTERESIS : 3.0 PARTS IN 3.870 = 0.08%

Calibration per MIL-STD-45662, traceable to NIST.

S-1150

Appendix B. Tabulated Relaxation Experiment Data and Relaxation Graphs

This Appendix presents the raw relaxation experiment data (output voltages, time of measurement, and temperature) on pages 80 and 81. Page 82 is a tabulated summary of the clampup force relaxation behavior of the ten joint specimens, with clampup force expressed both in pounds and in a dimensionless form, obtained by dividing the measured force by the initial force. Pages 83 through 94 are plots of the relaxation data, as follows:

Relaxation Experiment Data

27 April 1700
T=81F

Specimen	Time	Volts Out	Force (lb)
R-1	1654	0.619	1474
R-2	1655	0.388	925
R-3	1655	0.519	1257
R-4	1655	0.842	2028
R-5	1656	0.558	1316
R-6	1656	0.145	343
R-7	1657	0.152	369
R-8	1657	0.102	244
R-9	1657	0.167	400
R-10	1658	0.848	2016

28 April 0100
T=76F

Time	Volts Out	Force (lb)
0058	0.543	1293
0059	0.344	820
0059	0.455	1102
0111	0.741	1785
0100	0.478	1128
0103	0.103	244
0103	0.102	247
0103	0.100	239
0104	0.105	251
0104	0.796	1892

28 April 0900
T=73F

Specimen	Time	Volts Out	Force (lb)
R-1	0900	0.523	1246
R-2	0900	0.331	789
R-3	0900	0.437	1058
R-4	0901	0.717	1727
R-5	0901	0.459	1083
R-6	0902	0.102	242
R-7	0902	0.102	247
R-8	0903	0.100	239
R-9	0903	0.101	242
R-10	0903	0.778	1850

28 April 1700
T=77F

Time	Volts Out	Force (lb)
1707	0.526	1253
1707	0.336	801
1708	0.441	1068
1709	0.719	1732
1709	0.460	1085
1710	0.103	244
1710	0.102	247
1711	0.101	242
1711	0.102	244
1712	0.787	1871

29 April 0100
T = 74F

Specimen	Time	Volts Out	Force (lb)
R-1	0057	0.512	1220
R-2	0058	0.328	782
R-3	0058	0.429	1039
R-4	0059	0.692	1667
R-5	0059	0.448	1057
R-6	0101	0.102	242
R-7	0101	0.101	245
R-8	0102	0.099	237
R-9	0102	0.101	242
R-10	0102	0.774	1840

29 April 0900
T = 74F

Time	Volts Out	Force (lb)
0917	0.506	1205
0917	0.324	773
0917	0.424	1027
0918	0.699	1683
0918	0.442	1043
0919	0.102	242
0919	0.102	247
0919	0.100	239
0920	0.101	242
0920	0.768	1826

29 April 1700
T = 76F

Specimen	Time	Volts Out	Force (lb)
R-1	1737	0.508	1210
R-2	1738	0.325	775
R-3	1738	0.427	1034
R-4	1739	0.699	1683
R-5	1739	0.441	1040
R-6	1739	0.103	244
R-7	1740	0.102	247
R-8	1740	0.100	239
R-9	1740	0.102	244
R-10	1741	0.773	1838

30 April 0100
T = 75F

Time	Volts Out	Force (lb)
0124	0.501	1193
0125	0.328	782
0125	0.419	1014
0125	0.686	1652
0126	0.433	1021
0127	0.102	242
0128	0.101	245
0128	0.100	239
0129	0.101	242
0129	0.765	1819

Relaxation Experiment Data (Continued)

30 April 0900
T = 75F

Specimen	Time	Volts Out	Force (lb)
R-1	0907	0.497	1184
R-2	0908	0.315	751
R-3	0908	0.415	1005
R-4	0909	0.683	1645
R-5	0909	0.429	1012
R-6	0909	0.102	242
R-7	0910	0.100	243
R-8	0910	0.099	237
R-9	0911	0.100	239
R-10	0911	0.762	1811

30 April 1700
T = 78F

Time	Volts Out	Force (lb)
1749	0.502	1196
1749	0.320	763
1749	0.421	1019
1750	0.691	1664
1750	0.432	1019
1751	0.102	242
1752	0.101	245
1752	0.100	239
1752	0.101	242
1753	0.771	1833

1 May 0100
T = 76F

Specimen	Time	Volts Out	Force (lb)
R-1	0107	0.496	1181
R-2	0108	0.314	749
R-3	0108	0.414	1002
R-4	0109	0.684	1647
R-5	0110	0.425	1003
R-6	0111	0.102	242
R-7	0111	0.101	245
R-8	0111	0.100	239
R-9	0112	0.101	242
R-10	0112	0.764	1816

1 May 0900
T = 75F

Time	Volts Out	Force (lb)
1007	0.490	1167
1008	0.311	742
1008	0.409	990
1009	0.676	1628
1009	0.420	991
1010	0.101	239
1010	0.101	245
1011	0.100	239
1011	0.101	242
1011	0.759	1804

1 May 2100
T = 75F

Specimen	Time	Volts Out	Force (lb)
R-1	2043	0.490	1167
R-2	2043	0.311	742
R-3	2044	0.409	990
R-4	2044	0.673	1621
R-5	2045	0.419	988
R-6	2045	0.102	242
R-7	2046	0.101	245
R-8	2046	0.100	239
R-9	2046	0.101	242
R-10	2047	0.759	1804

2 May 0100
T = 74F

Time	Volts Out	Force (lb)
0109	0.485	1155
0110	0.307	732
0110	0.404	978
0111	0.669	1611
0112	0.413	974
0112	0.101	239
0112	0.101	245
0113	0.099	237
0113	0.100	239
0114	0.755	1795

2 May 1100
T = 74F

Specimen	Time	Volts Out	Force (lb)
R-1	1042	0.482	1148
R-2	1043	0.305	727
R-3	1043	0.401	971
R-4	1043	0.662	1594
R-5	1043	0.410	967
R-6	1044	0.101	239
R-7	1044	0.100	243
R-8	1045	0.099	237
R-9	1045	0.094	225
R-10	1045	0.749	1781

Clampup Force Relaxation, Countersunk Bolted Joints in GRP

Clampup Force (lbs)

Time (hrs):	0	8.01	16.1	24.233	32.05	40.3833	48.7167
Specimen							
R-1 (60 ft-lb)	1474	1293	1246	1253	1220	1205	1210
R-2 (60 ft-lb)	925	820	789	801	782	773	775
R-3 (60 ft-lb)	1257	1102	1058	1068	1039	1027	1034
R-4 (60 ft-lb)	2028	1785	1727	1732	1667	1683	1683
R-5 (60 ft-lb)	1316	1128	1083	1085	1057	1043	1040
R-6 (35 ft-lb)	343	244	242	244	242	242	244
R-7 (35 ft-lb)	369	247	247	247	245	247	247
R-8 (35 ft-lb)	244	239	239	242	237	239	239
R-9 (35 ft-lb)	400	251	242	244	242	242	244
R-10 (35 ft-lb)	2016	1892	1850	1871	1840	1826	1838

Normalized Clampup Force

Time (hrs):	0	8.01	16.1	24.233	32.05	40.3833	48.7167
Specimen							
R-1 (60 ft-lb)	1	0.877	0.845	0.850	0.828	0.818	0.821
R-2 (60 ft-lb)	1	0.886	0.853	0.866	0.845	0.836	0.838
R-3 (60 ft-lb)	1	0.877	0.842	0.850	0.827	0.817	0.823
R-4 (60 ft-lb)	1	0.880	0.852	0.854	0.822	0.830	0.830
R-5 (60 ft-lb)	1	0.857	0.823	0.824	0.803	0.793	0.790
R-6 (35 ft-lb)	1	0.711	0.706	0.711	0.706	0.706	0.711
R-7 (35 ft-lb)	1	0.669	0.669	0.669	0.664	0.669	0.669
R-8 (35 ft-lb)	1	0.980	0.980	0.992	0.971	0.980	0.980
R-9 (35 ft-lb)	1	0.628	0.605	0.610	0.605	0.605	0.610
R-10 (35 ft-lb)	1	0.938	0.918	0.928	0.913	0.906	0.912

Clampup Force (lbs)

Time (hrs):	56.5167	64.2167	72.9167	80.2333	89.2167	99.8167	104.2667	113.80
Specimen								
R-1 (60 ft-lb)	1193	1184	1196	1181	1167	1167	1155	1148
R-2 (60 ft-lb)	782	751	763	749	742	742	732	727
R-3 (60 ft-lb)	1014	1005	1019	1002	990	990	978	971
R-4 (60 ft-lb)	1652	1645	1664	1647	1628	1621	1611	1594
R-5 (60 ft-lb)	1021	1012	1019	1003	991	988	974	967
R-6 (35 ft-lb)	242	242	242	242	239	242	239	239
R-7 (35 ft-lb)	245	243	245	245	245	245	245	243
R-8 (35 ft-lb)	239	237	239	239	239	239	237	237
R-9 (35 ft-lb)	242	239	242	242	242	242	239	225
R-10 (35 ft-lb)	1819	1811	1833	1816	1804	1804	1795	1781

Normalized Clampup Force

Time (hrs):	56.5167	64.2167	72.9167	80.2333	89.2167	99.8167	104.2667	113.80
Specimen								
R-1 (60 ft-lb)	0.809	0.803	0.811	0.801	0.792	0.792	0.784	0.779
R-2 (60 ft-lb)	0.845	0.812	0.825	0.810	0.802	0.802	0.791	0.786
R-3 (60 ft-lb)	0.807	0.800	0.811	0.797	0.788	0.788	0.778	0.772
R-4 (60 ft-lb)	0.815	0.811	0.821	0.812	0.803	0.799	0.794	0.786
R-5 (60 ft-lb)	0.776	0.769	0.774	0.762	0.753	0.751	0.740	0.735
R-6 (35 ft-lb)	0.706	0.706	0.706	0.706	0.697	0.706	0.697	0.697
R-7 (35 ft-lb)	0.664	0.659	0.664	0.664	0.664	0.664	0.664	0.659
R-8 (35 ft-lb)	0.980	0.971	0.980	0.980	0.980	0.980	0.971	0.971
R-9 (35 ft-lb)	0.605	0.598	0.605	0.605	0.605	0.605	0.598	0.563
R-10 (35 ft-lb)	0.902	0.898	0.909	0.901	0.895	0.895	0.890	0.883

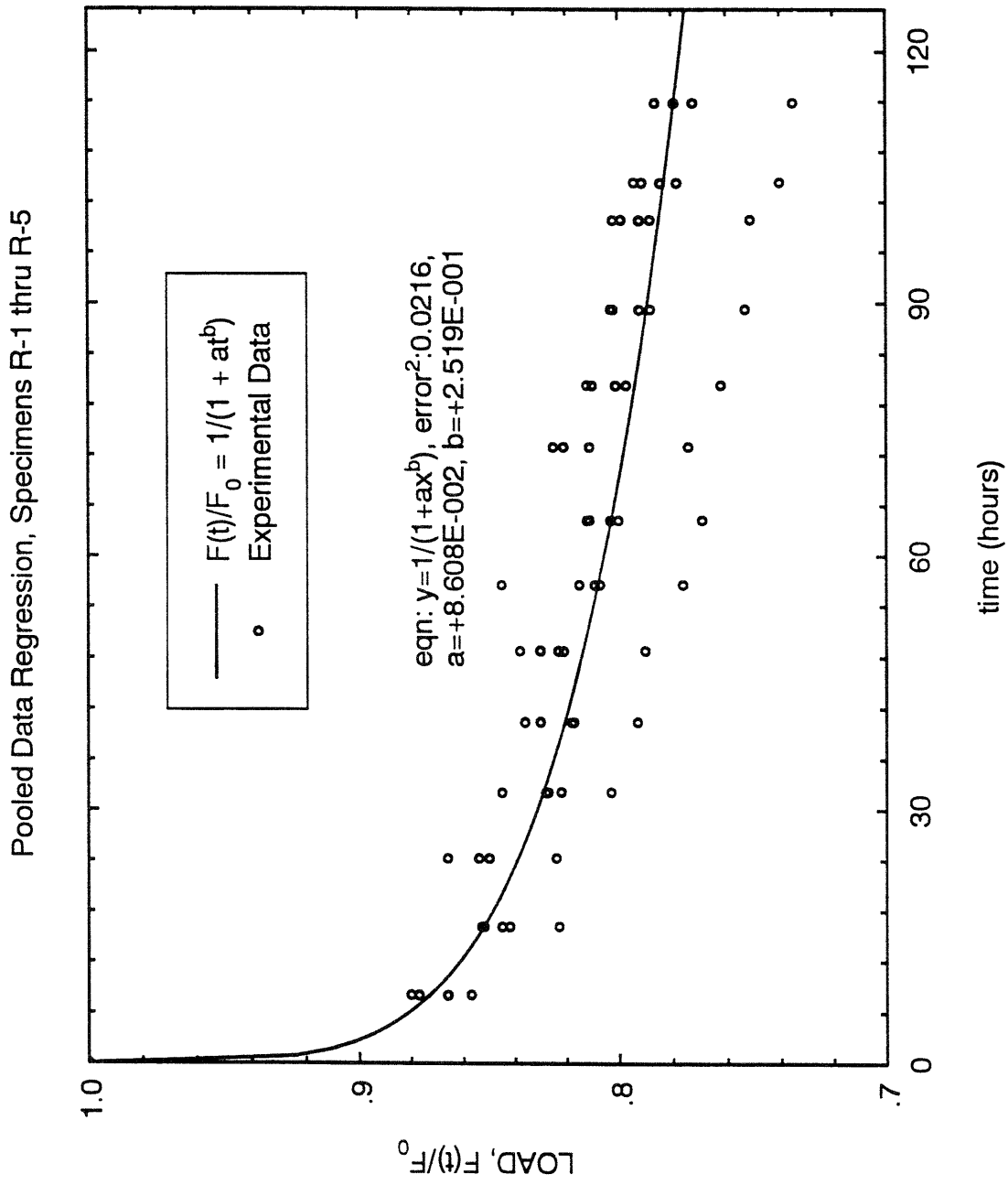
Pooled Data Regression, Specimens R-1 thru R-5
F(t)/F0 = 1/(1 + atb)
Experimental Data
eqn: y=1/(1+axb), error2:0.0216,
a=+8.608E-002, b=+2.519E-001
LOAD, F(t)/Fo
1.0
.9
.8
.7
0
30
60
90
120
time (hours)

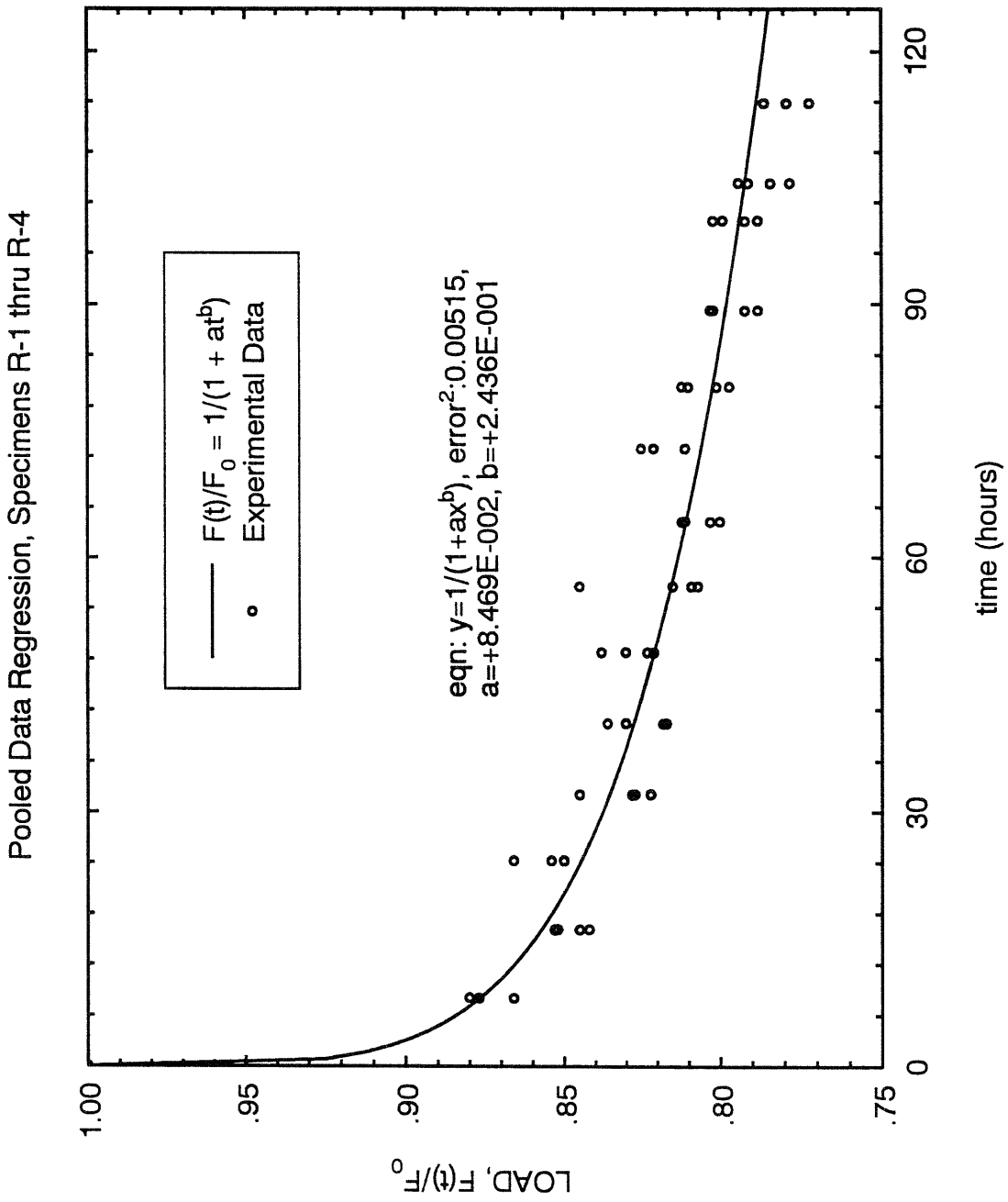
Pooled Data Regression, Specimens R-1 thru R-4
F(t)/F0 = 1/(1 + atb)
Experimental Data
eqn: y=1/(1+axb), error2:0.00515,
a=+8.469E-002, b=+2.436E-001
LOAD, F(t)/F0
1.00
.95
.90
.85
.80
.75
0
30
60
90
120
time (hours)

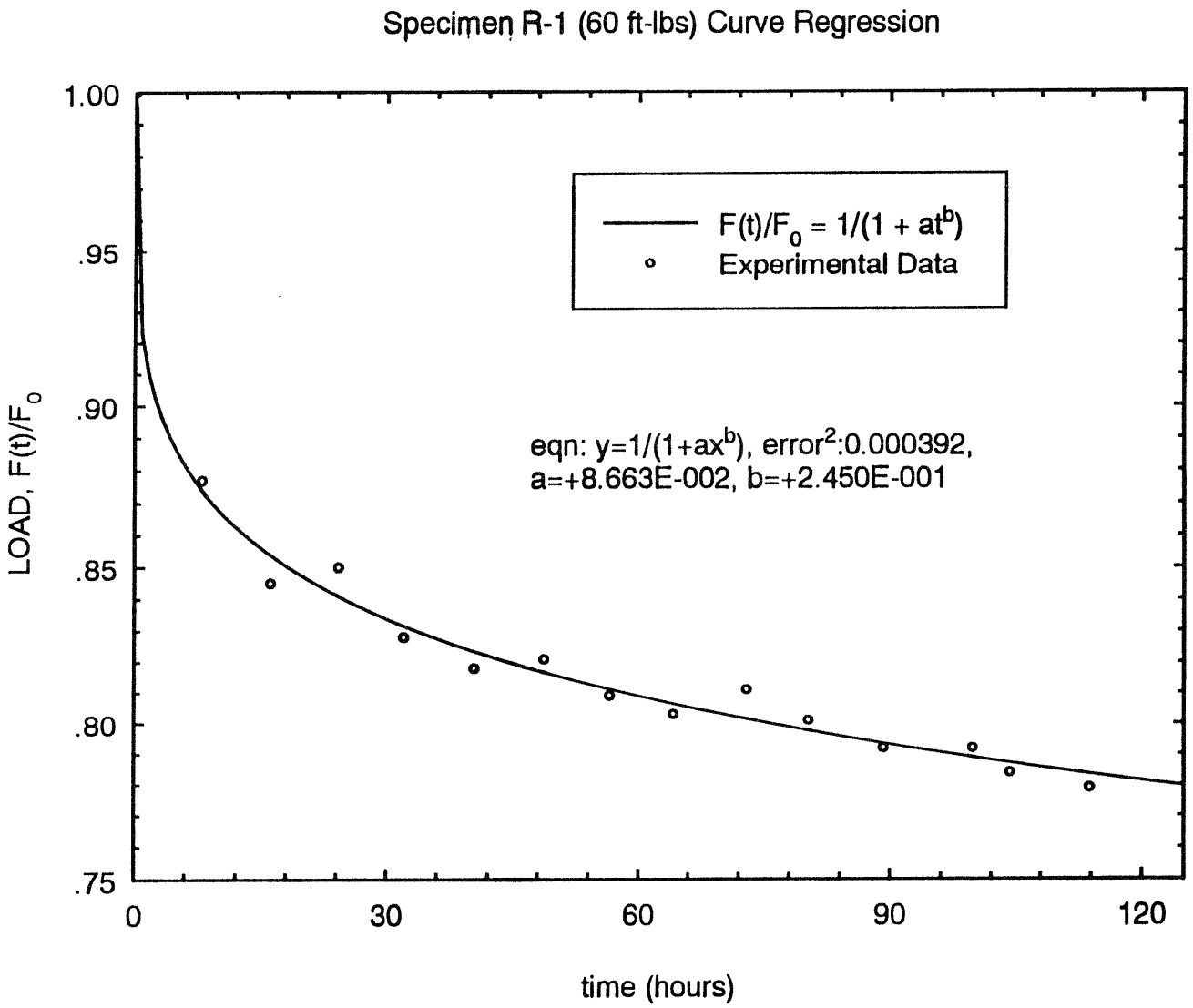
Specimen R-1 (60 ft-lbs) Curve Regression
1.00
.95
.90
.85
.80
.75
LOAD, F(t)/F0
0
30
60
90
120
time (hours)
F(t)/F0 = 1/(1 + at^b)
Experimental Data
eqn: y=1/(1+ax^b), error^2:0.000392,
a=+8.663E-002, b=+2.450E-001

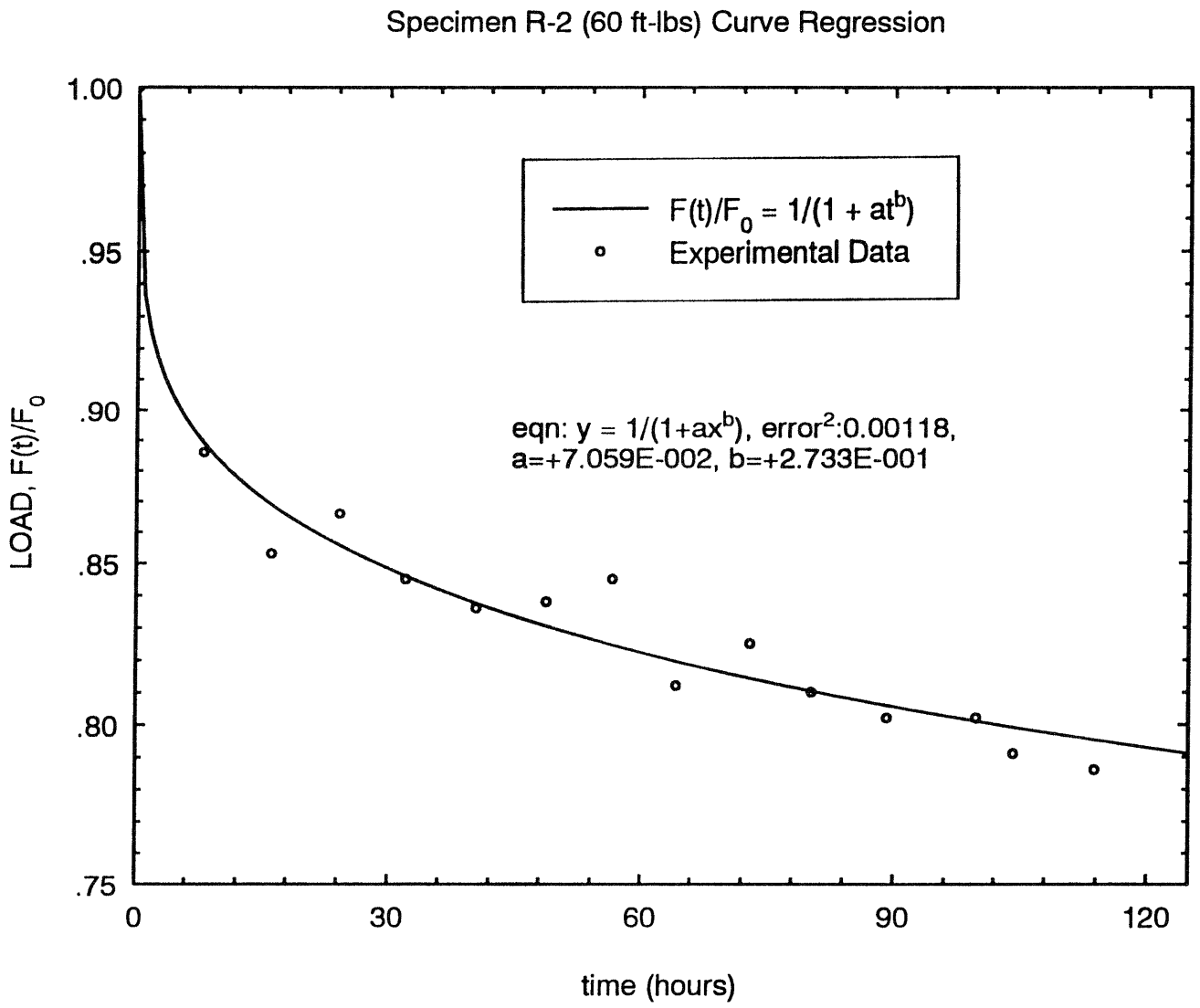
Specimen R-2 (60 ft-lbs) Curve Regression
1.00
.95
.90
.85
.80
.75
LOAD, F(t)/F0
0
30
60
90
120
time (hours)
F(t)/F0 = 1/(1 + atb)
Experimental Data
eqn: y = 1/(1+axb), error2:0.00118,
a=+7.059E-002, b=+2.733E-001

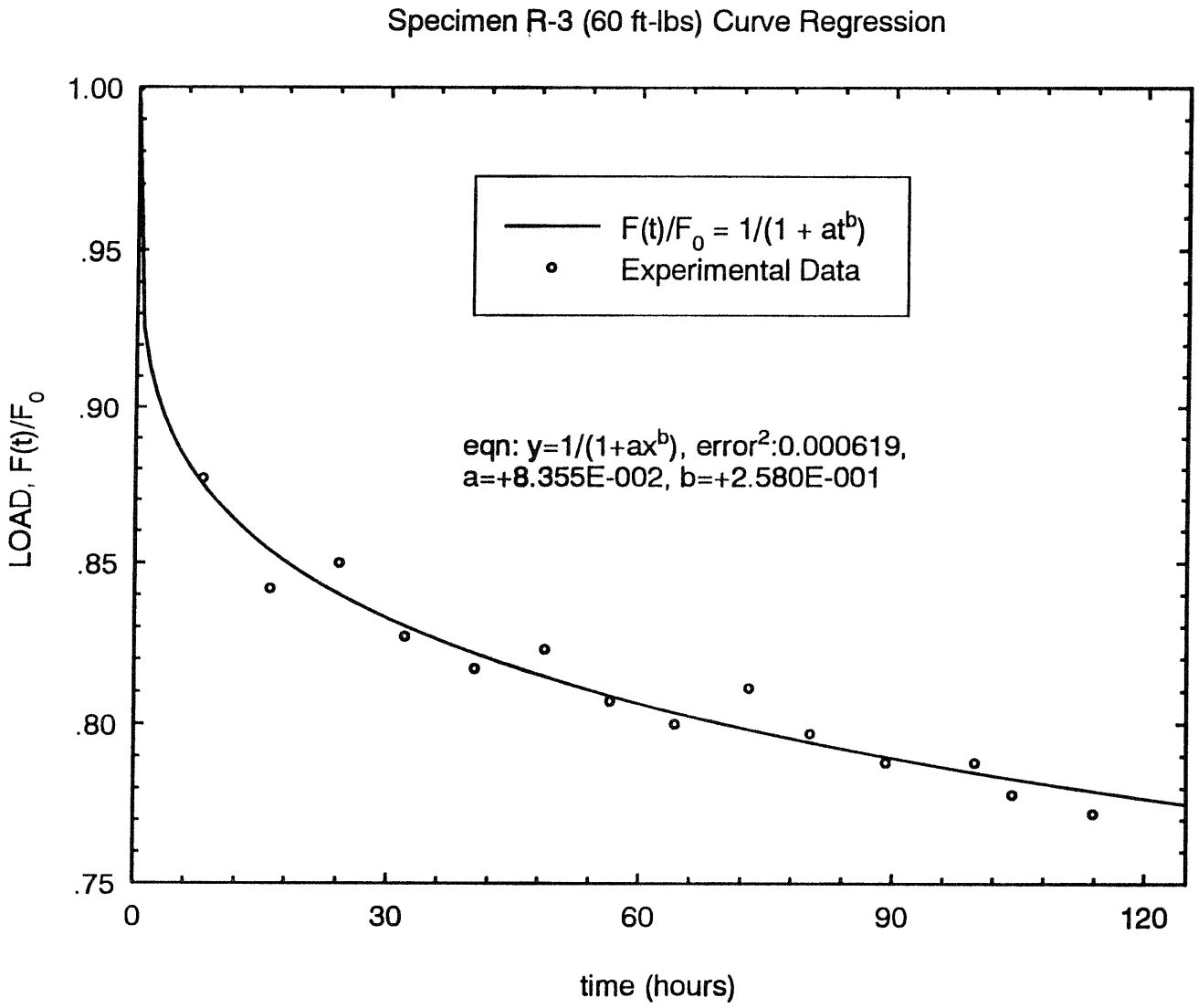
Specimen R-3 (60 ft-lbs) Curve Regression
1.00
.95
.90
.85
.80
.75
LOAD, F(t)/F0
0
30
60
90
120
time (hours)
F(t)/F0 = 1/(1 + at^b)
Experimental Data
eqn: y=1/(1+ax^b), error^2:0.000619,
a=+8.355E-002, b=+2.580E-001

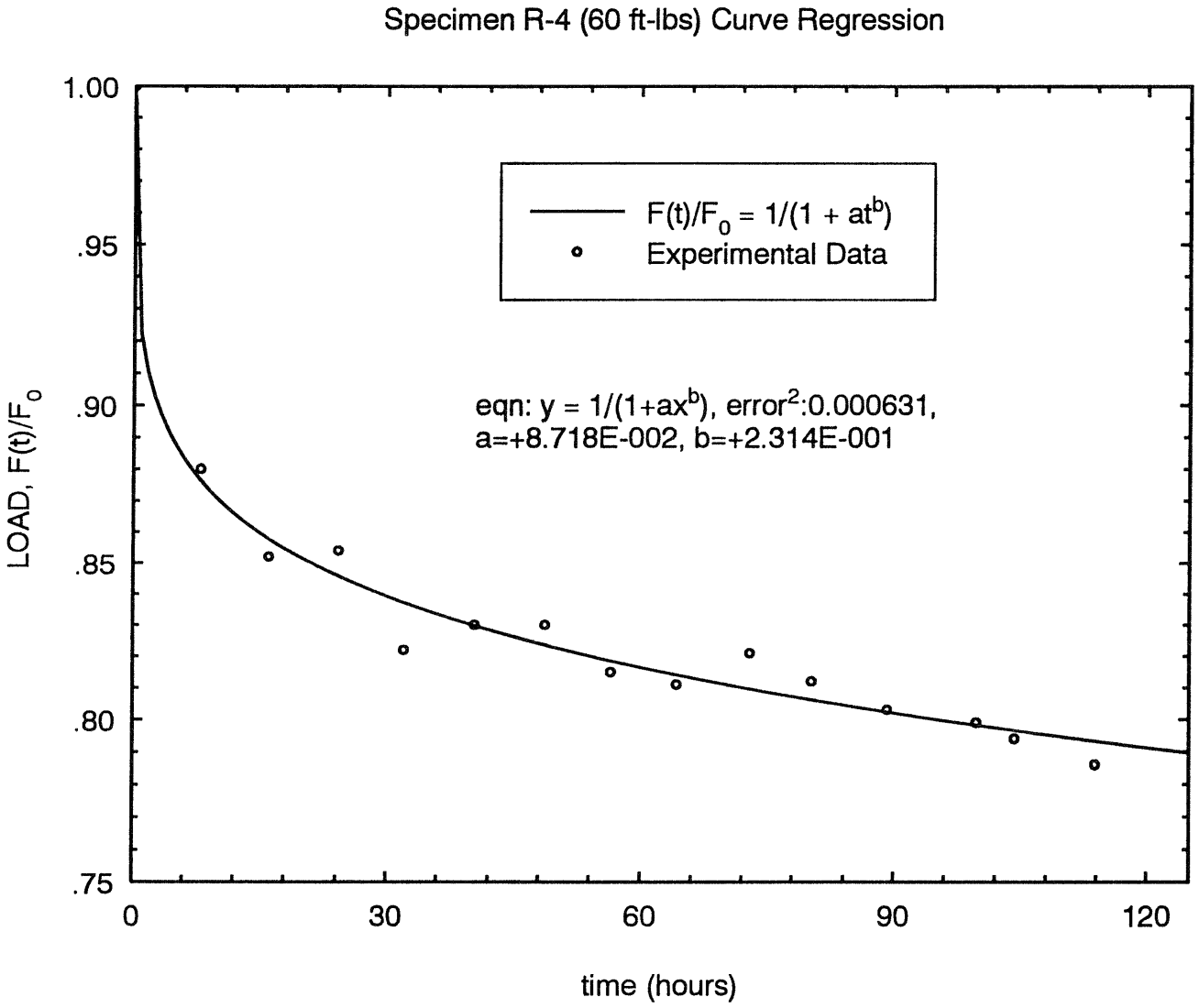
Specimen R-4 (60 ft-lbs) Curve Regression
1.00
.95
.90
.85
.80
.75
LOAD, F(t)/F0
0
30
60
90
120
time (hours)
F(t)/F0 = 1/(1 + at^b)
Experimental Data
eqn: y = 1/(1+ax^b), error^2:0.000631,
a=+8.718E-002, b=+2.314E-001

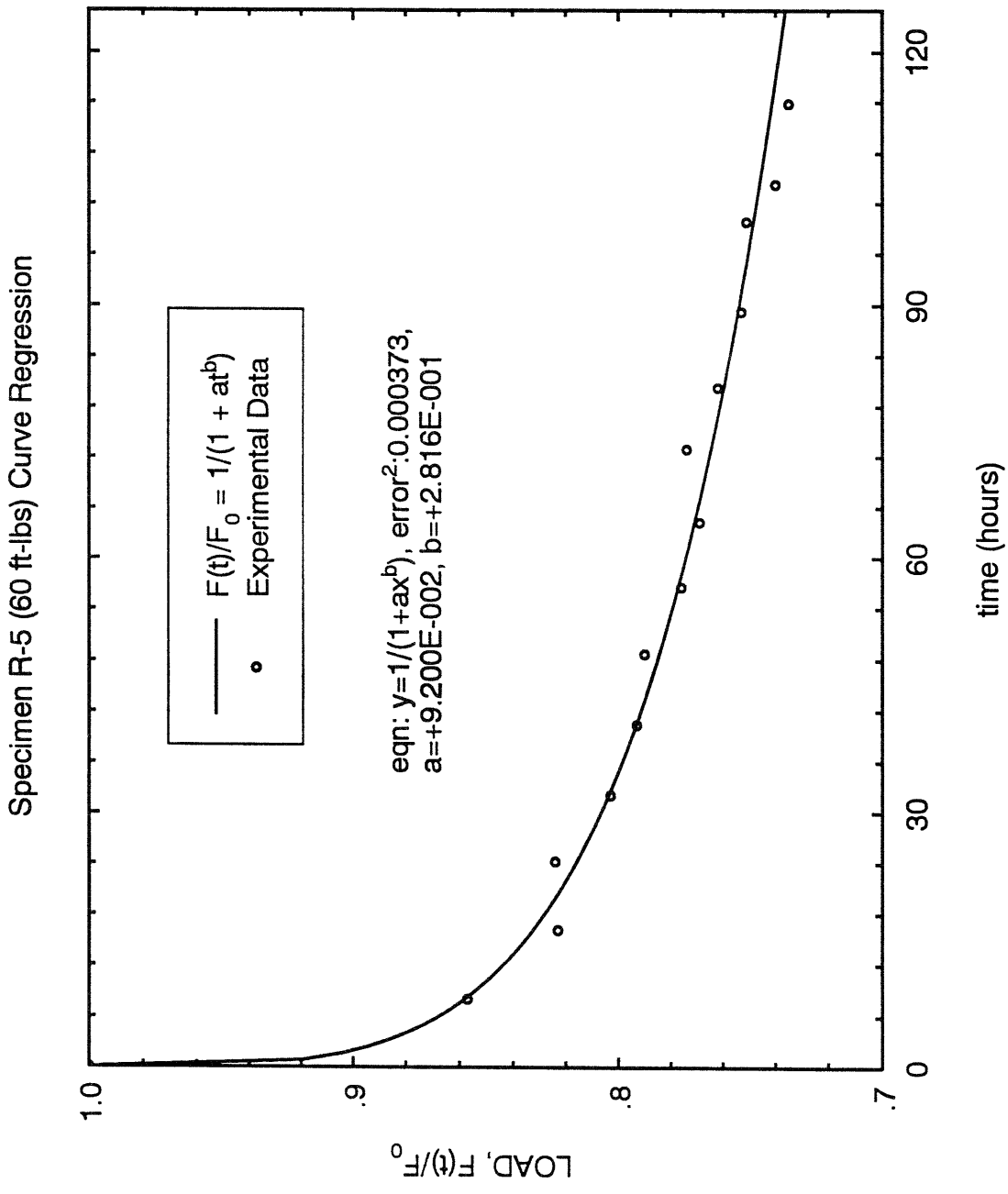
Specimen R-5 (60 ft-lbs) Curve Regression
F(t)/F0 = 1/(1 + at^b)
Experimental Data
eqn: y=1/(1+ax^b), error^2:0.000373,
a=+9.200E-002, b=+2.816E-001
LOAD, F(t)/Fo
time (hours)
1.0
.9
.8
.7
0
30
60
90
120

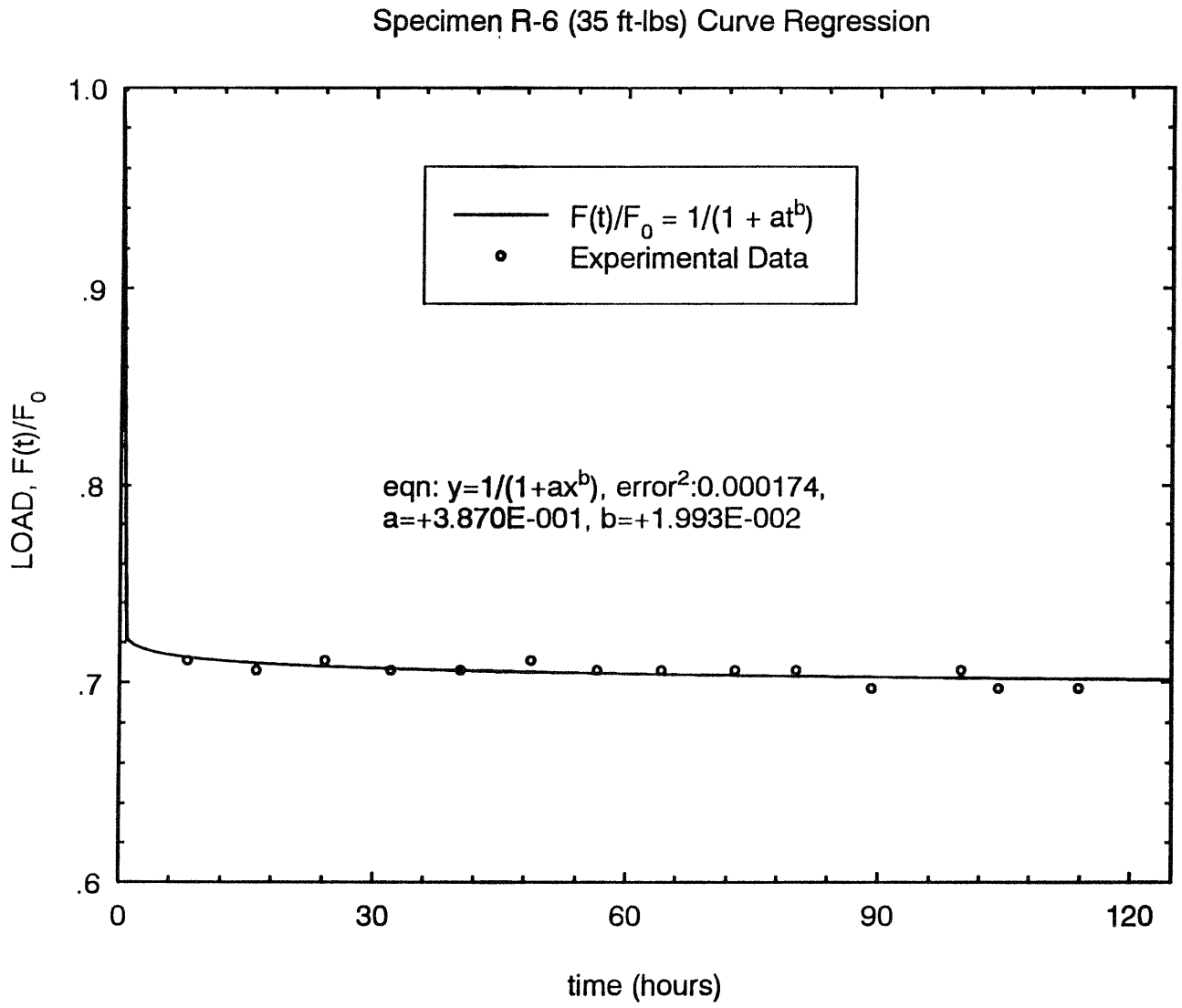
Specimen R-6 (35 ft-lbs) Curve Regression
1.0
.9
.8
.7
.6
LOAD, F(t)/F0
F(t)/F0 = 1/(1 + atb)
Experimental Data
eqn: y=1/(1+axb), error2:0.000174,
a=+3.870E-001, b=+1.993E-002
0
30
60
90
120
time (hours)

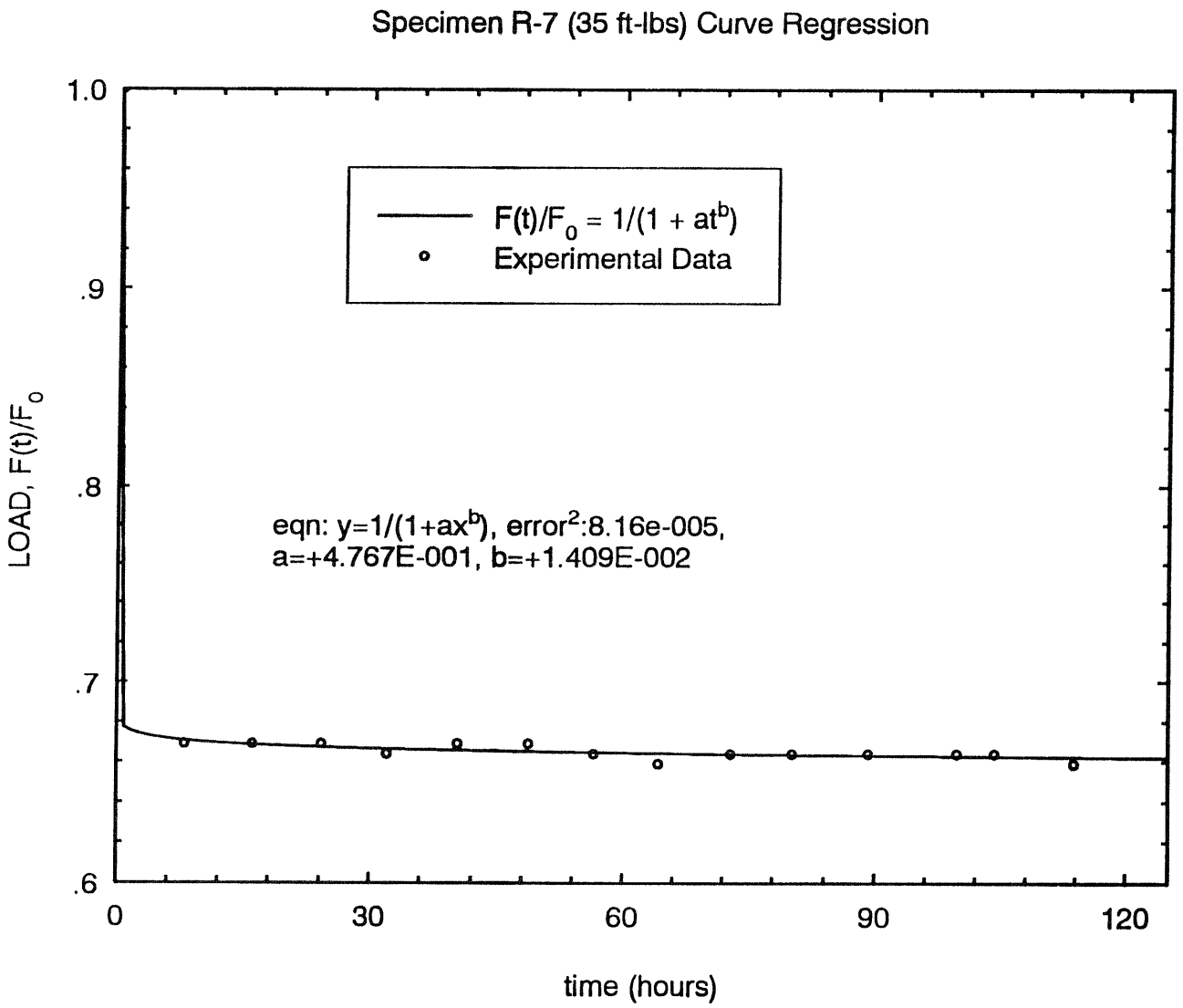
Specimen R-7 (35 ft-lbs) Curve Regression
1.0
.9
.8
.7
.6
LOAD, F(t)/F0
F(t)/F0 = 1/(1 + atb)
Experimental Data
eqn: y=1/(1+axb), error2:8.16e-005,
a=+4.767E-001, b=+1.409E-002
0
30
60
90
120
time (hours)

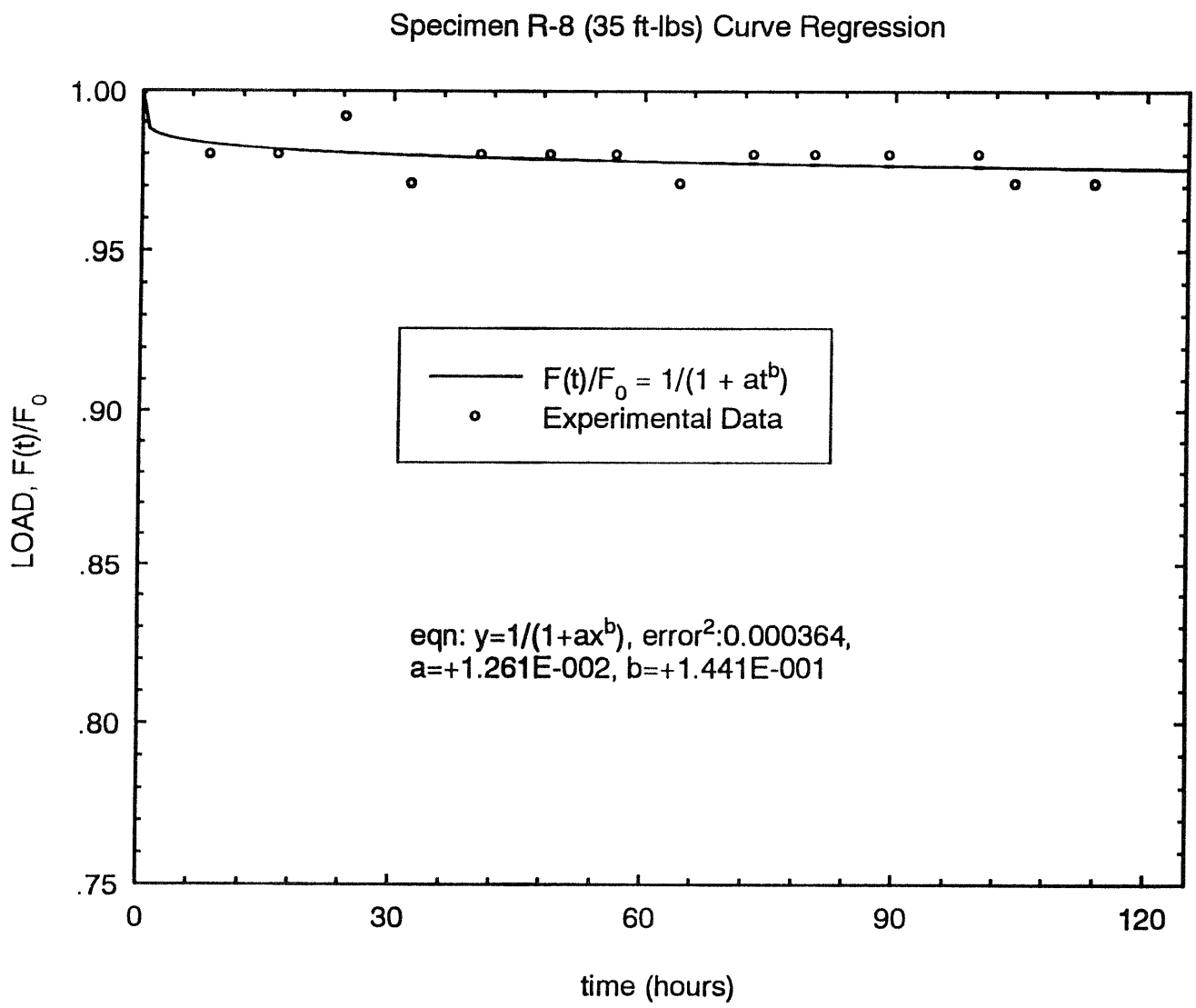
Specimen R-8 (35 ft-lbs) Curve Regression
1.00
.95
.90
.85
.80
.75
LOAD, F(t)/F0
0
30
60
90
120
time (hours)
F(t)/F0 = 1/(1 + at^b)
Experimental Data
eqn: y=1/(1+ax^b), error^2:0.000364,
a=+1.261E-002, b=+1.441E-001

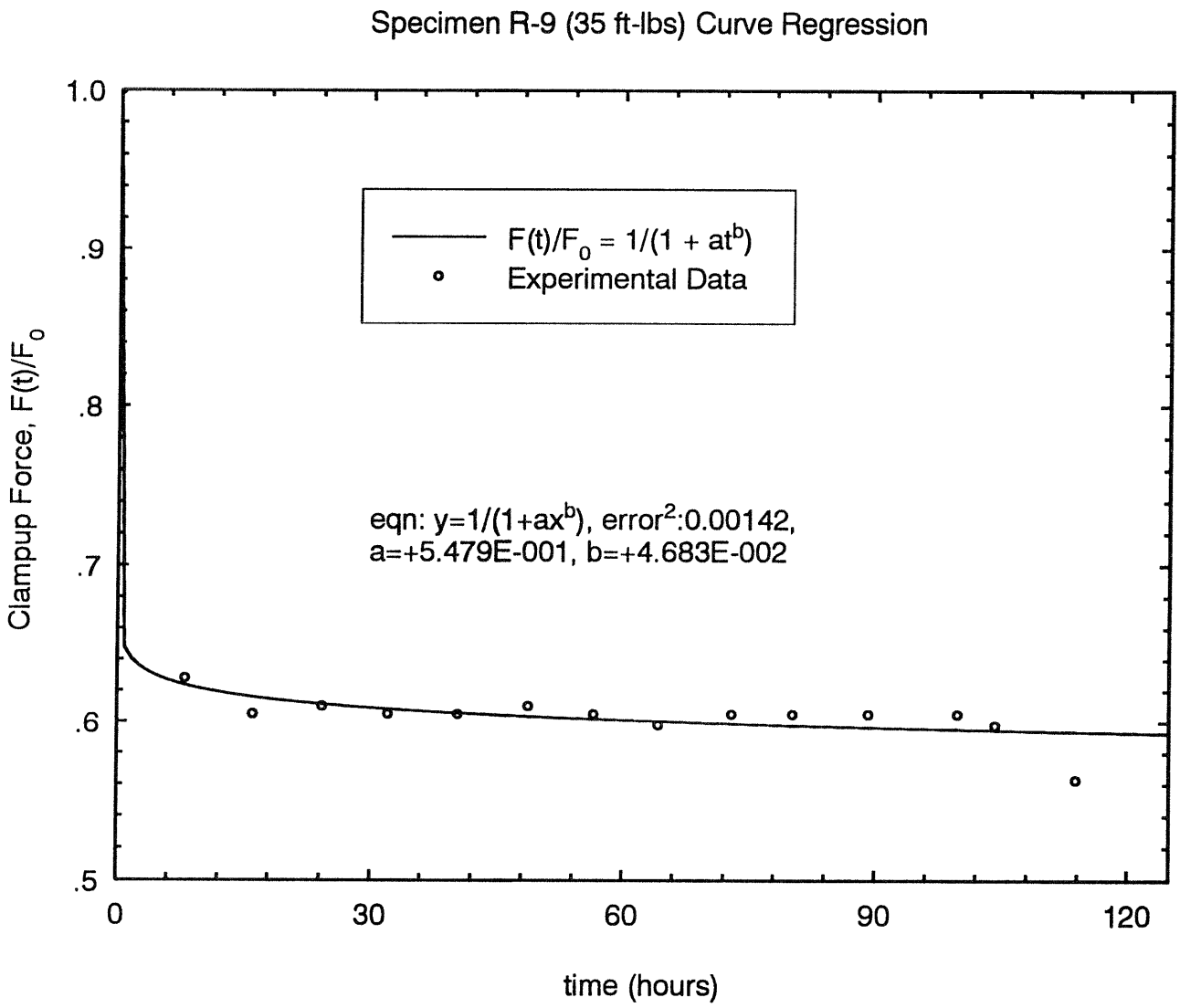
Specimen R-9 (35 ft-lbs) Curve Regression
1.0
.9
.8
.7
.6
.5
Clampup Force, F(t)/F0
0
30
60
90
120
time (hours)
F(t)/F0 = 1/(1 + at^b)
Experimental Data
eqn: y=1/(1+ax^b), error^2:0.00142,
a=+5.479E-001, b=+4.683E-002

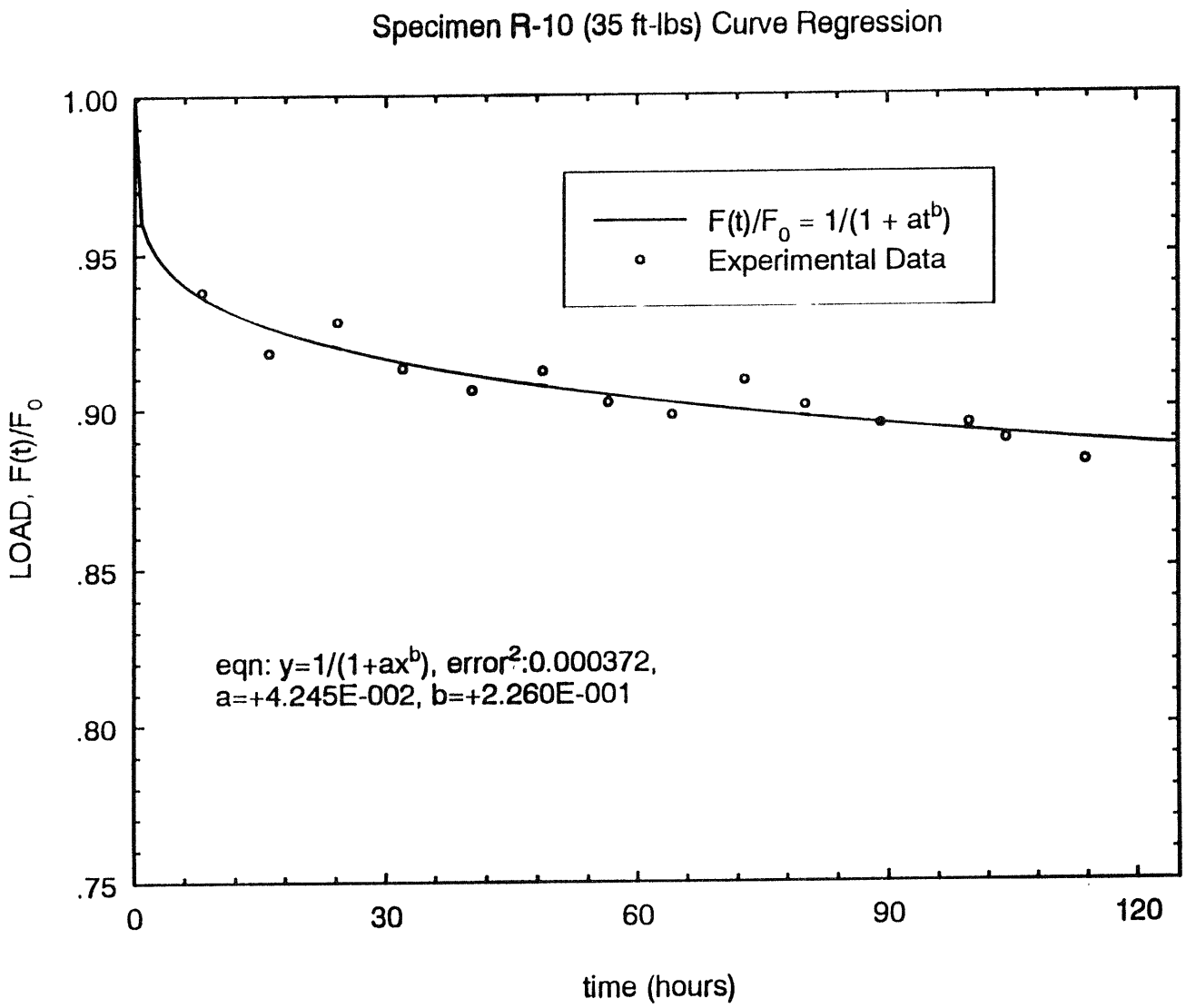
Specimen R-10 (35 ft-lbs) Curve Regression
1.00
.95
.90
.85
.80
.75
LOAD, F(t)/F0
0
30
60
90
120
time (hours)
F(t)/F0 = 1/(1 + atb)
Experimental Data
eqn: y=1/(1+axb), error2:0.000372,
a=+4.245E-002, b=+2.260E-001

Appendix C. Bearing Strength Experiment Load-Displacement Curves

This Appendix contains the testing machine-generated load-displacement curves for the twenty bearing strength specimens. The curves for specimens BS-1, BS-2, BS-3, BS-5, BS-13, and BS-14 are not continuous; this was a result of an initial plotting scale setting that was too high. On the graphs for the indicated specimens, the plotting scale was changed when the pen approached the edge of the paper during the experiment. This caused the pen to re-position itself on the paper, and accounts for the discontinuities in the curves.

SPECIMEN BS-1
Protruding Head Bolt
50 ft-lbs Torque
11 April 1994

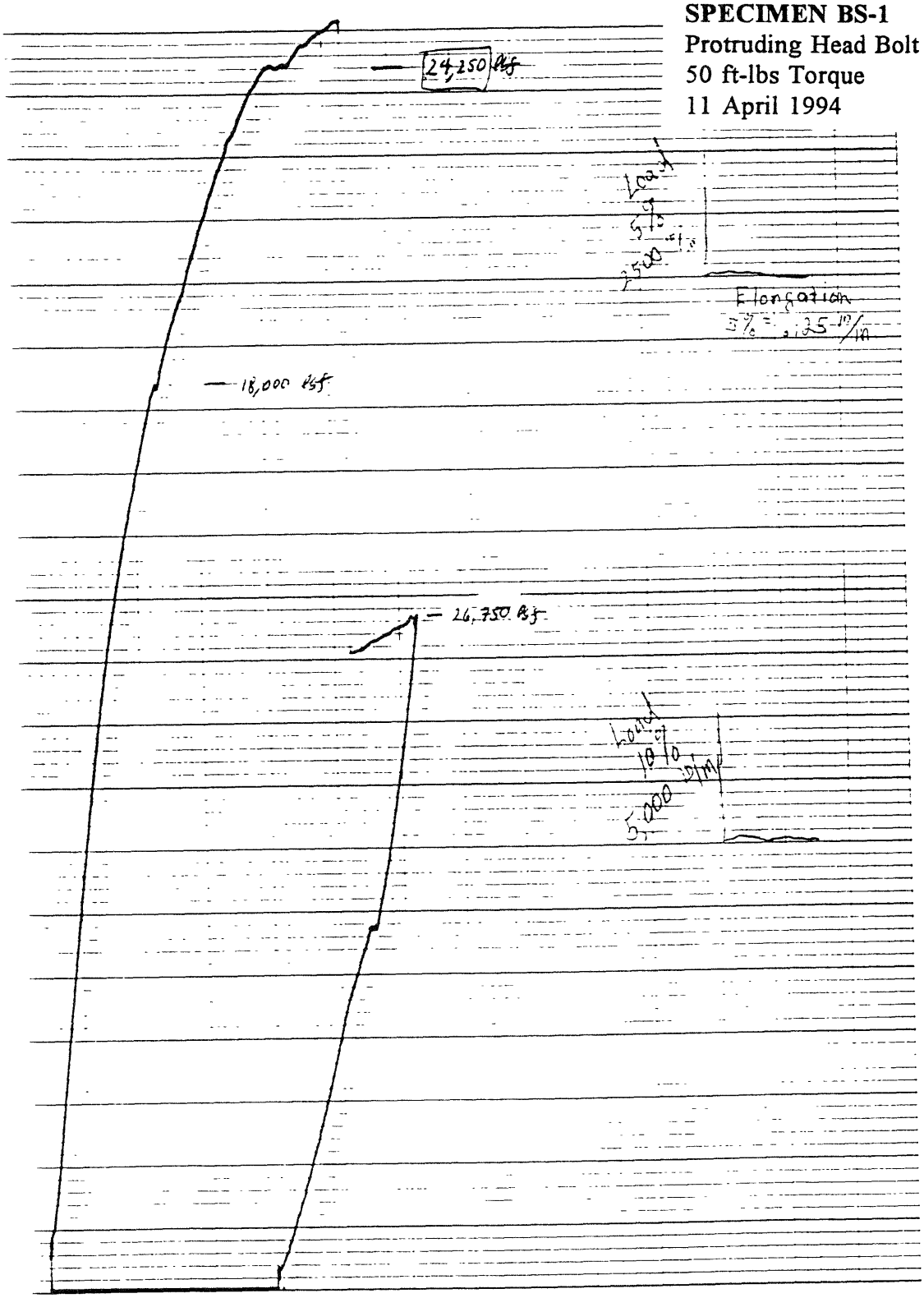

SPECIMEN BS-2
Countersunk Bolt
50 ft-lbs Torque
11 April 1994

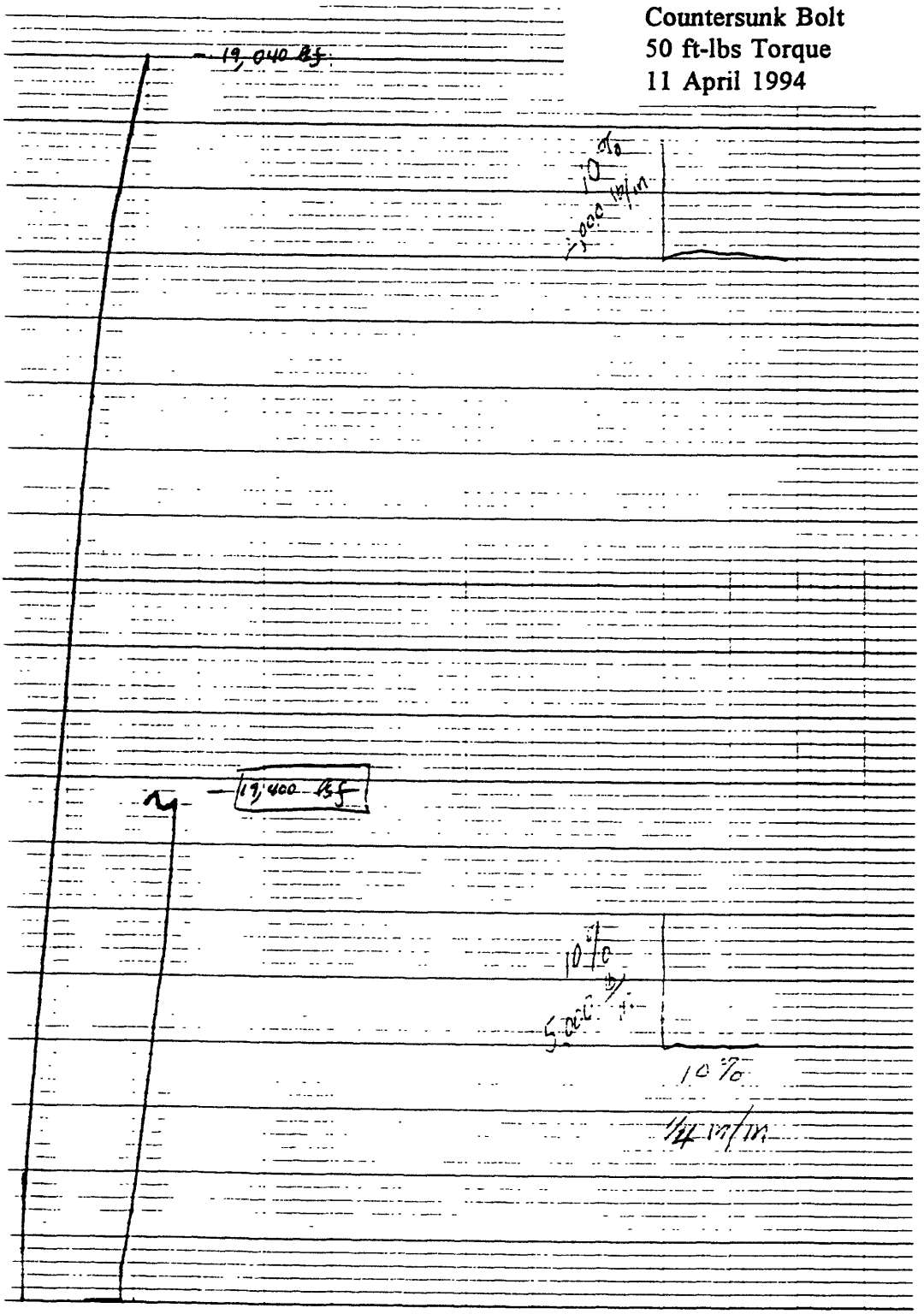

SPECIMEN BS-3
Countersunk Bolt
50 ft-lbs Torque
19 April 1994

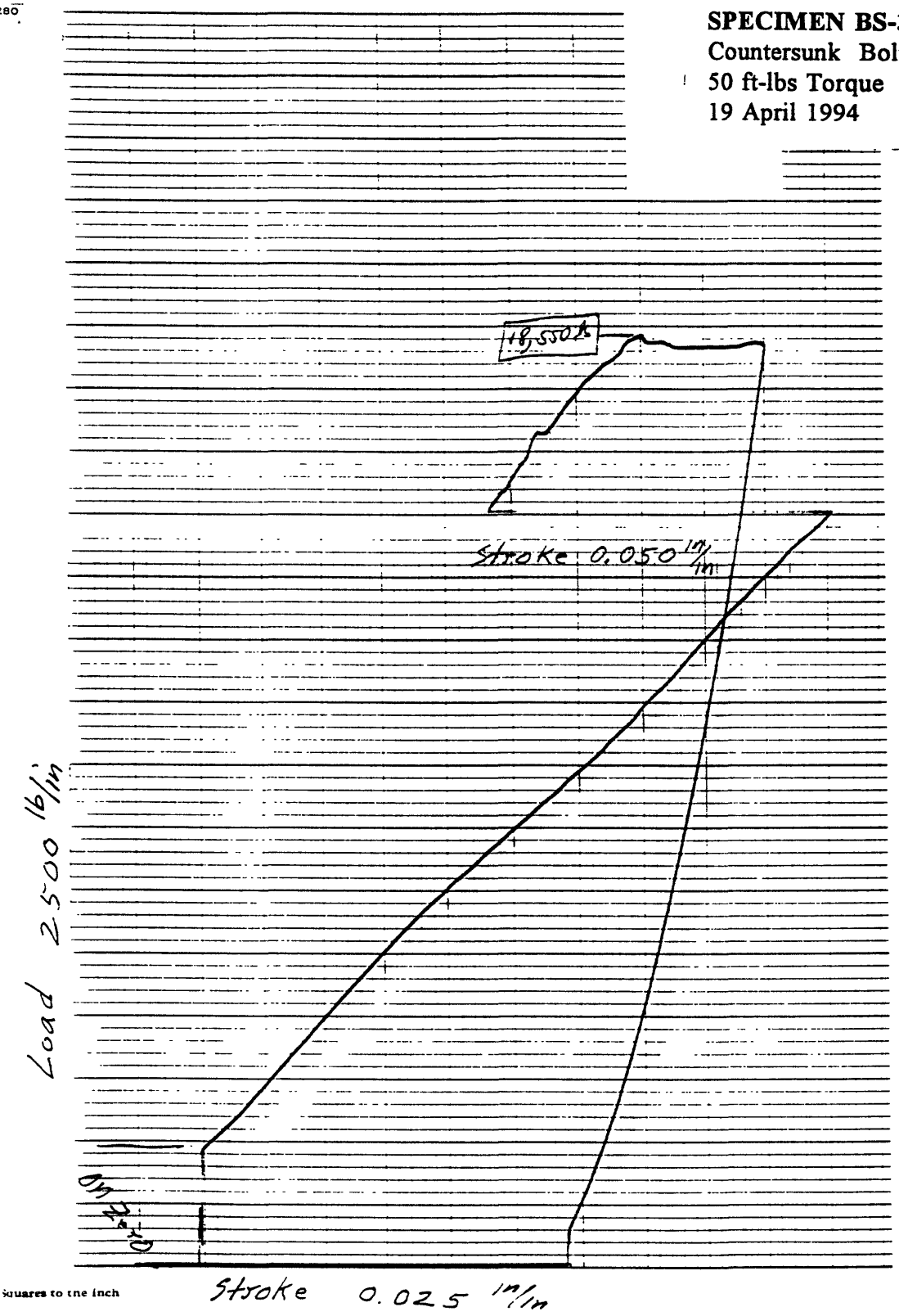

Squares to the inch

SPECIMEN BS-4
Countersunk Bolt
50 ft-lbs Torque
19 April 1994

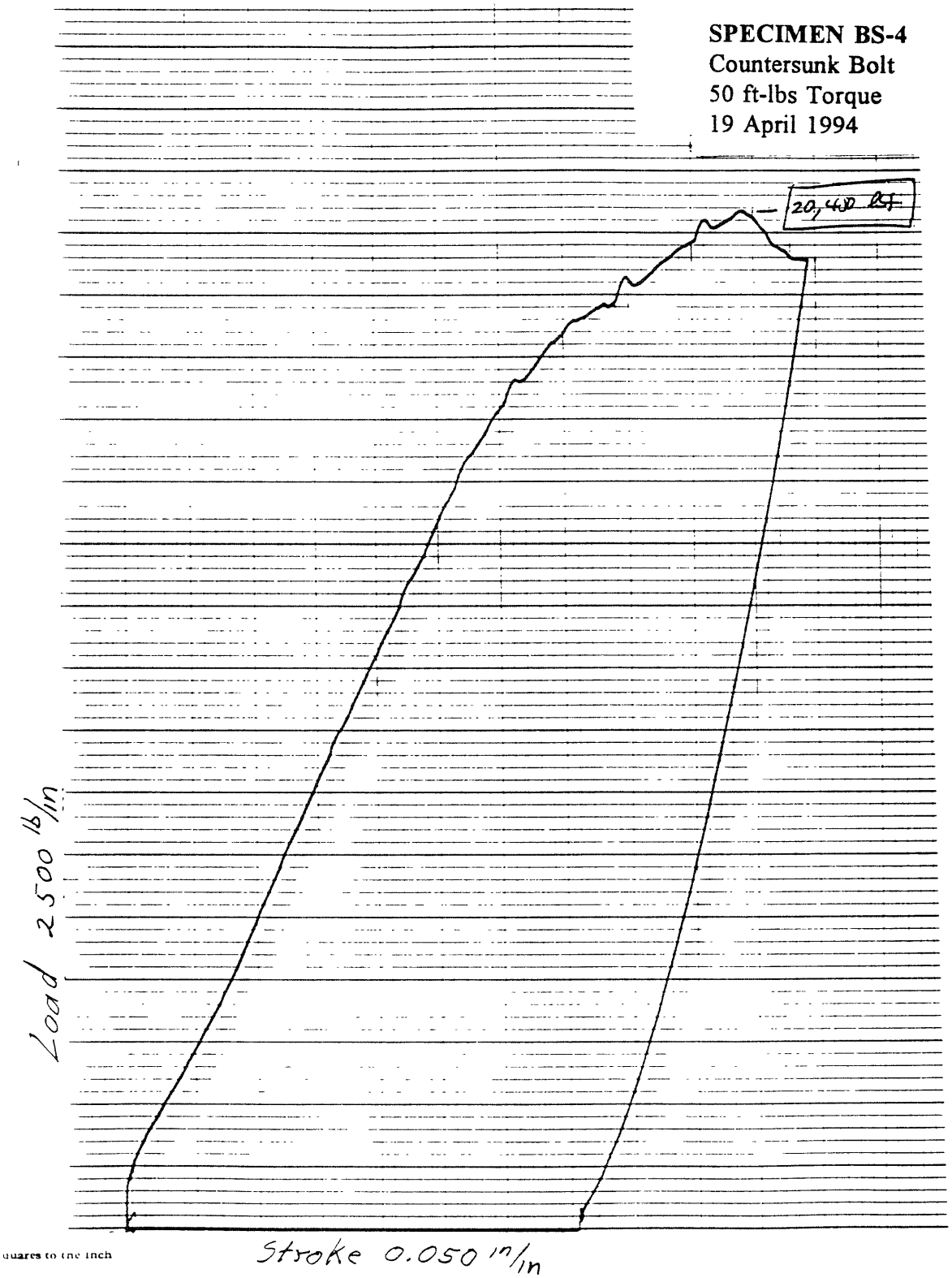

SPECIMEN BS-5
Countersunk Bolt
50 ft-lbs Torque
19 April 1994

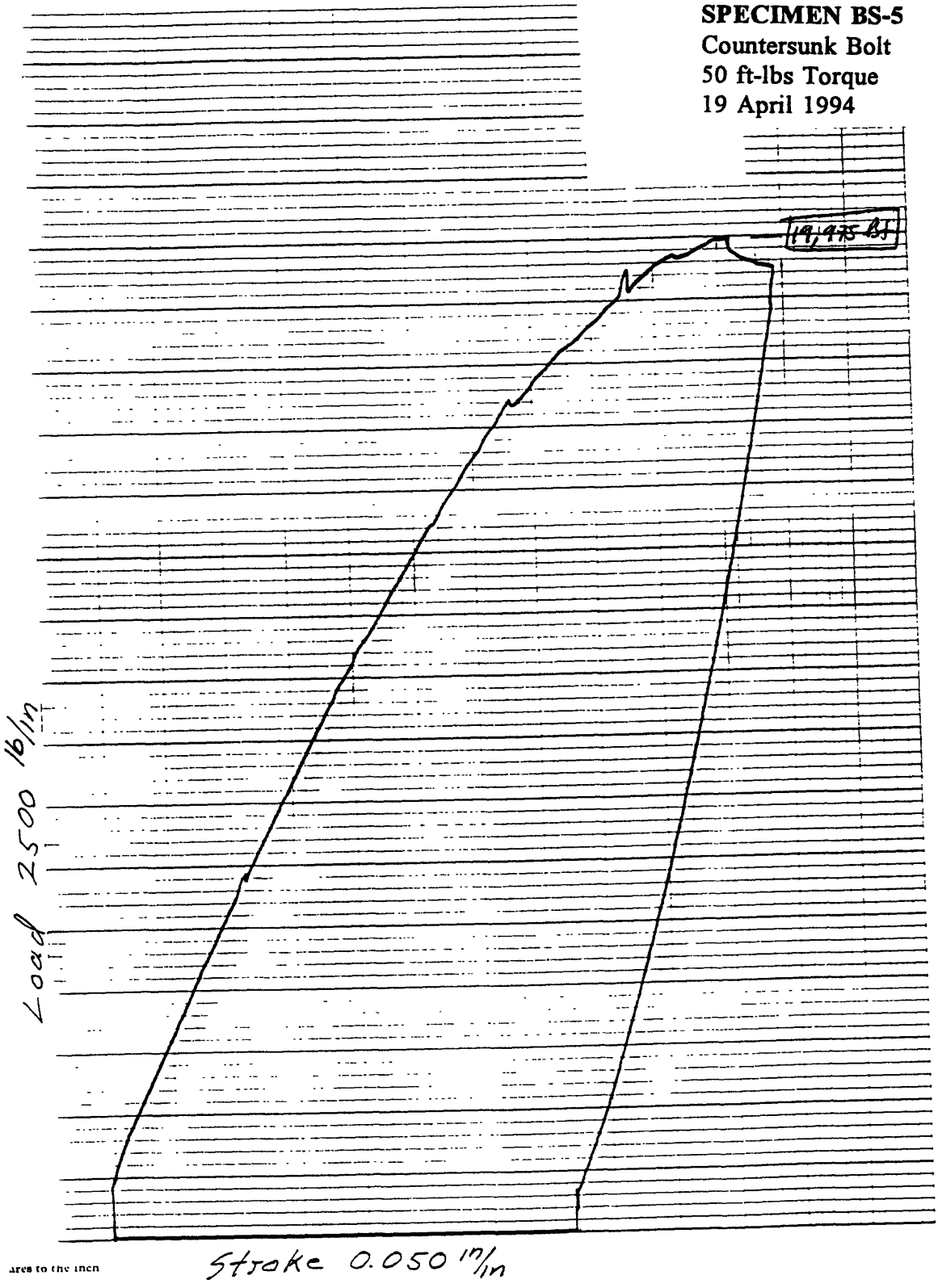

SPECIMEN BS-6
Protruding Head Bolt
33 ft-lbs Torque
19 April 1994

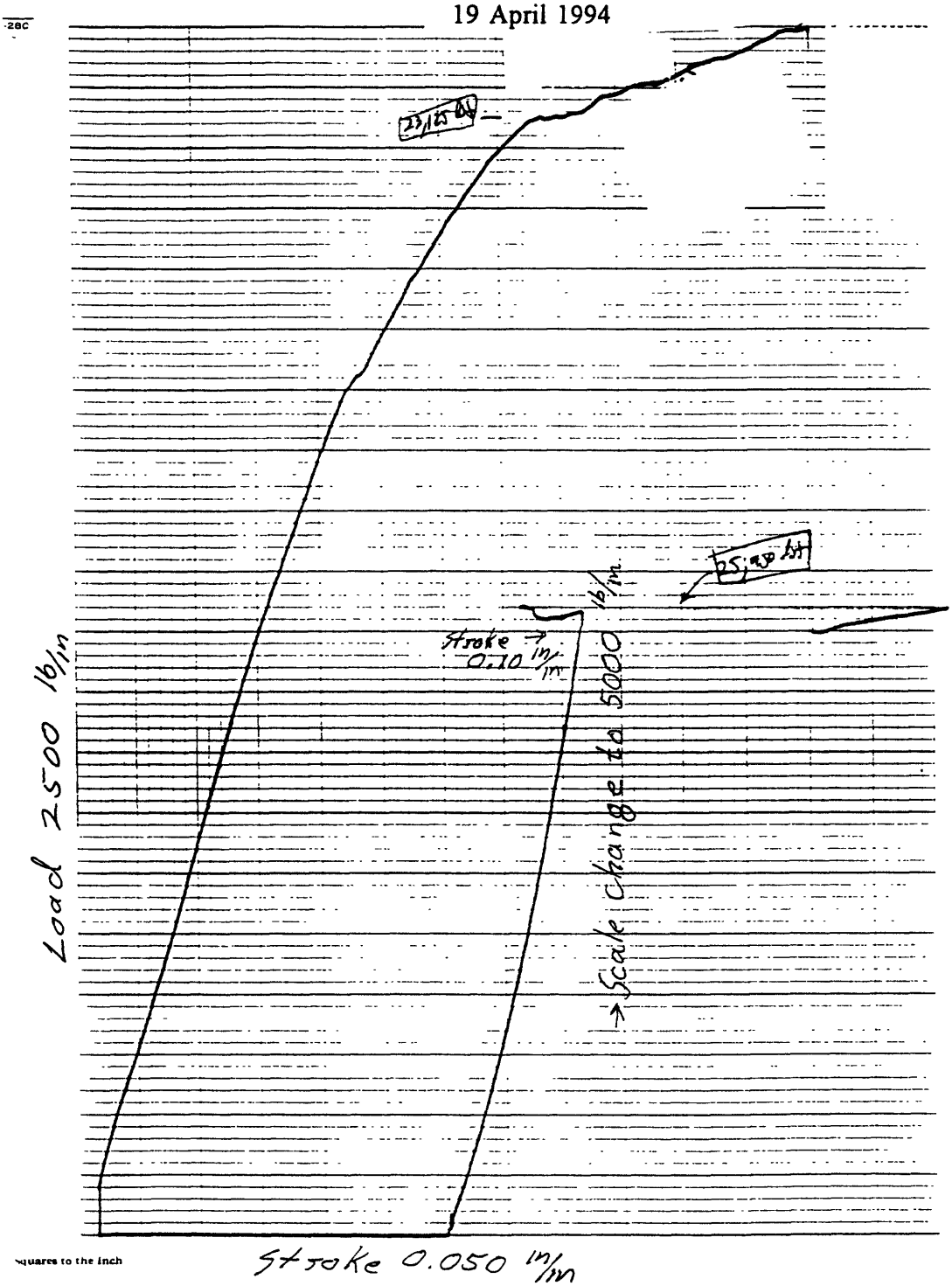

SPECIMEN BS-7
Countersunk Bolt
33 ft-lbs Torque
14 April 1994

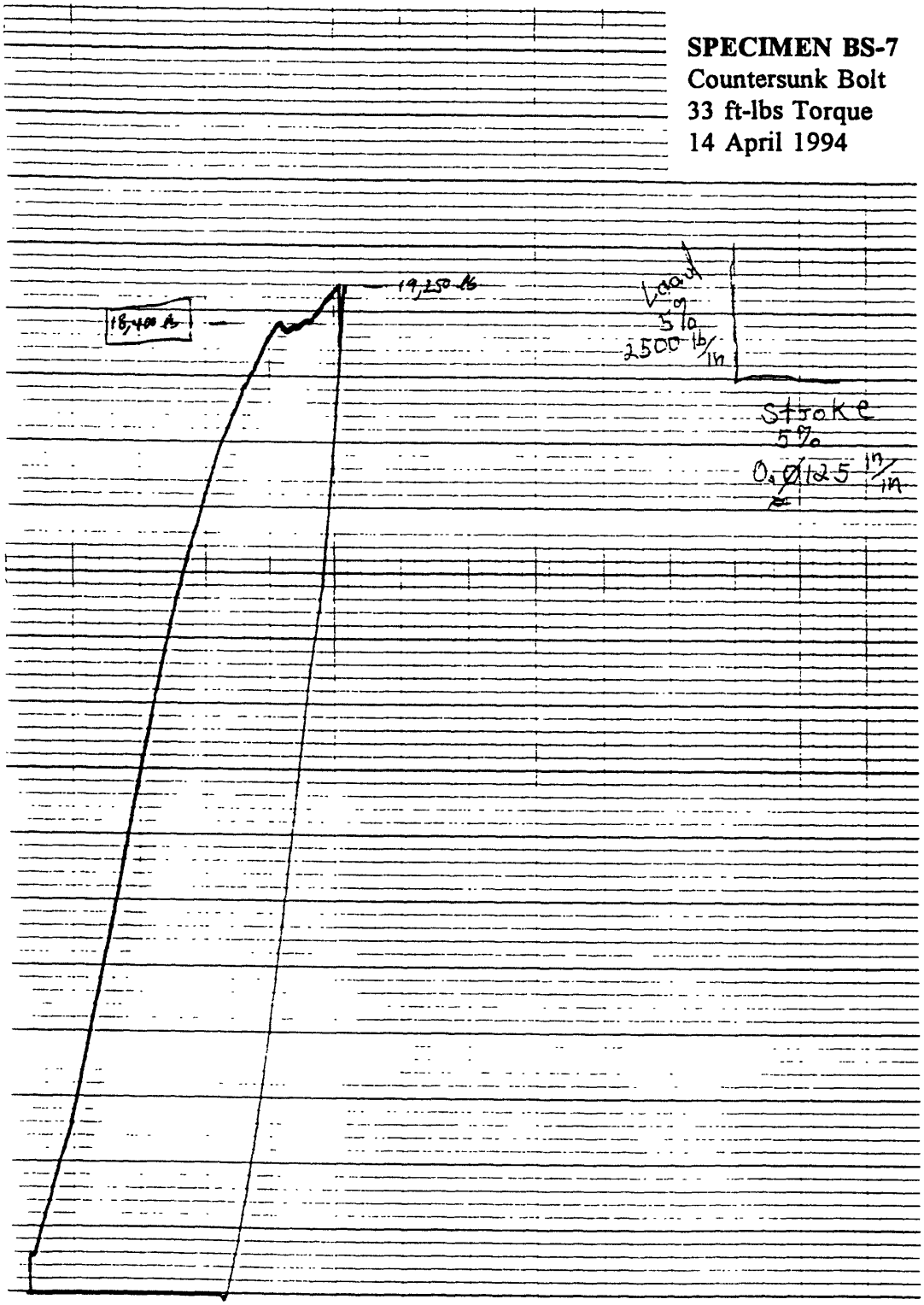

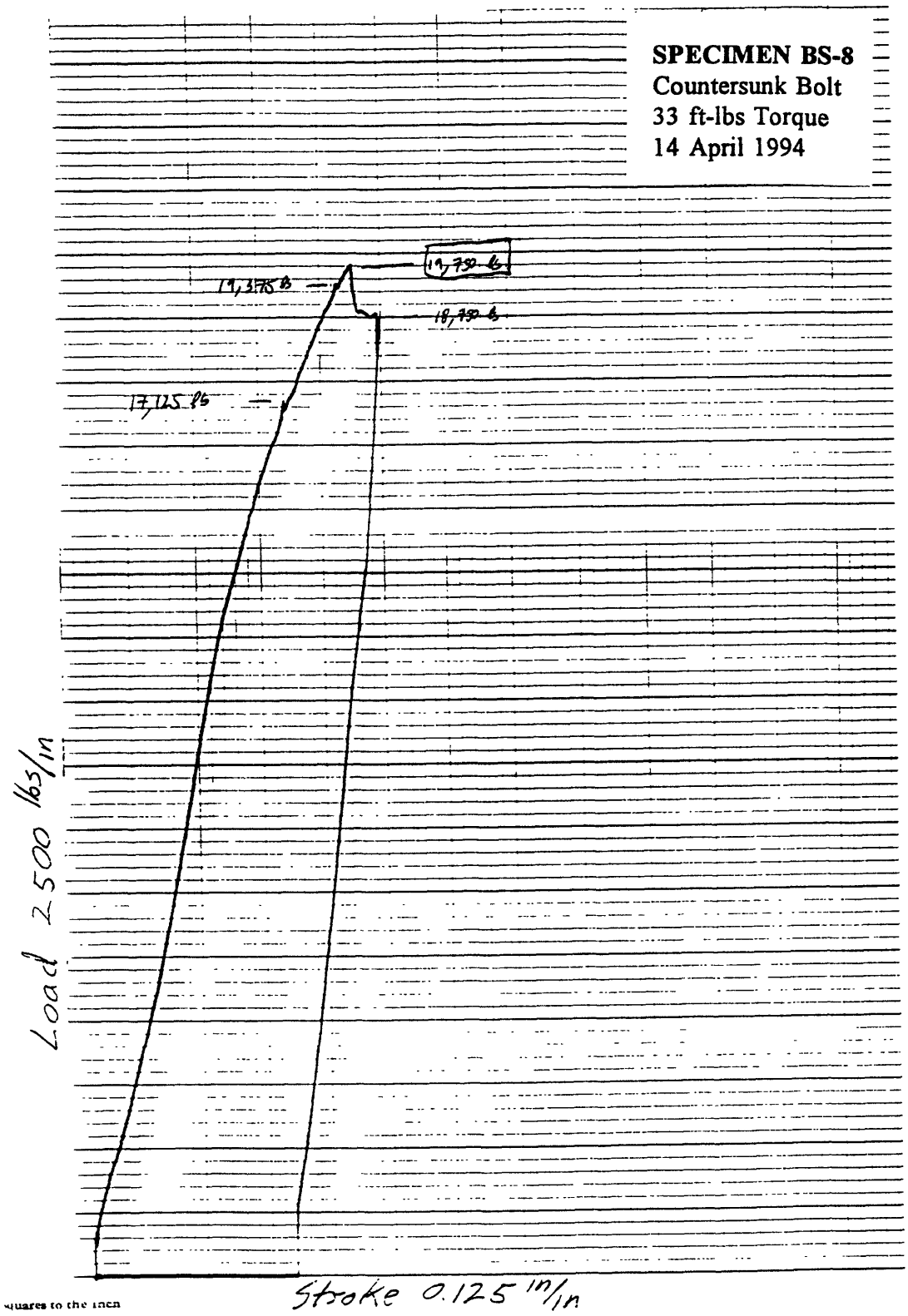
SPECIMEN BS-8
Countersunk Bolt
33 ft-lbs Torque
14 April 1994
19,750 lb
19,375 lb
18,750 lb
17,125 lb
Load 2500 lbs/in
Stroke 0.125 in/in
squares to the inch

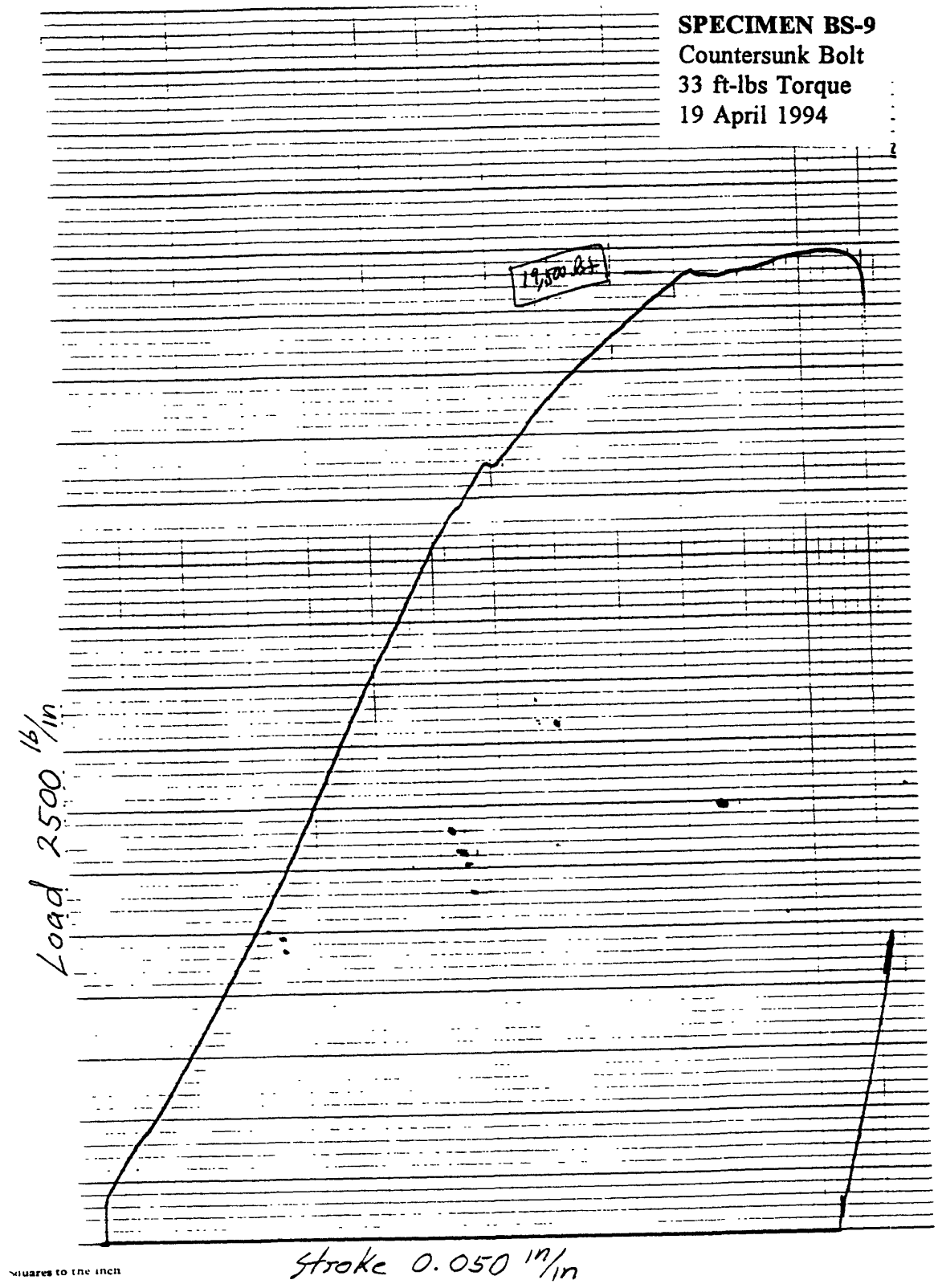
SPECIMEN BS-9
Countersunk Bolt
33 ft-lbs Torque
19 April 1994
19,500 lbf
Load 2500 lb/in
Stroke 0.050 in/in
squares to the inch

SPECIMEN BS-10
Countersunk Bolt
33 ft-lbs Torque
19 April 1994

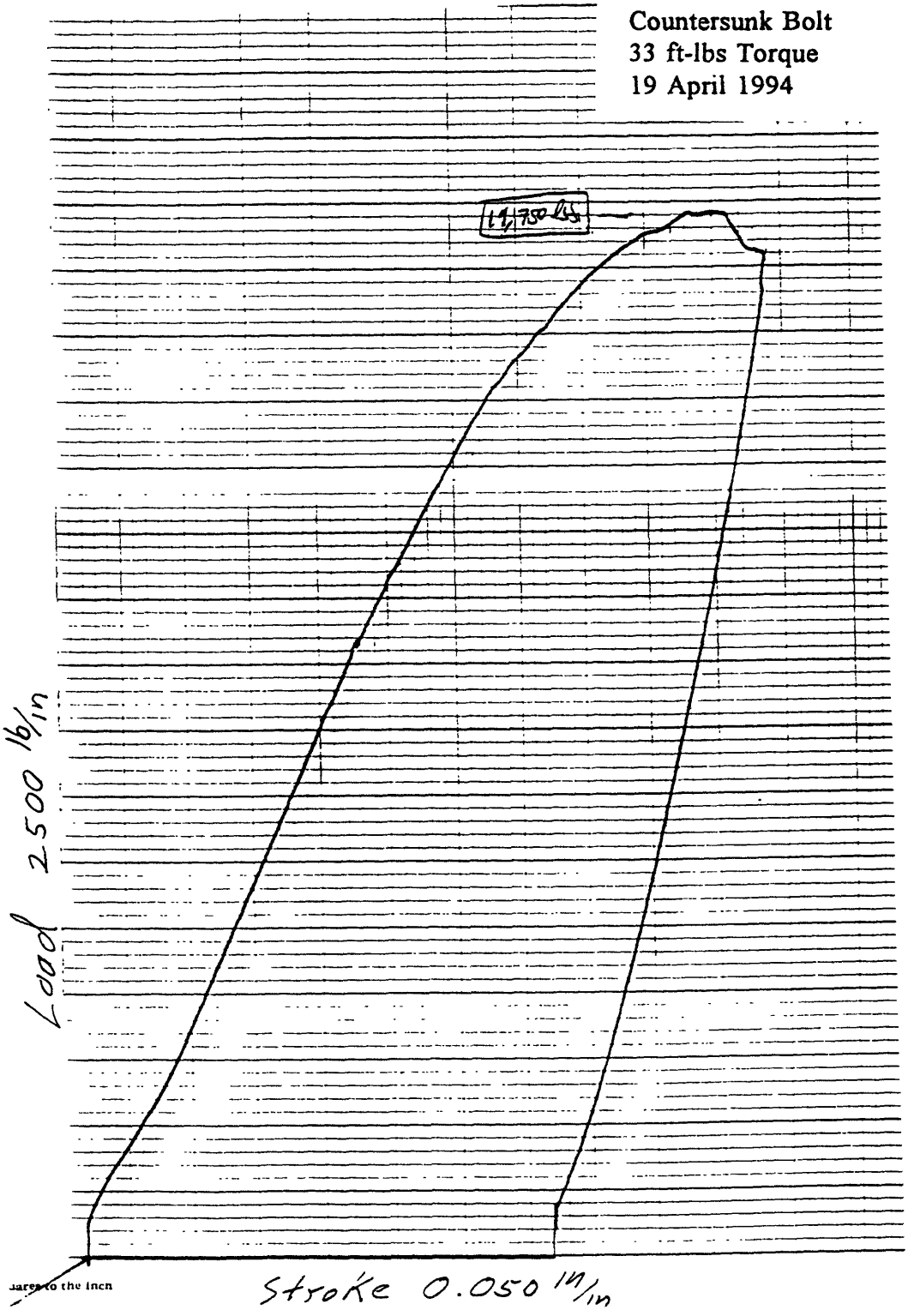

SPECIMEN BS-11
Protruding Head Bolt
17 ft-lbs Torque
19 April 1994

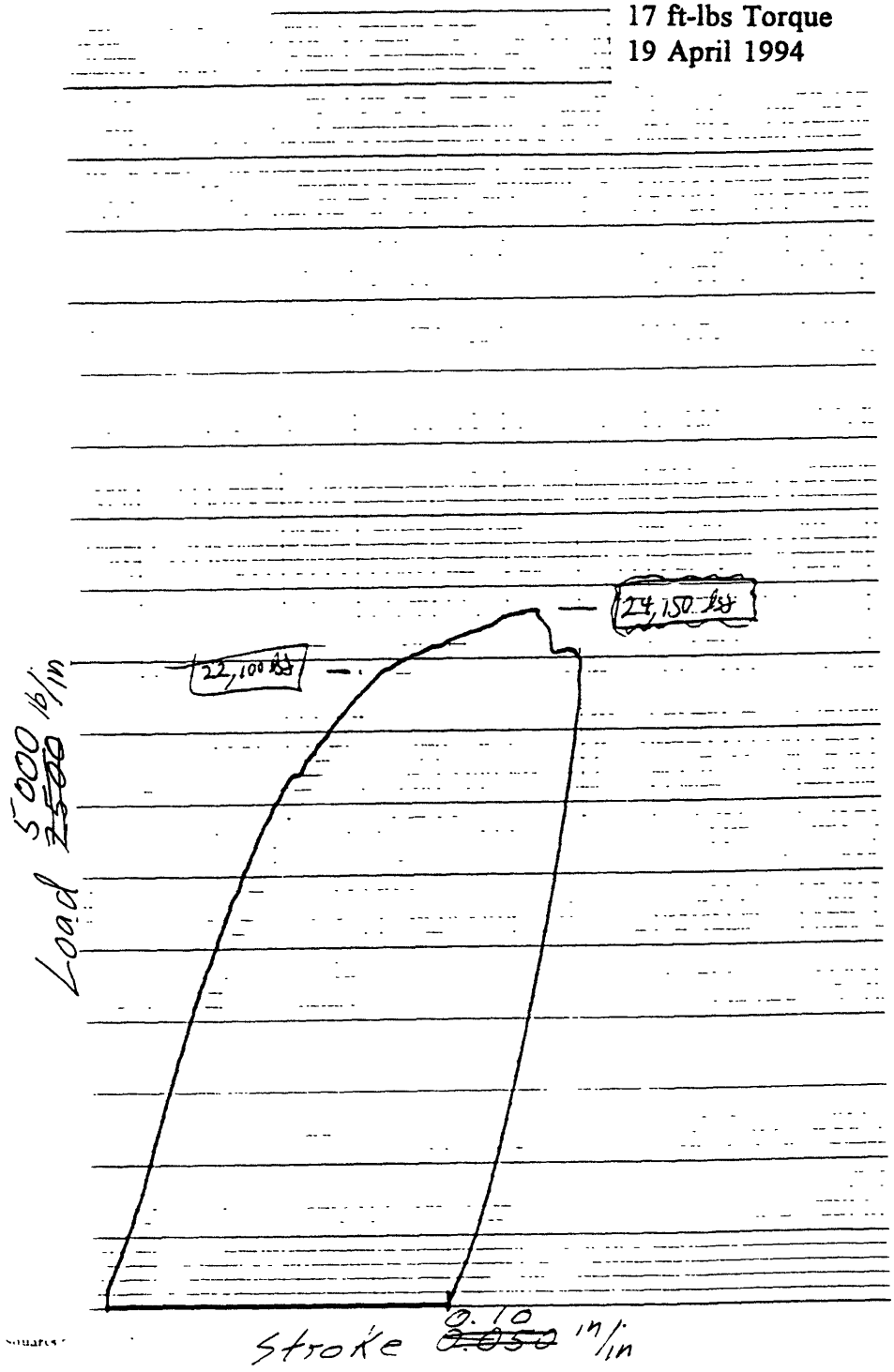

SPECIMEN BS-12
Countersunk Bolt
17 ft-lbs Torque
19 April 1994

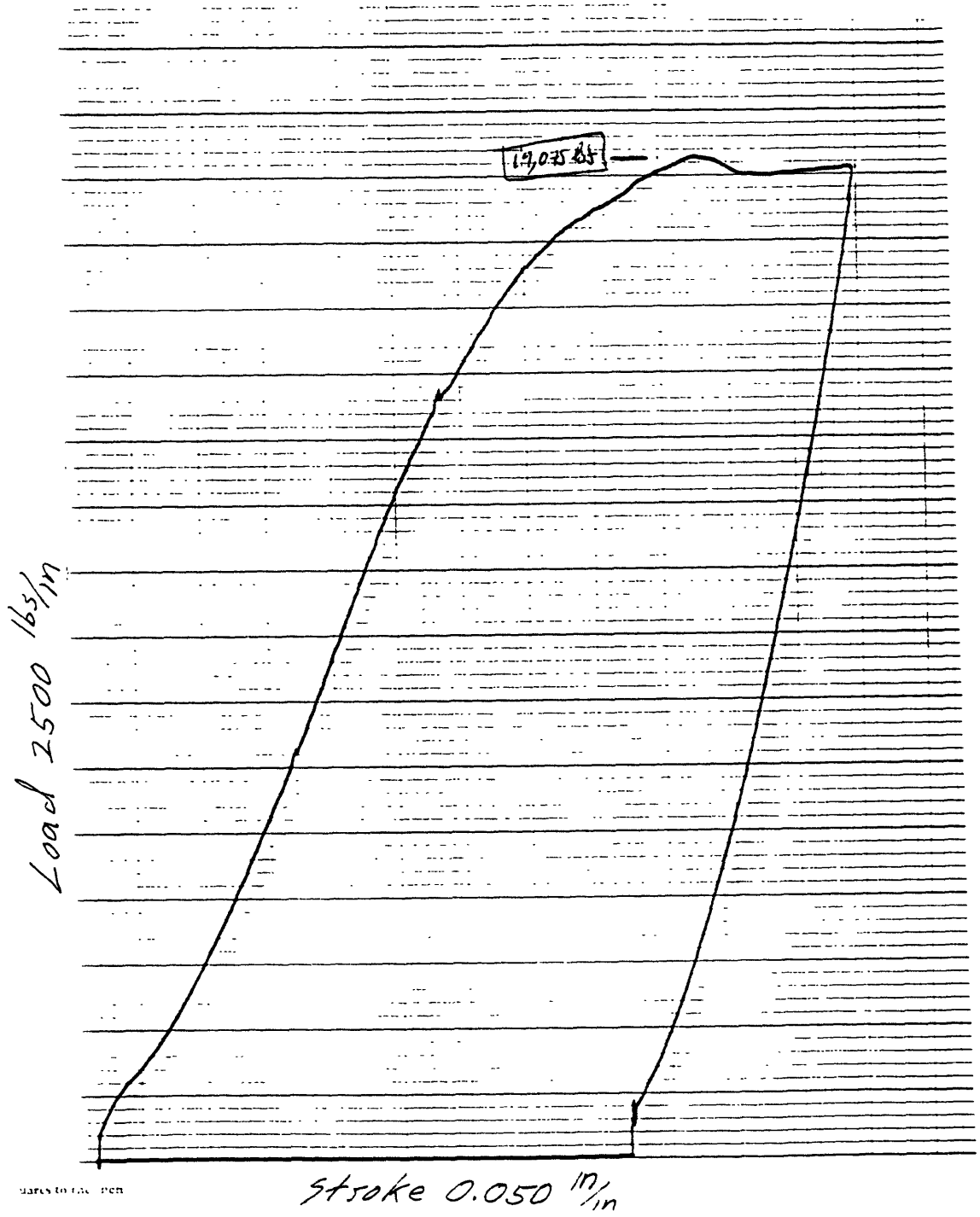

SPECIMEN BS-13
Countersunk Bolt
17 ft-lbs Torque
19 April 1994

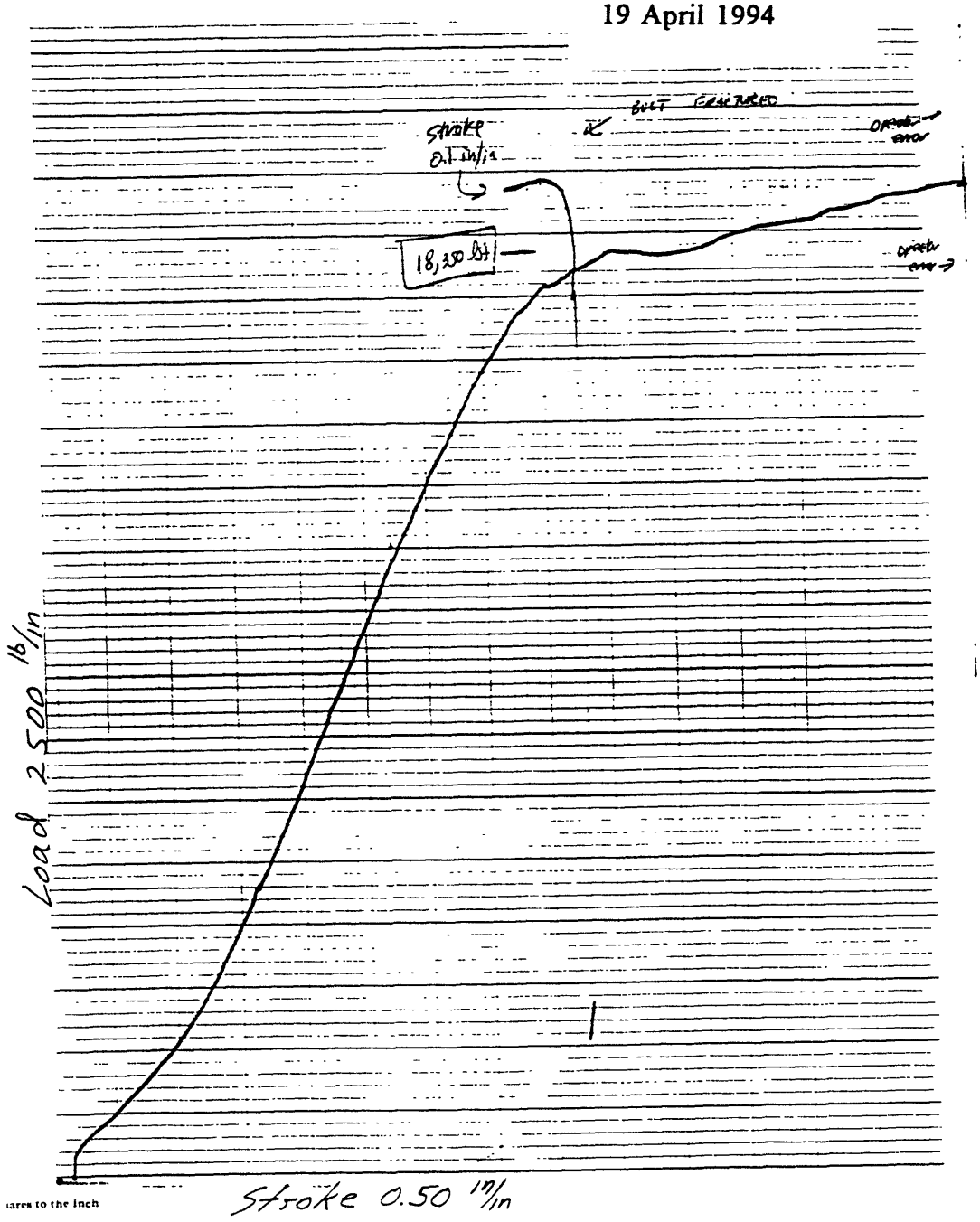

SPECIMEN BS-14
Countersunk Bolt
17 ft-lbs Torque
19 April 1994

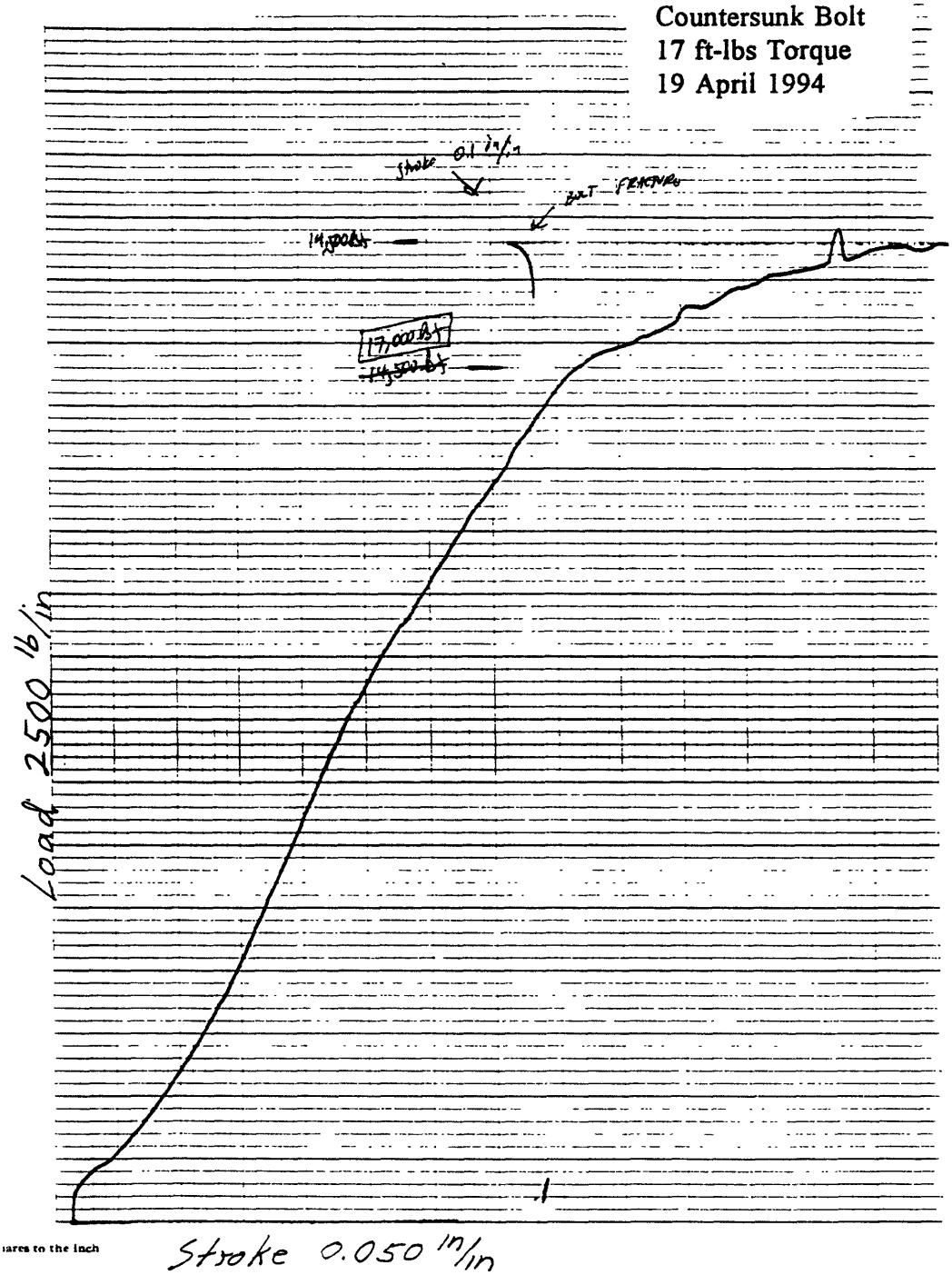

iares to the inch

SPECIMEN BS-15
Countersunk Bolt
17 ft-lbs Torque
19 April 1994

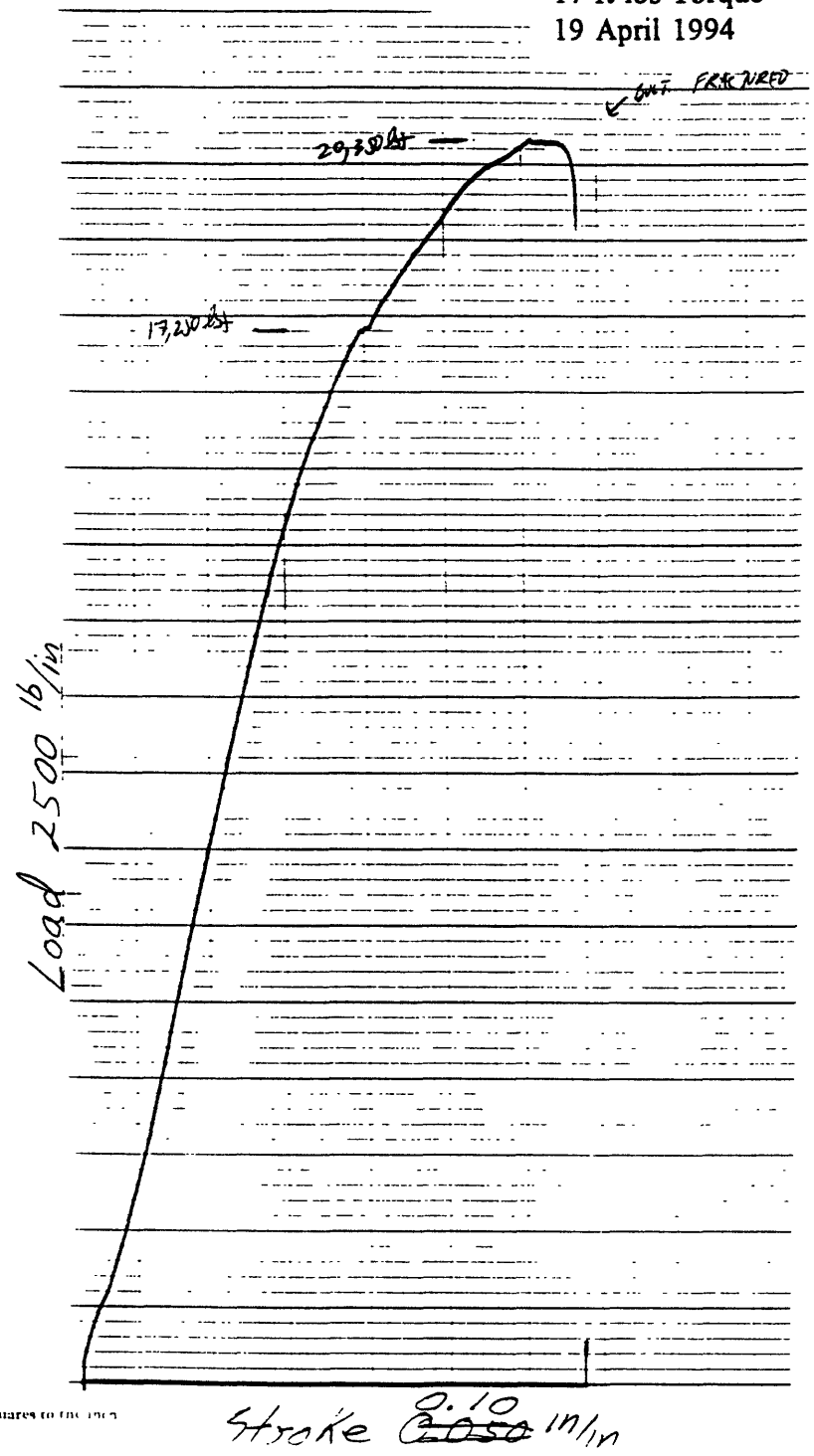

SPECIMEN BS-16
Protruding Head Bolt
0 ft-lbs Torque
19 April 1994

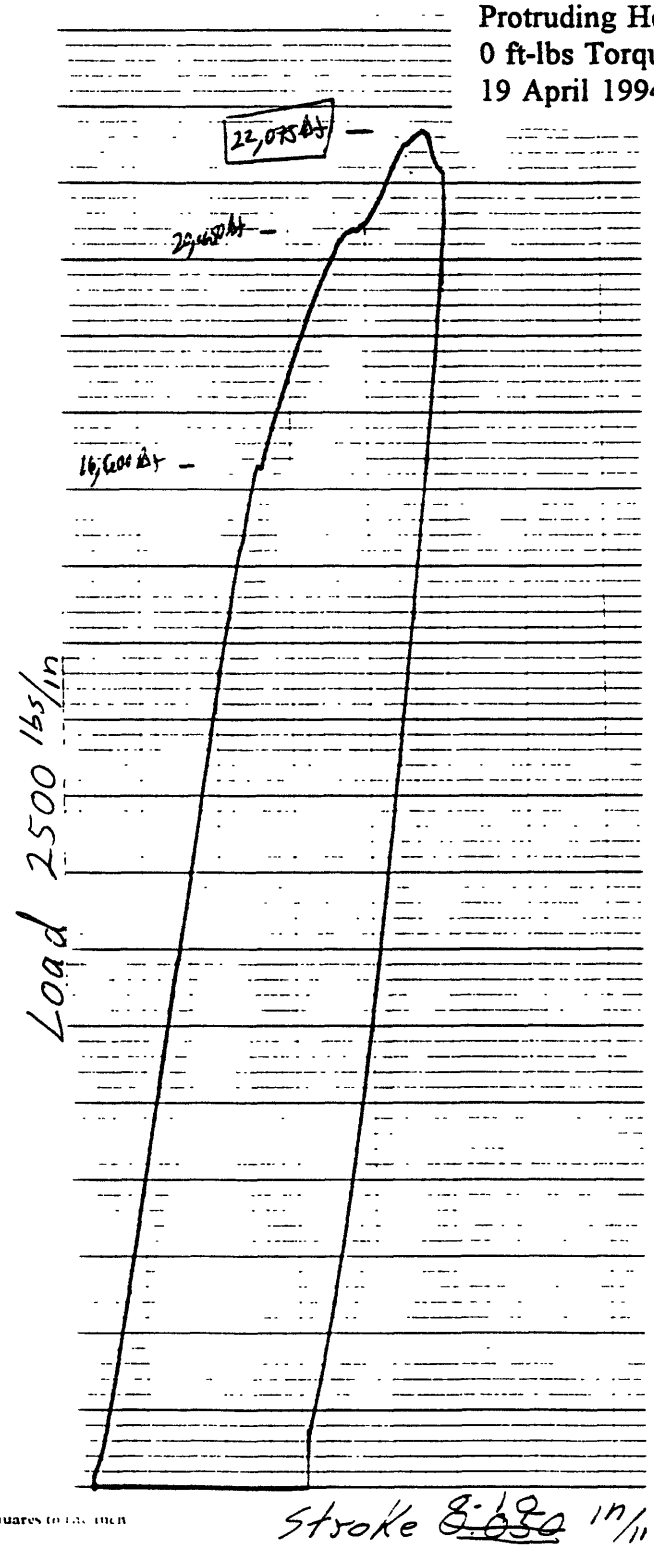

SPECIMEN BS-17
Countersunk Bolt
0 ft-lbs Torque
19 April 1994

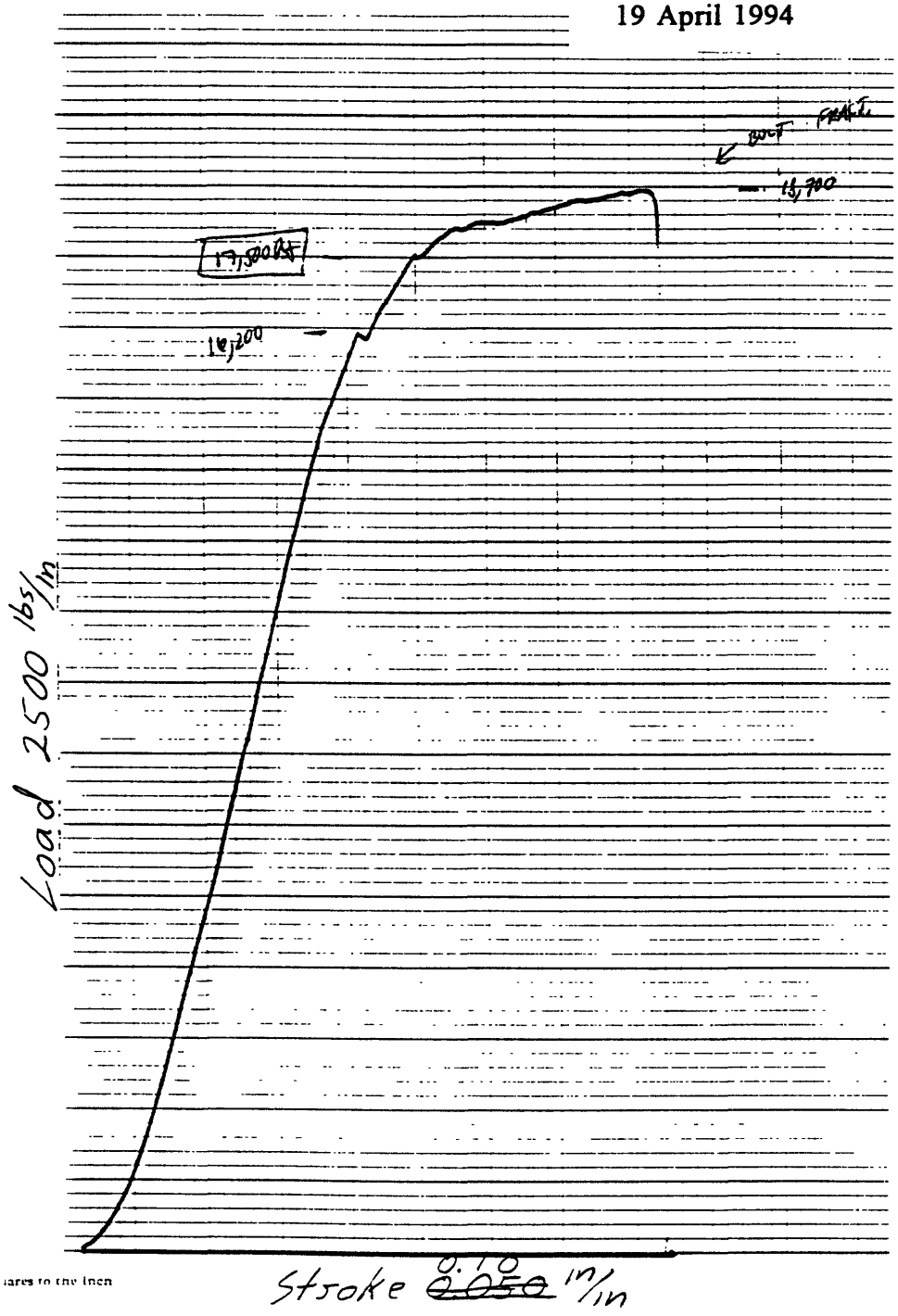

SPECIMEN BS-18
Countersunk Bolt
0 ft-lbs Torque
19 April 1994

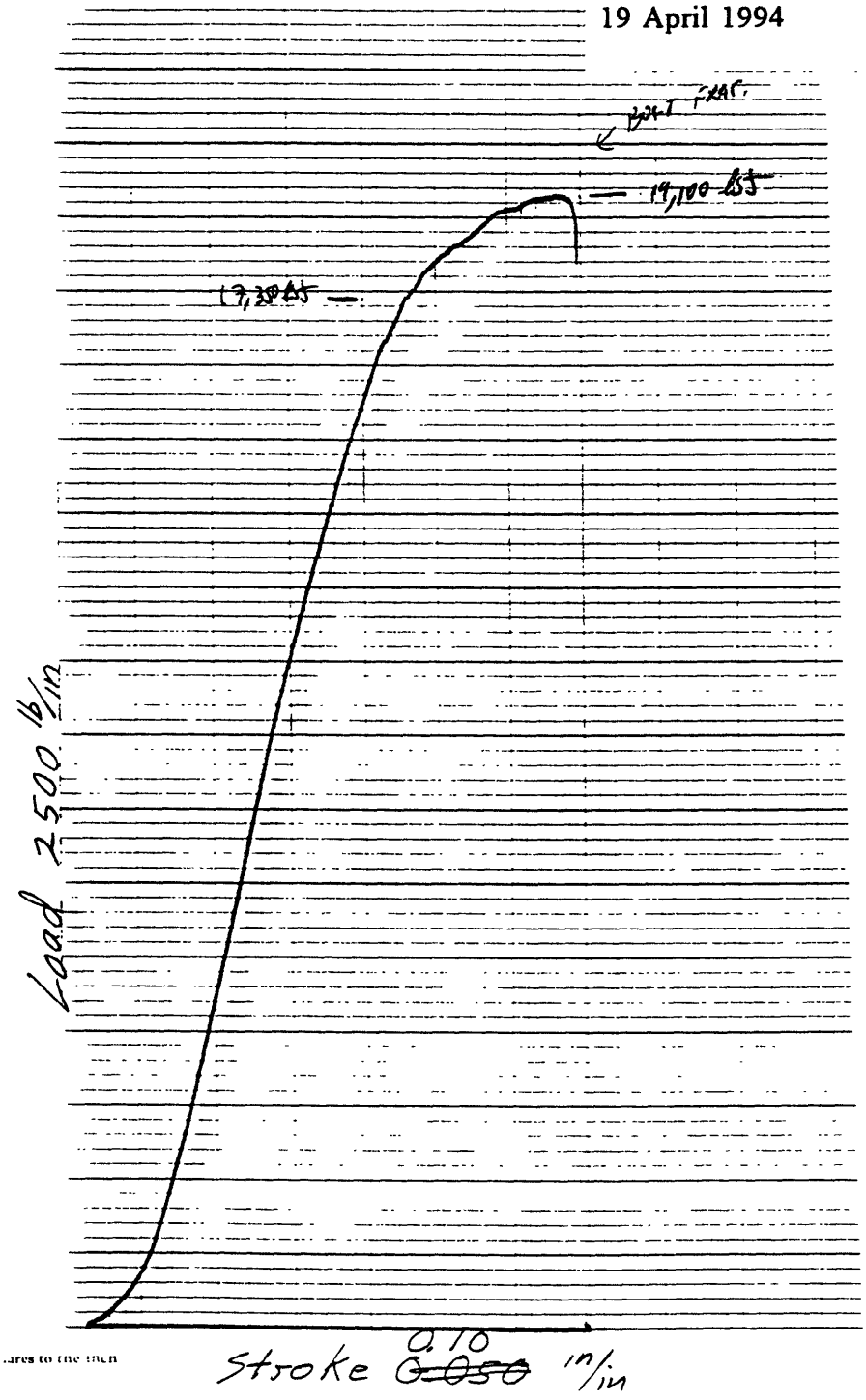

SPECIMEN BS-19
Countersunk Bolt
0 ft-lbs Torque
19 April 1994

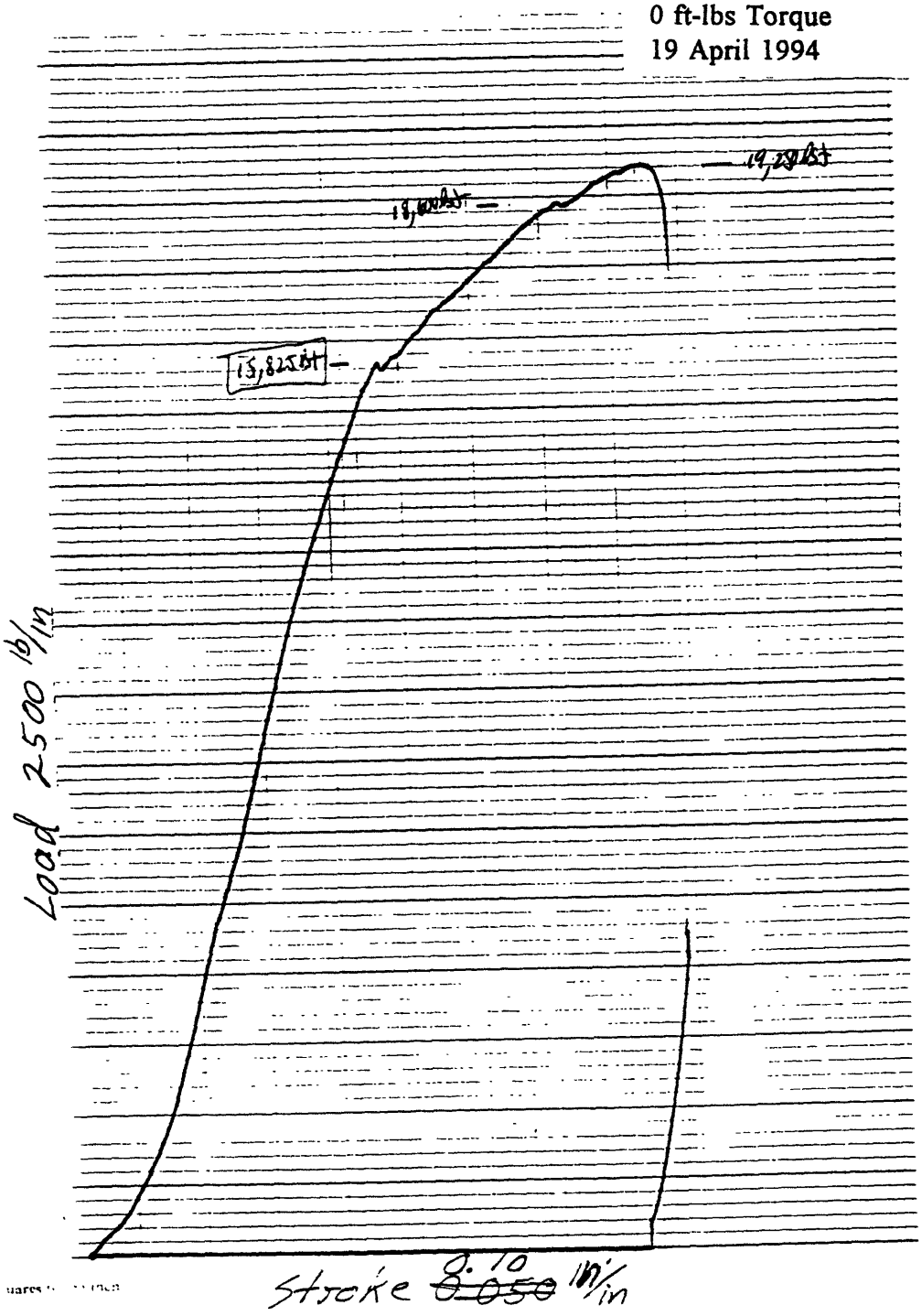

SPECIMEN BS-20
Countersunk Bolt
0 ft-lbs Torque
19 April 1994

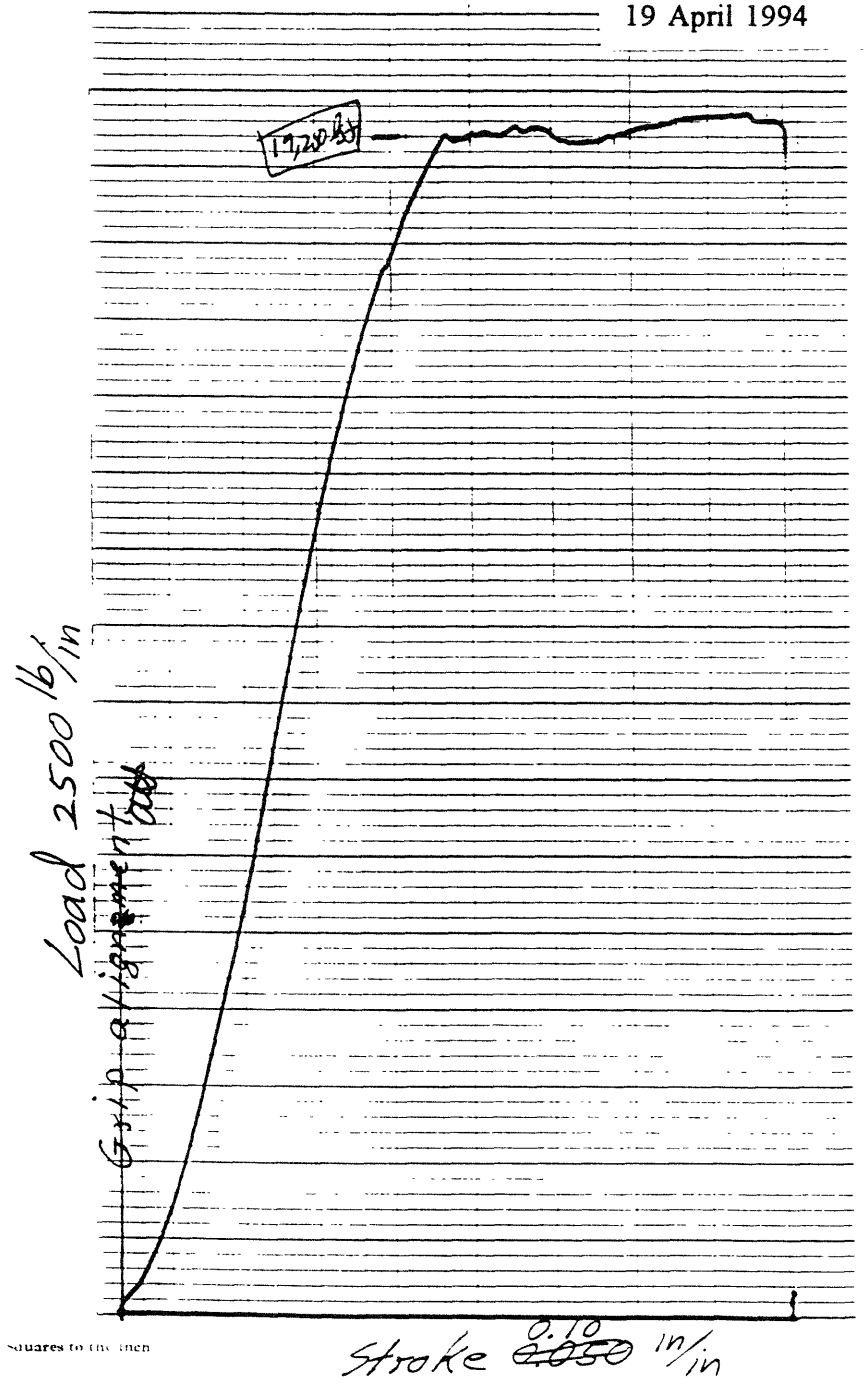

Appendix D. Photographs of Failed Bearing Strength Specimens

The following six pages contain photographs of representative failed specimens from the bearing strength experiments. These photos illustrate the delamination and brooming which precipitated bearing failure in the experiments, as well as hole deformation and bolt bending. Additionally, the photos illustrate some of the differences between countersunk and protruding-head bolted joint failure behavior.

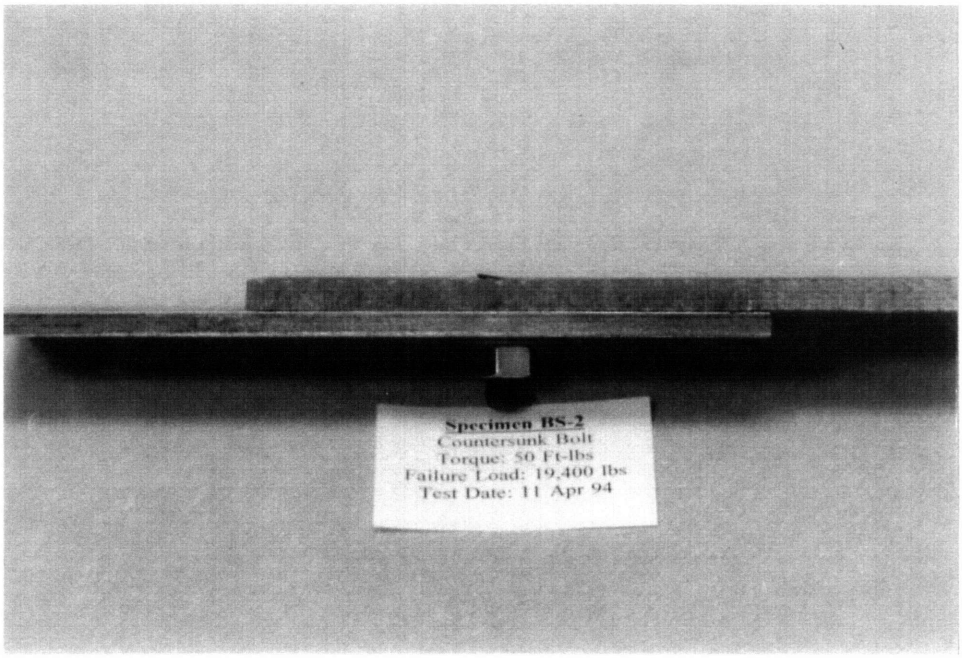

Specimen BS-2, Countersunk Bolt, 50 ft-lbs torque. Edge view of joint showing bolt bending and surface brooming.

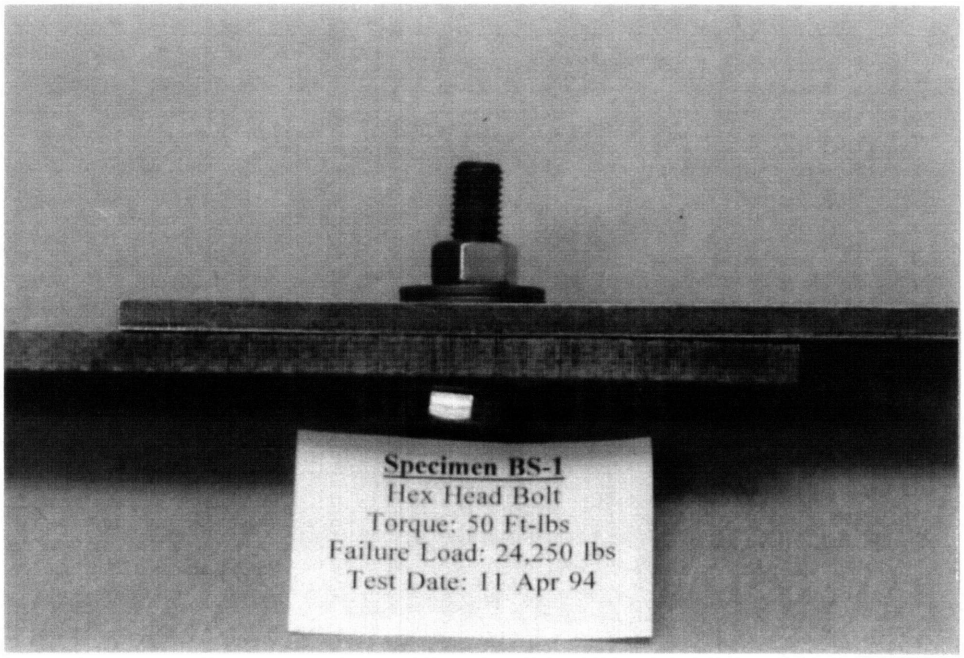

Specimen BS-1, Hex Head Bolt, 50 ft-lbs torque. Edge view of joint showing bolt bending and washer dishing.

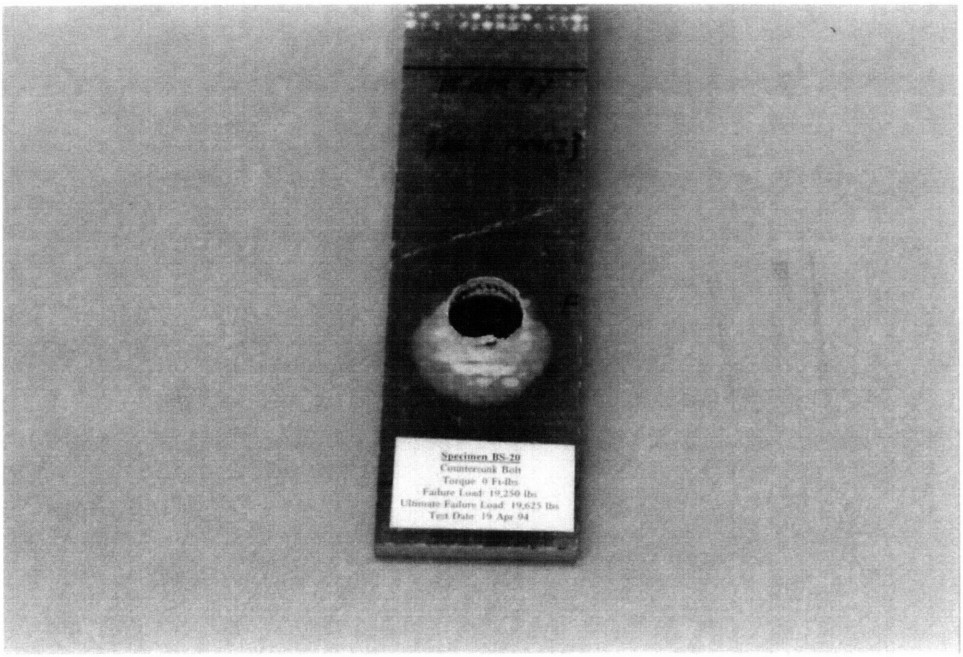

Specimen BS-20, Countersunk Bolt, 0 ft-lbs torque. View of outer GRP surface showing massive delamination and brooming, and bolt bending. The bolt fractured during the test.

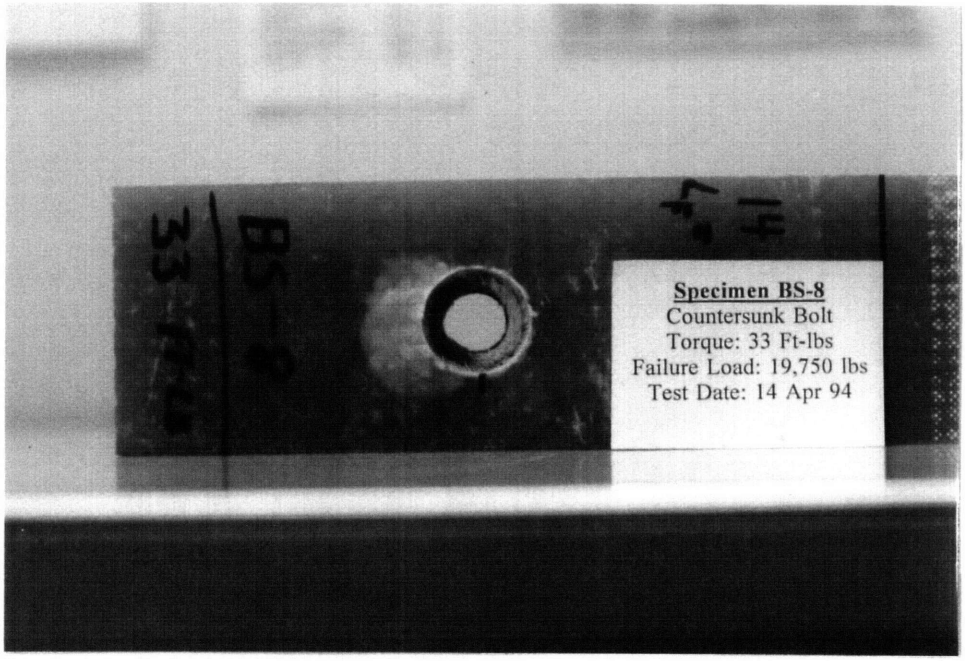

Specimen BS-8, Countersunk Bolt, 33 ft-lbs torque. View of outer GRP surface showing delamination and hole distortion. (Bolt removed from specimen.)

Specimen BS-1, Hex Head Bolt, 50 ft-lbs torque. Edge view, GRP panel, showing moderate brooming.

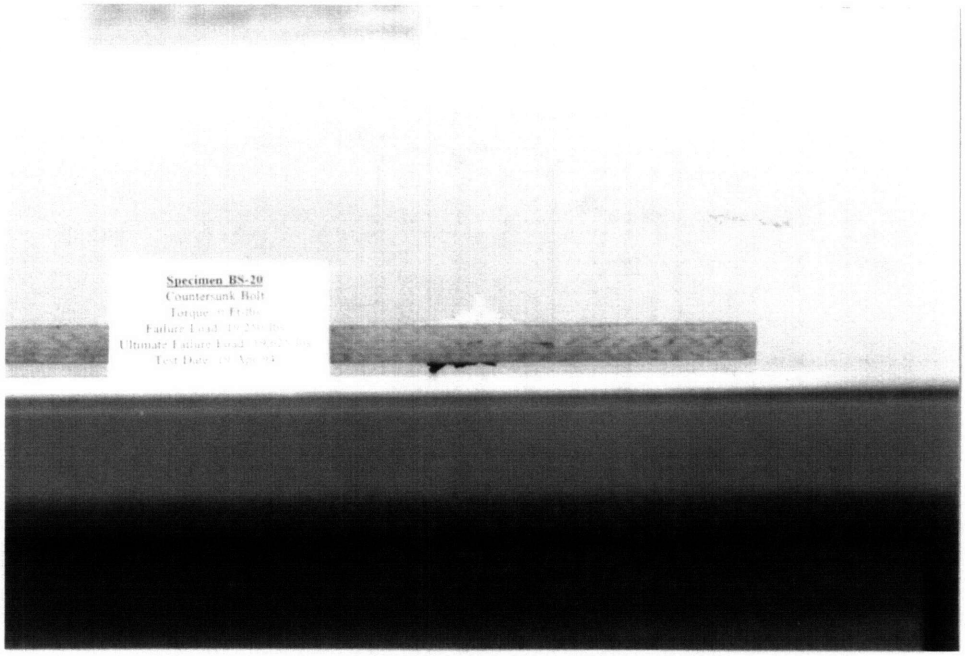

Specimen BS-20, Countersunk Bolt, 0 ft-lbs torque. Edge view, GRP panel, showing extensive delamination/brooming. (Bolt fractured during test.)

Specimen BS-19, Countersunk Bolt, 0 ft-lbs torque. View of inner GRP surface showing delamination, brooming, and hole deformation.

Specimen BS-1, Hex Head Bolt, 50 ft-lbs torque. View of outer GRP surface showing delamination, moderate brooming and hole deformation.

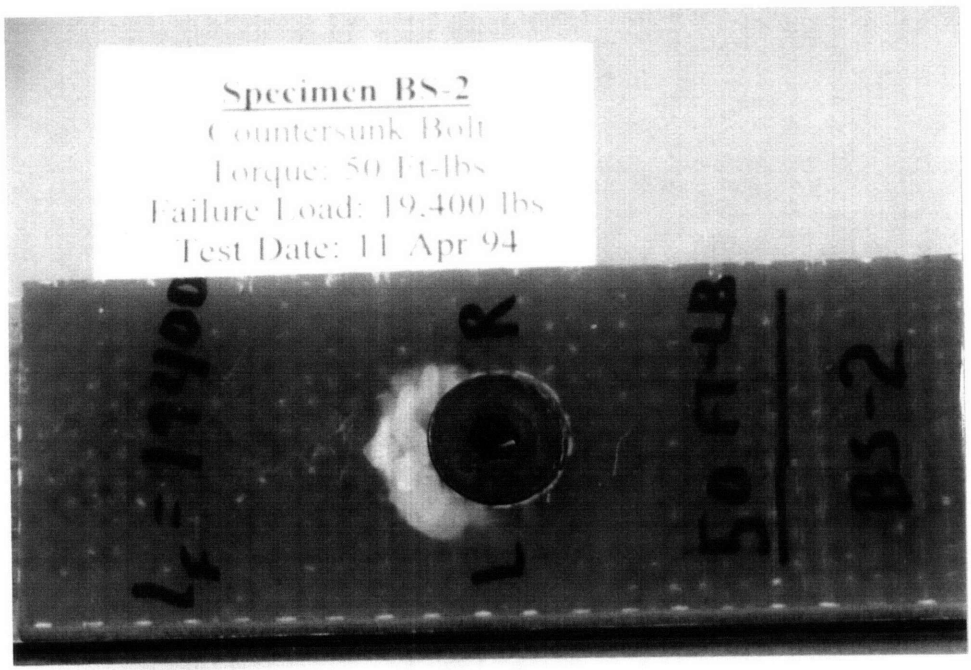

Specimen BS-2, Countersunk Bolt, 50 ft-lbs torque. View of outer GRP surface/bolt head, showing delamination and bolt bending.

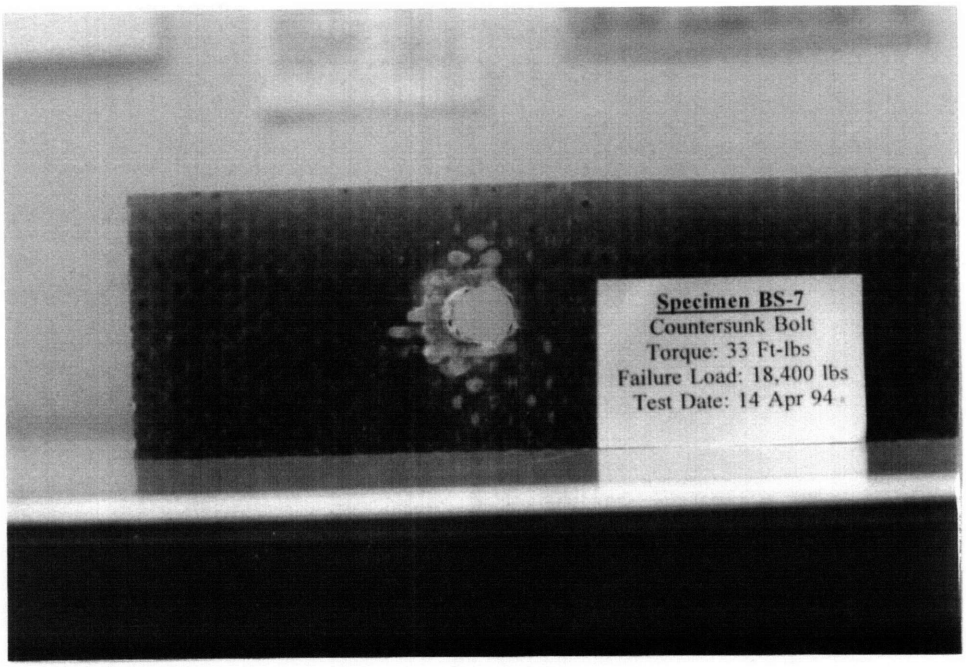

Specimen BS-7, Countersunk Bolt, 33 ft-lbs torque. View of inner GRP surface showing delamination, brooming, and hole deformation.

Specimen BS-1, Hex Head Bolt, 50 ft-lbs torque. View of bolt showing moderate bending. Impressions from the panels can be seen on the shank.

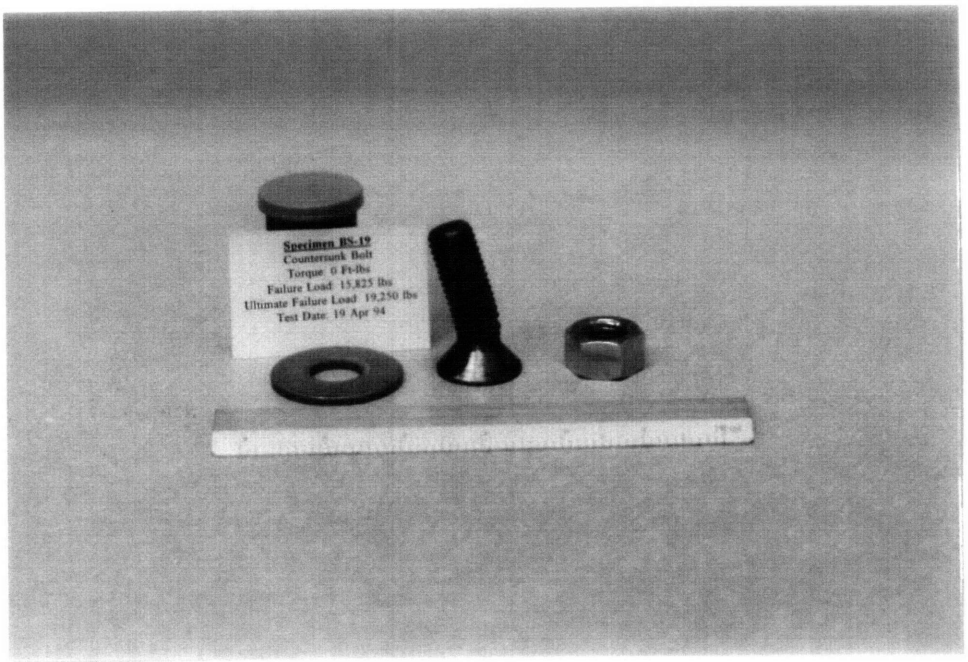

Specimen BS-19, Countersunk Bolt, 0 ft-lbs torque. View of bolt showing severe bending. Note fracture which has initiated between threads.

Bibliography

[1] Hart-Smith, L. J., "Design and Empirical Analysis of Bolted or Riveted Joints", in *Joining Fibre Reinforced Plastics*, ed. by F. L. Matthews (London: Elsevier Applied Science, 1987), pp. 227-269.

[2] Shivakumar, K. N. and J. H. Crews, Jr., "Bolt Clampup Relaxation in a Graphite/Epoxy Laminate", in *Long-Term Behavior of Composites*, ed. by T. K. O'Brien (Philadelphia: American Society for Testing and Materials, 1983), pp. 5-22.

[3] Savin, G. N., *Stress Distribution Around Holes* (NASA TT F-607, Translated from Russian, 1966), pp. 1-59.

[4] Ward, I. M., *Mechanical Behavior of Solid Polymers*, (Chichester: John Wiley and Sons, 1990), pp. 246-250.

[5] Matthews, F. L., "Theoretical Stress Analysis of Mechanically Fastened Joints", in *Joining Fibre Reinforced Plastics*, ed. by F. L. Matthews (London: Elsevier Applied Science, 1987), pp. 65-103.

[6] Stockdale, J. H. and F.L. Matthews, "The Effect of Clamping Pressure on Bolt Bearing Loads in Glass-Reinforced Plastics, *Composites*, Vol. 7, No. 1 (January 1976), pp. 34-38.

[7] Herrington, P. D. and M. Sabbaghian, "Effect of Radial Clearance between Bolt and Washer on the Bearing Strength of Composite Bolted Joints", *Journal of Composite Materials*, Vol. 26, No. 12 (1992), pp. 1826-1843.

[8] Shigley, J. E. and L. D. Mitchell, *Mechanical Engineering Design* (New York: McGraw-Hill Book Company, 1983), pp. 377-379.

[9] Hogg, R. V. and J. Ledolter, *Applied Statistics for Engineers and Physical Scientists* (New York: Macmillan Publishing Company, 1992), p. 450.

[10] Collings, T. A., "Experimentally Determined Strength of Mechanically Fastened Joints", in *Joining Fibre Reinforced Plastics*, ed. by F. L. Matthews (London: Elsevier Applied Science, 1987), pp. 9-63.

Biographical Note

The author, who is a Lieutenant in the U.S. Navy, was born and raised in Beech Grove, Indiana. He received his Bachelor's Degree in Chemical Engineering, Cum Laude, in 1984 from Rose-Hulman Institute of Technology, where he was elected to Tau Beta Pi and Omega Chi Epsilon. He received his Naval commission in 1985. After serving in the nuclear submarines USS Snook and USS Scamp and qualifying in submarines, Lieutenant Fox was designated as an Engineering Duty Officer, in 1988. Before coming to MIT, he was assigned to the Naval Underwater Systems Center in Newport, R.I., as the military liaison to the Torpedo MK 48/ADCAP Program Manager.

In his off-duty time, Lieutenant Fox enjoys sailing, skiing, and collecting and playing musical instruments.